12-2001

Cold-Temperature Adaptation of Muscle Creatine Kinase from an Antartic Teleost (*Chaenocephalus Aceratus*)

Paul Winnard Jr.

COLD-TEMPERATURE ADAPTATION OF MUSCLE CREATINE KINASE FROM AN ANTARCTIC TELEOST (*CHAENOCEPHALUS ACERATUS*)

By

Paul Winnard Jr.

B.S. Merrimack College, 1984

M.S. The University of New Hampshire, 1987

A THESIS

Submitted in Partial Fulfillment of the

Requirements for the Degree of

Doctor of Philosophy

(in Biochemistry and Molecular Biology)

The Graduate School

The University of Maine

December, 2001

Advisory Committee:

Michael E. Vayda, Professor of Biochemistry and Molecular Biology, Advisor

Bruce Sidell, Professor of Marine Sciences and Biology

Robert Cashon, Assistant Professor of Biochemistry

Keith Hutchinson, Professor of Biochemistry

John Singer, Professor of Microbiology

Ione Hunt von Herbing, Assistant Professor of Marine Sciences

LIBRARY RIGHTS STATEMENT

In presenting this thesis in partial fulfillment of the requirements for an advanced degree at The University of Maine, I agree that the Library shall make it freely available for inspection. I further agree that permission for "fair use" copying of this thesis for scholarly purposes may be granted by the Librarian. Any copying or publication of this thesis for financial gain shall not be allowed without my written permission.

30 Nov '01
Date


Signature

COLD-TEMPERATURE ADAPTATION OF MUSCLE CREATINE KINASE FROM AN ANTARCTIC TELEOST (*CHAENOCEPHALUS ACERATUS*)

By Paul Winnard Jr.

Thesis Advisor: Dr. Michael E. Vayda

An Abstract of the Thesis Presented
in Partial Fulfillment of the Requirements for the
Degree of Doctor of Philosophy
(in Biochemistry and Molecular Biology)
December, 2001

The white muscle of *Chaenocephalus aceratus*, an Antarctic teleost of the Channicthyidae family, has a compromised glycolytic capacity and this fish cannot depend on glycolysis for rapid ATP generation. For *C. aceratus*, creatine kinase (CK) and phosphocreatine (PCr) reserves comprise the metabolic pathway that may supplement and overcome this deficiency in energy transduction. Two conditions, low glycolytic capacity and evolution in a chronically cold habitat (–1.86° C), give us reason to believe that *C. aceratus* muscle CK (MMCK) has been subjected to strong selective pressure. Thus, the hypothesis of this thesis is that MMCK from *C. aceratus* white muscle exhibits a high specific activity. In order to test this hypothesis, MMCK from *C. aceratus* white (glycolytic) muscle was purified. This revealed that *C. aceratus* expresses two cytosolic isoforms of MMCK. Mammals, birds, and most fish express only one MMCK. Thermal stability studies indicate that *C. aceratus* MMCKs exhibit thermal denaturation after a 30 minute incubation at temperatures greater-than 10° C. At 0° C,

the average apparent V_{max} was found to be 3-to-5 times higher than that predicted from a Q_{10} analysis. The estimate of activation enthalpy for *C. aceratus* MMCK was 7 kcal/mol lower than that of rabbit MMCK and the activation free energy estimate of *C. aceratus* MMCK was 1 kcal/mol lower. This helps explain *C. aceratus* MMCK's high catalytic activity at low temperature, which was found to be greater-than eurythermal fish MMCK activities at 25° C. Kinetic constant estimates indicate that *C. aceratus* MMCKs have an affinity for ADP (K_m = 0.06 mM) and PCr (K_m = 17 mM) that is similar to what has been reported for other MMCKs. All *C. aceratus* CK cDNAs were cloned and sequenced, which confirmed that *C. aceratus* expresses two distinct isoforms of MCK. The tissues that express muscle, brain, and mitochondrial CK mRNAs were determined. This is a characteristic of each CK isoform and *C. aceratus* MCK mRNAs were obsevered only in skeletal muscle. The evidence presented in this thesis demonstrates that one or both MMCKs have undergone cold-temperature adaptation.

ACKNOWLEDGMENTS

Dedicated to my parents,

Paul Thomas Winnard Sr. and Isabella Carmen Barile Winnard.

Their unwavering love and moral support greatly bolstered my ability to complete this thesis.

TABLE OF CONTENTS

LIST OF TABLES

LIST OF FIGURES

Chapter 1

INTRODUCTION

1.1. Creatine kinase's important function in energy transduction in vertebrate skeletal muscle.

Vertebrate skeletal muscle requires a steady supply of energy to sustain a variety of contraction states. Muscle fuels its contractions with ATP and unlike most other tissue muscle's ATP turnover rate can increase by 2-to-3 orders of magnitude in going from rest to full activity (Hochachka *et al.*, 1983; Hochachka, 1985). Myocytes do not maintain high concentrations of free adenylate nucleotides because these are regulators of metabolic enzymes (Atkinson, 1970; Hochachka *et al.*, 1983). In addition, fluctuations in the ATP/ADP ratio must be avoided because such fluctuations would result in fluctuations in ATP's chemical potential (Hochachka *et al.*, 1983). Muscle circumvents these metabolic obstacles and is endowed with metabolic pathways that ensure that a ready supply of ATP is made available throughout its range of metabolic rates. Sustained anaerobic work relies on glycolysis for ATP generation and once engaged, provides ATP until exhaustion occurs (Hochachka, 1985). Another important metabolic pathway involves creatine kinase (CK) isozymes and the high-energy phosphate reserves of phosphocreatine (PCr). During sustained muscle work, the CK pathway is coupled to oxidative phosphorylation by the phosphocreatine shuttle (Bessman and Geiger, 1981; Hochachka, 1983). During a burst response, the CK pathway replenishes ATP pools at ATPase sites. (Hochachka *et al.*, 1983; Sweeney, 1994).

CK (E.C. 2.7.3.2) catalyzes the reversible phosphorylation of creatine:

$$\text{creatine} + MgATP^{2-} \leftarrow \rightarrow PCr^{2-} + MgADP^{-} + H^{+}.$$

The majority of CK found in vertebrate skeletal muscle consists of two isoforms: a cytosolic dimer CK (MMCK) and a mitochondrial CK (MtCK) that is functional as an octamer (Wallimann *et al.*, 1992). At sites of ATP utilization ATP production is favored, that is, the reverse reaction (Hochachka *et al.*, 1983; Khan *et al.*, 1989). Myosin ATPase is coupled to M-line bound MMCK (Wallimann and Eppenberger, 1985; Wallimann *et al.*, 1992). At these sites, MMCK is capable of matching rapid ATP usage with rapid ATP production. This ensures that a high ATP/ADP ratio is maintained and thus, the high free energy associated with ATP hydrolysis (Sweeney, 1994). During recovery and sustained work, cytosolic PCr pools are largely replenished in mitochondria by the forward reaction by mitochondrial CK isoform present in the intramembrane space (Wallimann *et al.*, 1992). Therefore, *in vivo* the forward and reverse CK reactions are associated with different CK isozymes that are located in separate cellular compartments (Wallimann *et al.*, 1992). The CK reaction is particularly crucial when ATP must be rapidly supplied to muscle during circumstances of prey capture or predator avoidance (Sweeney, 1994) and perhaps, also when competing for sexual partners (Crockett and Sidell, 1990; Clarke, 1991). MMCK's significance during these types of burst activities is apparent from studies of transgenic mouse skeletal muscles that are deficient in MMCK and incapable of burst activity (van Deursen *et al.*, 1993). MMCK's role of minimizing fluctuations in ATP concentration during burst activity means that MMCK is likely subjected to strong selective pressure.

Comparative studies between homologous enzymes of ectotherms and endotherms provide a means of evaluating natural selection processes (Hochachka and Somero, 1984). Endotherms have warm stable body temperatures while an ectotherm's body temperature varies with its environmental temperature. The Southern Ocean that surrounds Antarctica is chronically cold and ectotherms that thrive there have cold stable body temperatures (Eastman, 1993). Teleosts from the Southern Ocean exhibit enzymes that have adapted to function at extremely cold temperatures (Hochachkka and Somero, 1984; Fields and Somero, 1998; Ciardiello et al., 2000). Comparative studies give us the opportunity to evaluate structural and functional differences that bring about enzymatic adaptations (Hochachka and Somero, 1984).

1.2. Antarctic teleosts are uniquely adapted to thrive in the chronically cold Southern Ocean.

The ichthyofauna of the Sourthern Ocean is uniquely adapted to a stenothermic environment. Thermal isolation of the Southern Ocean began approximately 25 million years ago with the development of a circumpolar current and establishment of the Polar Frontal Zone (Eastman, 1993; Eastman, 1995; Clarke and Johnston, 1996). Year-round temperature of Antarctic coastal waters in McMurdo Sound is -1.86° C and along the Antarctic Peninsula temperature fluctuates only from -1.86° C-to-$+1.0^{\circ}$ C (Eastman 1993). The coastal waters are devoid of estuaries, reefs, intertidal zones, and shallow continental shelves. Even with these constraints these coastal waters support a diversity of 49 families and 274 species of fish (Eastman, 1995). The perciform suborder Notothenioidei contains the majority (6 families and 122 species) of the classified

Antarctic teleosts (Eastman 1993). Diversification of the Notothenioid stock is considered to be a relatively recent event that occurred during the last 10-to-15 million years (Eastman, 1995). During this time, species within this group have successfully filled a variety of niches and nototheniids are found throughout the water column (Eastman, 1995). Particularly interesting are the Channicthyidae family (icefishes), which may have radiated as recently as 2.4-to-4.5 million years ago and are endemic to the Antarctic coastal waters (Eastman, 1995). During this short period of evolution icefishes have undergone a number of physiological adaptations that, in part, have been brought about as a response to life at subzero temperatures (Hemmingsen and Douglas, 1977; Fitch *et al.*, 1984; Eggington and Rankin, 1998; Vayda *et al.*, 1999). Studies on icefish white anaerobic muscle indicate that its structure and physiology is substantially different in comparison to the white musculature of other teleosts.

1.2.1. Icefish thrive despite a white musculature with low glycolytic capacity.

Relative to temperate teleosts, white muscle of several Notothenioids exhibit a compromised glycolytic capacity (Walesby and Johnston, 1979; Dunn and Johnston, 1986; Johnston, 1987; Dunn *et al.*, 1989; Sidell and Crockett, 1989; Crockett and Sidell, 1990). In these fishes, this group of enzymes does not exhibit cold-temperature adaptation. These fishes do not generate large amounts of lactate during burst swimming, which is consistent with this finding (Dunn and Johnston, 1986; Johnston, 1989). These data indicate that these teleosts cannot depend on anaerobic glycolysis for ATP generation. Relatively large CK activities are present in white muscle homogenates from these fishes (Dunn and Johnston, 1986; Johnston, 1987; Dunn, 1988). These results

indicate that for many nototheniids MMCK apparently has a particularly important role in replenishing ATP pools during anaerobic activities.

The CK reaction functions as a spatial and temporal energy buffer (Sweeny, 1994). The CK reaction plays a greater role in providing an energy reserve in muscle that is composed of large fibers with few mitochondria (Sweeney, 1994). In large fibers the CK reaction minimizes ATP/ADP gradients that might otherwise occur, because of the relatively large distances between mitochondria and the core of muscle fiber. The CK reaction also functions as a temporal energy buffer in these cells by using PCr reserves to extend the available fuel supply beyond the period that would otherwise be obtainable (Sweeney, 1994). White myotomal muscle from *Chaenocephalus. aceratus* (an icefish) can have fiber diameters greater-than 400 μm (Johnston, 1985). Similar white muscle fiber diameters (200-to-450 μm) have been reported for other nototheniids as well (Dunn *et al.*, 1989; Johnston, 1989). In contrast, temperate teleost species tend to have white muscle fibers with diameters that are less-than 100 μm (Johnston, 1989). In addition, the mitochondrial content of notothenid white muscle is less-than 2 volume percent (Londraville and Sidell, 1990). In comparison, the mitochondrial content of white muscle from striped bass acclimated to 5° C is 4 volume percent (Egginton and Sidell, 1989). In other words, *C. aceratus* white fibers have a low number of sites where ATP is generated by oxidative phosphorylation. Therefore, an ATP concentration gradient with high ATP concentrations near the surface of a fiber and low ATP concentrations at a fiber's core could develop in the very large white muscle fibers of *C. aceratus*. A compounding problem for icefishes is the cold, which hinders metabolite diffusion, for example ATP diffusion (Sidell, 1988). *C. aceratus* uses subcarangiform swimming to

propel them during a burst response and the myotomal fibers recruited at these times can not depend on glycolysis for ATP generation. Because of this, ATP generation by MMCK may be important to these Antarctic fish's swimming abilities when capturing prey and during predator avoidance (Johnston, 1987).

The hypothesis of this thesis is that MMCK from *C. aceratus* white muscle has a high activity at 0° C. An alternative explanation for high CK activity in *C. aceratus* white muscle would be a large protein concentration that would compensate for a MMCK of low catalytic activity. Molecular and kinetic characteristics of *C. aceratus* MMCK are not known. Therefore, whether this protein has undergone temperature compensation and achieved high catalytic efficiency is unknown. To test this hypothesis this research I have:

1. Purified MMCK from *C. aceratus* white muscle. The purification process indicated that white muscle from this icefish apparently has two cytosolic isoforms of MMCK. This is unusual, as most fish appear to express only one MMCK, except carp, which is polyploid.
2. Optimum pH for maximum activity, mean apparent V_{max}, and mean temperature stability of this fish's MMCKs were determined, at 0° C. Apparent V_{max} data showed that one or both of these MMCKs have undergone cold-temperature adaptation.
3. Estimates of the thermodynamic activation parameters and mean apparent kinetic constants (K_ms) have been obtained for *C. aceratus* MMCKs, at 0° C. The activation enthalpy and activation free energy for *C. aceratus* MMCKs proved to be lower than those of rabbit MMCK. This helps explain *C. aceratus* MMCK's high catalytic activity at low temperature. Apparent K_m estimates indicated that *C. aceratus*

MMCKs have an affinity for ADP and PCr that is similar to what has been reported for other MMCKs. The K_m data also showed that the rate determining substrate appears to be PCr.

4. *C. aceratus* CK-encoding cDNAs (MCK-b, MCK-a, MtCK, and brain CK (BCK)) were cloned and sequenced. This data firmly established that *C. aceratus* expresses two isoforms of MMCK that are distinct from other CK isoforms.
5. The tissues that express MCK, BCK, and MtCK mRNAs were determined. This is a characteristic of each isoform and this data supplemented the sequencing data in establishing the distinction between isoforms.
6. The deduced amino acid sequences of MMCK-b and MMCK-a were compared with mammalian and fish homologues. This comparison provided information about the potential amino acid differences that bring about *C. aceratus* MMCKs efficient function at 0^{o} C.

Chapter 2

OPTIMUM CONDITIONS FOR KINETIC MEASUREMENTS ON *C. aceratus* CK

2.1. Evaluation of the optimum concentrations of $NADP^+$, glucose-6-phosphate dehydrogenase, and hexokinase in the coupled kinetic assay at pH 7.55 and 0° C.

Creatine kinase activity was measured using a coupled kinetic assay (Oliver, 1954). In this assay ATP produced by CK is coupled to the production of NADPH by glucose-6-phosphate dehydrogenase (G-6-PDH) through an intermediate reaction where the CK produced ATP is used by hexokinase (HK) to produce glucose-6-phosphate. NADPH production is followed as a function of time at an absorbance of 340 nm. Figure 1 indicates how varying the concentrations of $NADP^+$, G-6-P-DH, and HK in the coupled assay affected V_{max} measurements of CK activity at 0° C. At assay concentrations of 10 U/ml of HK and 0.5 U/ml of G-6-P-DH the highest apparent V_{max}s were obtained at final assay concentrations of $NADP^+$ of $\geq$ 2 mM (Fig. 1A). In Figure 1B it is shown that maximum apparent V_{max}s were obtained at G-6-PDH concentrations of 5 or 10 U/ml, at assay concentrations of 5 mM $NADP^+$ and 10 U/ml HK. The G-6-PDH used here was supplied as a 2.6 M ammonium sulfate suspension. In the experiment that tested 50 U/ml of G-6-P-DH the assay concentration of sulfate anion was 45 mM. G-6-PDH is 80% inhibited at 10 mM sulfate (Sigma data sheet). MMCK is also inhibited by sulfate anion (K_i for sulfate 4 mM; Nihei *et al.*, 1960). Therefore, the most likely reason for the large decrease in apparent V_{max} at 50 U/ml of G-6-PDH was the high sulfate concentration in

the assay (Fig. 1B). Figure 1C indicates that V_{max} measurements were independent of HK concentration at concentrations of 5 U/ml of G-6-PDH and 5 mM $NADP^+$. From these results, the standard final assay concentrations were set at 5 mM $NADP^+$, 5 U/ml of G-6-PDH, and 25 U/ml of HK. A final evaluation of the validity of these conditions showed that at a final assay concentration of 2.5 U/ml of G-6-P-DH (all other reagents being held constant) the apparent V_{max} was only about 60% of what was found when using the standard assay.

2.2. Optimum pH for maximum apparent V_{max} determinations of MMCK from *C. aceratus* at 0° C.

An enzyme's function is affected by pH. That is, changes in net charge affect an enzymes ability to function and enzymes exhibit pH optima where their activities are at a maximum (Cornish-Bowden, 1995). In addition, temperature has a profound affect on intracellular muscle pH of ectotherms, which varies inversely with temperature (Howell *et al.*, 1970, Cameron, 1984). Therefore, in order to obtain physiologically relevant (0° C) activity measurements during ATP production by CK from *C. aceratus* it was necessary to determine its pH optimum at this temperature. It can be seen in Figure 2 that preparations of CK from *C. aceratus* have near maximum activity over a narrow pH range of 7.50-to-7.65 with maximum activity at pH 7.60. From these results the pH used in the standard kinetic assay was set at 7.55-to-7.60.

2.3. Determination of *C. aceratus* MMCK's Apparent V_{max} within its Linear Concentration Range.

Valid kinetic values were obtained at enzyme concentrations that are directly proportional to the rates. Measurements taken outside such a range give erroneous results. Therefore, it was necessary to determine the range of protein concentrations over which the assay was linear, at 0° C. The samples that were analyzed were from various steps in the purification of CK from *C. aceratus* white muscle (see Chp. 3). Figure 3 shows the protein concentration ranges (μg/ml) over which the change in absorbance at 340 nm per minute (ΔA_{340}/min) was linear. For white muscle homogenates the linear range was approximately 1.0-to-3.0 μg/ml (Panel A), for post homogenate supernatants the linear range was approximately 0.45-to-1.0 μg/ml (Panel B), and for affinity column eluants the linear range was approximately 0.08-to-0.30 μg/ml (Panel C). In each case the regression line extends through the theoretical lower limit of zero protein (enzyme) concentration. However, the actual lower limit of the assay was a protein concentration that gave a ΔA_{340}/min of about 0.05. These experiments established that the final determinations of V_{max} had to be conducted at a ΔA_{340}/minute between 0.06 and 0.18. Under these conditions the assay ran for 20-to-30 minutes and was linear during steady-state for at least 3-to-10 minutes. The CK concentration range (2-to-3 fold) reported here is similar to what has been reported earlier for this coupled assay (Oliver, 1954; Nielsen and Ludvigsen, 1963; Rosalki, 1967; Hess *et al.*, 1968).

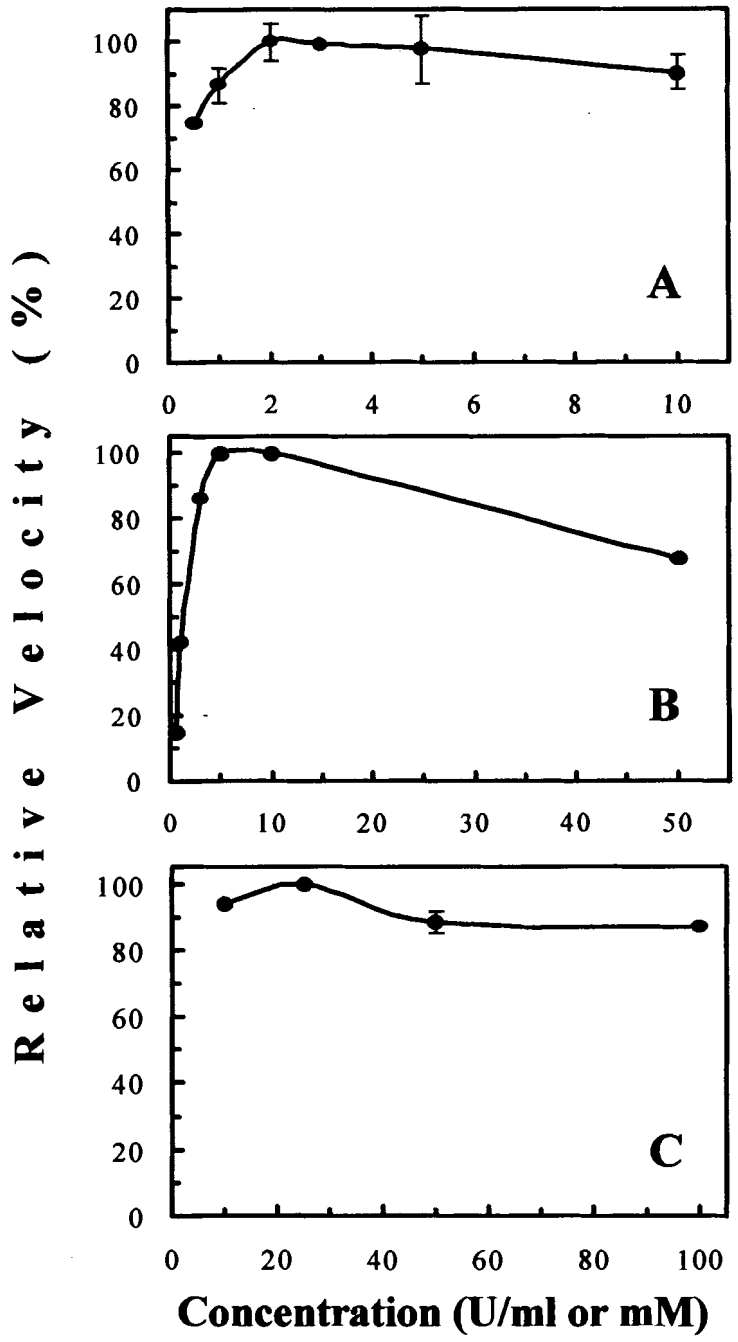

Figure 1. Determination of optimum concentrations of $NADP^+$, G-6-PDH, and HK used in the coupled kinetic assay at 0° C. Plots are of concentrations versus percent of maximum velocity for Panel A: $NADP^+$ (mM), Panel B: G-6-PDH (U/ml), and Panel C: HK (U/ml). Data-points with error bars represent means of n = 3-to-5 ±1 standard deviation. In all other cases data-points represent means of n = 2, except in Panel B where n = 1 for the 0.5, 2.0, and 50 U/ml data-points.

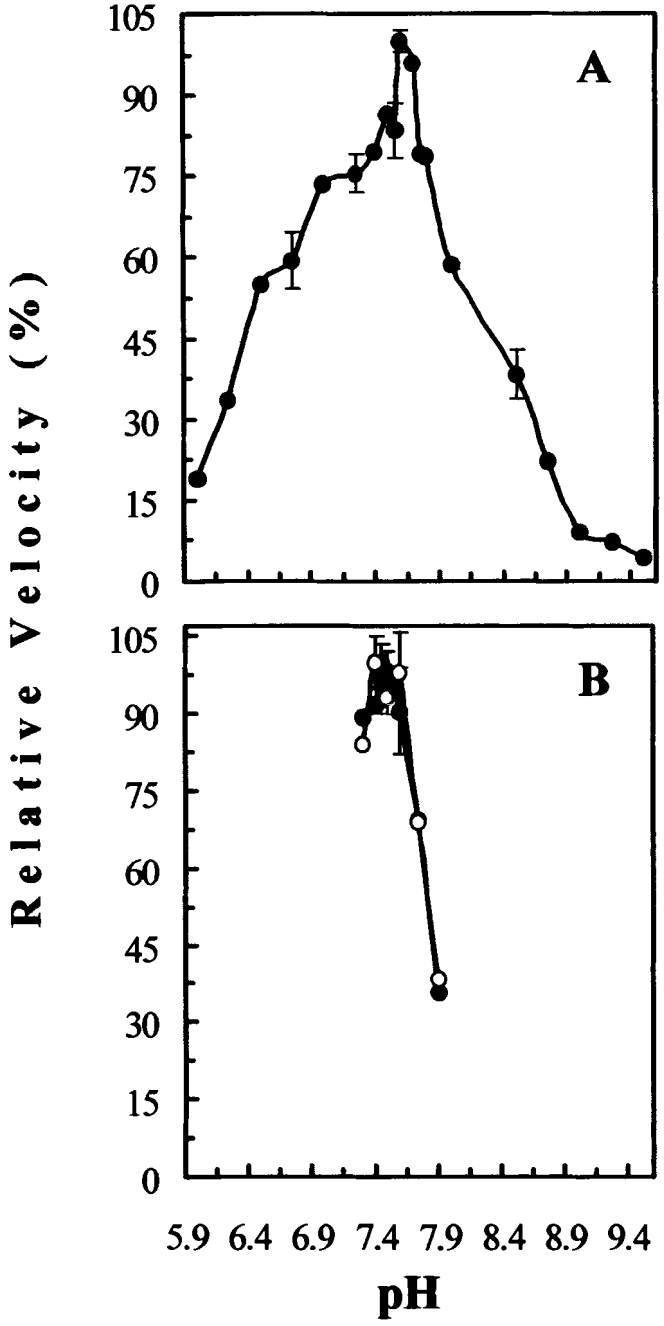

Figure 2. pH optimum for MMCKs from *C. aceratus* white muscle. Plots are of pH versus percent of maximum velocity. Panel A: Cibracon 3GA blue affinity column eluant. Panel B: DEAE Sepharose CL-6B anion exchange column eluants (CK-1 open symbols, CK-2 closed symbols). In Panel A data-points with error bars represent means of n = 3 or 4 ±1 S.D. all other data-points represent means of n = 2, except for those for pH 7.40, 7.50, 7.70, and 9.50 where n = 1. In Panel B all data-points with error bars represent means of n = 3 ±1 S.D. while all others are means of n = 2.

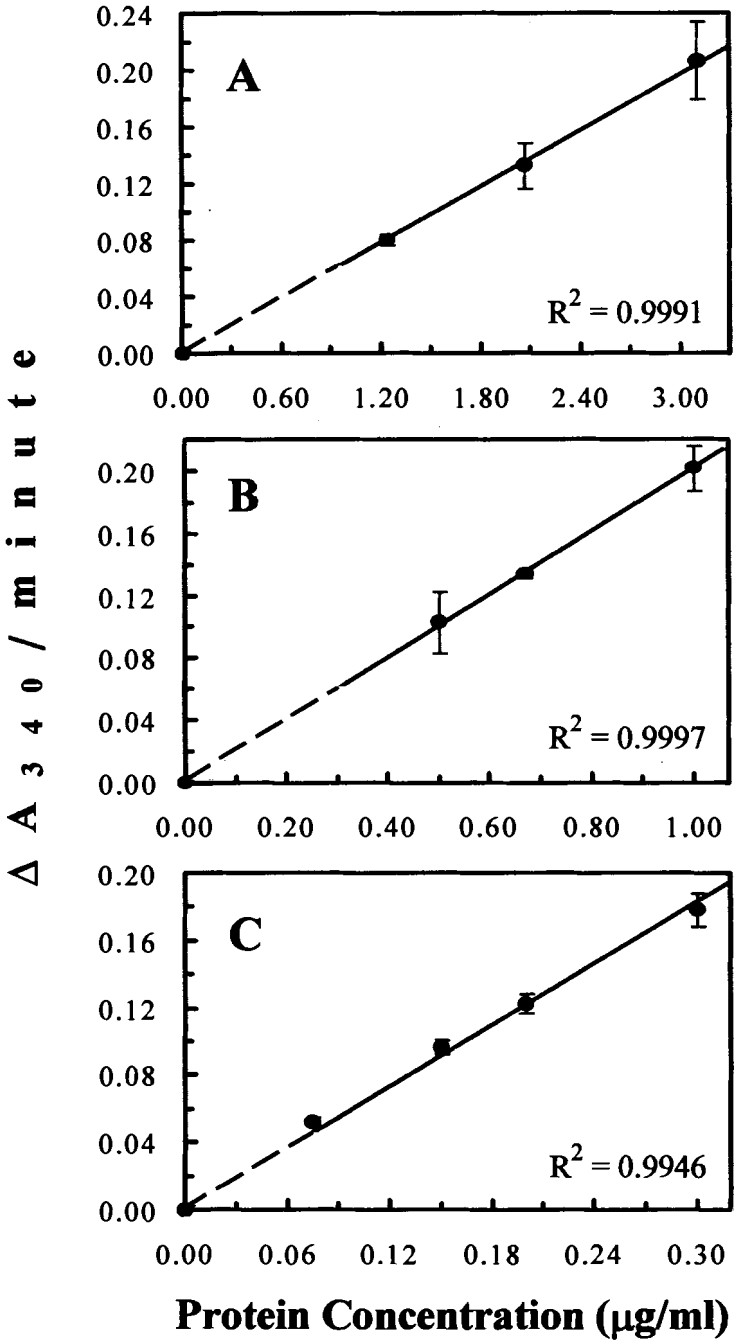

Figure 3. Determination of the range of protein concentrations that result in directly proportional rates for *C. aceratus* MMCK at 0° C. Plots are of protein concentration (μg/ml) versus rate (ΔA_{340}/min) for samples of homogenate (Panel A), samples of supernatant (Panel B), and samples of Cibracon 3GA blue affinity column eluant (Panel C). All data-points represent means of n = 3 ± 1 S.D. Lines were fitted by linear regression analysis and coefficients of determination (R^2) indicate the goodness of fit. The dotted portion of these lines indicates the theoretical extension of ΔA_{340}/min to zero protein concentration.

Chapter 3

PURIFICATION AND CHARACTERIZATION OF MMCK FROM *C. ACERATUS* WHITE MUSCLE

3.1. Purification of MMCK from *C. aceratus* white muscle.

3.1.1. Cibacron 3GA blue dye agarose affinity chromatography.

A difficulty in isolating some proteins from fish tissue is their inherent instability. For example, fish myosins readily undergo aggregation upon isolation (Sidell and Moreland, 1989). Isolation of enzymes from Antarctic fish tissue is also problematic (Low and Somero, 1976). The instability of MMCK isolated from *Torpedo marmorata* electric organ has been reported (Barrantes *et al.*, 1985). Barrantes *et al.* (1985) noted that recovery of torpedo MMCK's activity was enhanced after dialysis against 50% glycerol. This is consistent with glycerol's known ability to stabilize protein structure (Rabekas and Massey, 1996). This stabilization is brought about by enhancing protein hydration and minimizing unfolding tendencies by 'squeezing' proteins into tighter conformations with smaller volumes (Gekko and Timasheff, 1981; Timasheff, 1992). Glycerol also minimizes the adsorption of protein onto glass surfaces (Suelter and DeLuca, 1983). Therefore, the final formulations of buffer solutions used in this research included 30% glycerol. Fisher and Whitt (1979) noted that Cibacron 3GA blue dye matrix could be used as an affinity matrix that efficiently and selectively binds CK. Several other groups have reported the use of this matrix for the purification of CK (Miller *et al.*, 1982; Mickelson *et al.*, 1985; Quest *et al.*, 1989; and Appukuttan and Basu, 1992). The blue dye of this matrix selectively binds kinases because its ring structure

mimics an adenine nucleotide (Bohme *et al.*, 1972; Beissner and Rudolph, 1978a & 1978b; Biellmann *et al.*, 1979; and Amicon, 1980). In addition, the dye's sulfate anion may mimic the phosphate anion of ADP and coordinate Mg^{2+} in a manner analogous to CK's binding of $MgADP^-$ (Appukuttan and Basu, 1992). This method avoids several manipulations that might result in loss of CK's enzymatic activity (Fisher and Whitt, 1979; Barrantes *et al.*, 1985). For example, use of an ammonium sulfate precipitation step caused a total loss of CK's activity during its preparation from cod white muscle (Petrova et al., 1987) and 80% loss during its isolation from *T. marmorata* electric organ (Barrantes *et al.*, 1985). Thus, Cibacron 3GA blue dye agarose (referred to here as the affinity column) was adopted for the first step in the purification of CK from *C. aceratus* white muscle. Figure 4A shows a plot of UV absorbance versus fraction number and the corresponding enzyme activity profile for an affinity column preparation of CK. Four of these types of plots were obtained and all were qualitatively identical. Our results indicate that *C. aceratus* CK's enzymatic activity (in this example, fractions 61-to-75) always coincided with a single protein peak and that the CK peak was well separated from the unbound protein peak (in this example, Fractions 6-to-30). *C. aceratus* MMCK did not efficiently bind the affinity column unless creatine and Mg^{2+} were included in the binding buffer solution. The importance of Mg^{2+} role in CK's binding to this matrix is known (Appukuttan and Basu, 1992). However, no report has indicated that addition of creatine is necessary. Perhaps creatine stabilizes the binding CK from *C. aceratus* to the matrix by participating in an enzyme-substrate complex at the dye's adenine-moiety. Similar to Fisher and Whitt's (1979) introductory note, we also found that concentration of preparations of *C. aceratus* CK led to precipitation of protein and no protein

concentration was done. Overall the affinity method is simple and consistently provided a highly active preparation of CK from *C. aceratus* white muscle in a single step.

3.1.2. DEAE Sepharose CL-6B anion exchange chromatography.

Denaturing sodium dodecylsulfate polyacrylamide gel electrophoretic (SDS-PAGE) analysis indicated that affinity column purified CK contained various amounts of other proteins (see below). Further purification was attempted using DEAE anion exchange column chromatography. A DEAE column elution profile of CK activity is shown in Figure 4B. This activity profile indicated that anion exchange chromatography resolved the affinity column eluant into two CKs, which differed in net negative charge (Fig. 4B). To achieve this resolution it was necessary to apply the elution gradient of 0-to-200 mM KCl as 4 narrow gradient steps. The first three of these are shown in Figure 4B, as indicated by the numbered arrowheads. No CK activity appeared during the fourth portion of the gradient, and thus, that part of the profile is not shown. Elution with a single linear gradient of either 0-to-60 mM or 0-to-100 mM or 0-to-200 mM KCl abolished resolution. Fractions 379-387 were pooled and designated CK-b (b denotes basic) while fractions 430-442 were pooled and designated CK-a (a denotes acidic) (Fig. 4B). Every fifth fraction of the elution was analyzed by SDS-PAGE. This analysis indicated that a single polypeptide with a molecular weight corresponding to that of monomer CK eluted only in fractions 362-to-455 (data not shown). These SDS-PAGE gels also clearly showed that two peak concentrations of protein were distributed between fractions 362-to-455.

Compared to affinity column eluants, CK-b and CK-a had very low specific activities of about 22 U/mg, which may have been caused by alkaline denaturation. In

the example shown in Figure 4B the pH of the loading and elution buffer solutions was pH 8.3. When pH 8.6 was used a UV profile identical to that shown in Figure 4B was obtained. In this case, SDS-PAGE analysis of every fifth fraction indicated that two CK peaks had again been resolved. However, elution and short periods of storage at pH 8.6 abolished CK activity. In experiments that used pH 7.6-to-7.8 during loading and elution, complete separation into two activity peaks was questionable. However, when pH 7.6-to-7.8 was used specific activities appeared to have been retained, and SDS-PAGE analysis indicated that complete separation of CK from the other protein contaminates had been achieved. One such preparation (apparent V_{max} = 93 U/mg) was used in experiments that provided an estimate of thermodynamic activation parameters (see below). Changing components of the buffer solution also affected resolution. For example, when the concentration of Tris base was increased from 2.5 mM-to-10 mM and Triton X-100 was lowered from 1.0 mM-to-0.1 mM, resolution was abolished and only a single protein peak was observed. Overall, these results indicate that further research is required if these two CKs are to be efficiently purified in active form. Possible alternative methods of purification include preparative native PAGE, isoelectric focusing, chromatofocusing, or expression of the cDNAs in an appropriate expression system.

3.1.3. SDS-PAGE and corresponding immunoblot analysis of the purification process.

Immunoblot analysis of proteins separated by SDS-PAGE provided strong evidence that the CK in affinity and DEAE eluants was the skeletal muscle isoenzyme. Figure 5 shows a 12.5% acrylamide gel after staining for protein (Panel A) and after development of an immunoblot (Panel B). Affinity column eluants contained a mixture

of polypeptides but the major component of these eluants appeared as a band that migrated at approximately 42.9 kDa (lane 3, Fig. 5A), as calculated from the molecular weight standards. This is the expected monomer molecular weight of CK. Various amounts of a 17.2 kDa polypeptide were observed in different affinity column eluants. It was not a major component of this preparation but was approximately 20-to-30% of some affinity column eluants. Small amounts of a 26 kDa polypeptide were sometimes observed in the affinity column eluants, as in this case (lane 3, Fig. 5A). High molecular weight polypeptides (4-to-5 ≥ 60 kDa) were also evident in the affinity column eluant (lane 3, Fig. 5A). Figure 5A shows that CK-b and CK-a (lanes 4 & 5) contained one major polypeptide component that migrated with the expected CK monomer molecular weight of approximately 43 kDa (Walliman *et al.*, 1992; Muhlebach *et al.*, 1994; Sun *et al.*, 1998). Small amounts of low molecular weight polypeptides (> 26 kDa) were visible in the CK-b preparation (lane 4) while CK-a (lane 5) contained minor amounts of high molecular weight polypeptides (> 66 kDa). Only small amounts (30-to-60 μg/ml) of CK-b and CK-a were obtained. Concentration of other DEAE CK preparations resulted in the formation of irreversible aggregates that migrated as high molecular weight contaminates. Therefore, it was not possible to load more than 0.5 μg of CK-b and CK-a onto SDS-PAGE gels. This was a limitation of the assessment of purity of CK-b and CK-a. Immunoblot analysis was used as direct evidence that the 42.9 kDa bands seen in lanes 3,4, and 5 of Figure 5A were the monomer polypeptide of the muscle isoform of CK. A western blot of an identical SDS-PAGE gel as shown in Figure 5A was probed with an antibody that was specific for the skeletal muscle isoform of CK (Biodesign's Product Specifications sheet). Development of this immunoblot showed that a single

band at 42.9 kDa was present at all stages of the purification process (Figure 5B). Strong support for the specificity of the anti-human MMCK antibody used in this analysis is the lack of non-specific binding to any one of the large mixture of polypeptides in homogenate (lane 1) and supernatant (lane 2) preparations (Fig. 5B). Therefore, Figure 5 provides strong evidence that the majority of the protein in affinity column eluants was the muscle isoform of CK (MMCK). Figure 5 also showed that further purification of *C. aceratus* MMCK was achieved using DEAE anion exchange chromatography.

3.1.4. Native gel activity stain analysis of purified enzyme.

Native acrylamide gel electrophoresis coupled to a CK specific activity stain was another method that was used to confirm the identity of CK in affinity and DEAE column eluants (CK-b and CK-a). The specificity of the stain is based on phosphocreatine, which is a substrate of CK and is not acted upon by any other enzyme (Sjovall, 1967; Anido *et al.*, 1974; Baba *et al.*, 1976). An advantage of using native acrylamide gels is that CK can be visualized directly in native form. Figure 6 shows an activity stain (Panel A) and a general protein stain (Panel B) of 12.5% native acrylamide gels. *C. aceratus* CK in the affinity column eluant shows a single band of activity in lane 4 of Figure 6A as do the DEAE column eluants (lane 6 & 8) and pure human MMCK in lane 2. Evidence that irreversible aggregation occurs during electrophoresis of CK-b and CK-a is seen as a fine band of activity staining near the top lane 6 and in the well of lane 8. In contrast, no activity was observed in lane 1 or 10, which contained alkaline phosphatase. It is very significant that only one major band of activity is seen in lanes 4, 6, and 8 of Figure 6A. If these preparations were contaminated with significant amounts of the brain isoform of CK (BBCK) and a muscle-brain heterodimer (BMCK) a second and third band of activity

would have been observed (Scholl and Eppenberger, 1972). The monomer polypeptide of BCK from *C. aceratus* is predicted as having a much larger net negative charge of –7 than that predicted for either MCK-b (–1.7) or MCK-a (–2.7) monomer (see Chp. 4). This is consistent with the net charge found for mammalian and bird MCK (–0.35-to-+0.5) versus BCK (–14-to- –6) polypeptide monomers (sequences extracted from GenBank). Protein staining of native acrylamide gels indicates that the affinity column eluant contains other proteins in addition to CK (lane 4, Fig. 6B). The majority of these contaminating bands migrate above the CK band (lane 4, Fig. 6B). Alkaline phosphatase is easily seen in lanes 1 and 6 of Figure 6B. Activity-stained gels swell during development and the activity patterns are somewhat diffuse (Fig. 6A). However, the ratio of human MMCK R_f values/*C. aceratus* affinity column CK R_f values are estimated to be 1.92 in the activity-stain gel and 1.91 in the Coomassie blue G-250 stained gel. Using MMCK specific antibody, immunoblots of native gels always showed bands that exactly coincided with those indicated by activity staining (data not shown). These latter experiments provided strong evidence that the activity staining does not represent another contaminating enzyme capable of producing a stain under these conditions. Overall, these results provide further evidence that MMCK is the isoform that has been isolated from *C. aceratus* white muscle.

These native acrylamide gels also allowed for a rough estimate of isoelectric point (pI) MMCKs from *C. aceratus* white muscle. Native alkaline phosphatase is a dimer that has a molecular weight of 94 kDa (Kim and Wyckoff, 1991), which is similar to MMCK's molecular weight of 85 kDa (Wallimann *et al.*, 1992). Therefore, these two proteins are of similar size. They are also of similar shape and are elongate globular

proteins. The long-axis/short-axis ratios are 1.63 and 1.61 for alkaline phosphatase and human MMCK respectively (Kim and Wyckoff, 1991; Shen *et al.*, 2001). Taken alone, one would predict from these characteristics that alkaline phosphatase and MMCK should have similar mobilities through the acrylamide matrix. This is a fair assumption because most size exclusion materials do not efficiently resolve proteins that are of very similar size and shape (data sheets available from Bio-Rad and Amersham). This means that any differences in their electrophoretic mobilities through native acrylamide gels should be due primarily to charge differences. Figure 6B shows that MMCKs *from C. aceratus* have higher net negative charge (lower pIs) than human MMCK (monomer pI ~7.0). However, *C. aceratus* MMCKs have lower net negative charge (higher pIs) than alkaline phosphatase (monomer pI of 5.49). This analysis indicates that *C. aceratus* MMCK monomers have apparent pIs between 5.5 and 7.0.

In summary, SDS-PAGE and native-PAGE experiments provide strong evidence that the muscle isoform of CK has been purified from *C. aceratus* white muscle.

3.1.5. Quantitative analysis of the purification process.

Quantitative analysis of the one-step affinity purification process is shown in Table 1. The specific activities of the homogenate and supernatant preparations shown in Table 1A were low when compared to those shown in Table 1B, 1C, & 1D. This was thought to be due to the presence of an inhibitor(s) that was removed during the purification process, as indicated by the specific activity of the affinity column preparation shown in Table 1A. The addition of EGTA along with an increase in β-mercaptoethanol concentration from 5-to-10 mM in the homogenization buffer solution appears to remove this anomaly, which is what the specific activities of homogenates and

supernatants of Table 1B-to-1D show. Specific activities increased from 3-to-12 U/(mg of protein) in muscle homogenates to 60-to-95 U/(mg of protein) in the affinity column eluant (Table 1A-1D). Hence, affinity chromatography resulted in a 5-to-8-fold purification of cytosolic MMCK from *C. aceratus* muscle homogenates and a yield of 50-to-65% (Table 1B-1D). This fold purification is similar to that previously reported during Cibacron 3GA affinity purification of CKs (Fisher and Whitt, 1979; Miller *et al.*, 1982; Quest *et al.*, 1989; Appukuttan and Basu, 1992). At the bottom of Table 1 it is seen that the total activity in *C. aceratus* white muscle homogenates was 615-to-640 U/g of frozen tissue. Accurate quantitative analysis of DEAE column eluants has not been obtained at this time. Estimation of yields indicates that CK-b and CK-a appear to be present in about equal amounts. In conclusion, affinity column chromatography consistently produced a stable preparation of MMCK with high activity from *C. aceratus* white muscle. Thus, affinity column preparations provided the source material for all further characterizations of *C. aceratus* MMCKs.

3.2. MMCKs from *C. aceratus* white muscle are thermally denatured at relatively low temperatures.

It has been established that MMCK from mammals undergoes conformational changes during substrate binding (Zhou *et al.*, 1993; Forstner *et al.*, 1997; Bai *et al.*, 1998; Lyubarev *et al.*, 1999; Cao *et al.*, 1999; Shen *et al.*, 2001). Relative to enzymes from warm-adapted vertebrates, enzymes from cold-adapted teleosts are thought to have tertiary and quaternary structures that are held in place by fewer H-bonds and ionic interactions (Hochachka and Somero, 1968; Somero, 1975; Hochachka and Somero,

1984; Sidell and Moreland, 1989). Thus, cold-adapted enzymes may have more flexible structures and it is thought that such increases in flexibility contribute to the enhanced activity that these enzymes exhibit at cold-temperature (Hochachka and Somero, 1968; Somero, 1975; Hochachka and Somero, 1984; Sidell and Moreland, 1989; Somero, 1995; Fields and Somero, 1998; Ciardiello *et al.*, 2000; Lonhienne *et al.*, 2000). It is also thought that such changes in protein structure result in increased susceptibility to thermal denaturation. Figure 7 shows a temperature versus percent activity remaining profile for muscle CK from *C. aceratus*. Figure 7 shows that the mean activity of *C. aceratus* MMCKs decreased to 50% of the maximum value after a 30 minute incubation at 25° C and *C. aceratus* MMCK was completely inactivated after 30 minutes at 30° C. Contrary to this, cod, nurse shark, mammalian, and bird MMCKs undergo complete thermal denaturation at temperatures in excess of 50° C (Dawson *et al.*, 1967; Grossman and Mollo, 1979; Gray *et al.*, 1986; Petrova *et al.*, 1988). These results provide indirect evidence that *C. aceratus* MMCKs apparently have a more flexible structure then homologous MMCKs from temperate fish and warm-bodied vertebrates, that is, *C. aceratus* MMCK is thermally denatured at relatively low temperatures of 20°-to-30° C. Therefore, *C. aceratus* MMCK's appear to remain in native form only at cold temperatures.

3.3. *C. aceratus* MMCK exhibits temperature compensation.

Cold-temperature adaptation is often evaluated by comparing the presumed cold-adapted enzyme's specific activity (V_{max}/mg) at cold temperature to the activity of its warm-adapted counterpart at the same temperature (Hochachka and Somero, 1984;

Somero, 1995; Fields and Somero, 1998). Therefore, the specific activities of *C. aceratus*, rabbit, and teleost MMCKs were compared, to determine whether *C. aceratus* MMCKs exhibit temperature compensation. The top section of Table 2 shows specific activities for rabbit and *C. aceratus* MMCKs, which were determined in our laboratory. The bottom section of Table 2 shows specific activities for sunfish (Fisher and Whitt, 1979), cod (Petrova *et al.*, 1987), and carp (Sun *et al.*, 1998) MMCKs. It is evident that rabbit MMCK is unable to function efficiently at cold temperature. At 0.5° C and 10° C rabbit MMCK has specific activities of only 10 and 45 U/mg respectively. Contrary to this, at 0.5° and 10° C *C. aceratus* MMCKs exhibit specific activities of 95 and 180 U/mg respectively. Table 2 also indicates that muscle CKs from *C. aceratus* have activities equal-to or greater-than the activity of muscle CK from teleosts that inhabit warmer environments. At 5° C and 15° C cod MMCK has activities similar to *C. aceratus* MMCKs. However, at 10° C–to-30° C carp MMCK's are only 10%-to-50% as active while at 25° C sunfish is only 60% as active as *C. aceratus* MMCKs. Moreover, affinity column preparations of *C. aceratus* MMCKs contain other proteins and thus, the mean specific activities for *C. aceratus* MMCKs are under estimates. These results show that at 0.5° C *C. aceratus* MMCKs are capable of producing ATP at ten times the rate of rabbit MMCK. Similary, *C. aceratus* MMCKs are as efficient or more efficient at producing ATP than other teleost MMCKs. These specific activity comparisons provide strong evidence that one or both *C. aceratus* MMCKs have undergone temperature compensation.

3.3.1. Estimation of thermodynamic activation parameters.

Cold-adaptated enzymes exhibit lower activation enthalpies ($\Delta H^{\ddagger}$) than their warm-adapted counterparts (Hochachka and Somero, 1984; Ciardiello *et al.*, 2000; Lonhienne *et al.*, 2000). Activation enthalpies can be evaluated once activation energies (Ea) have been obtained from an Arrhenius plot. A linear form of the Arrhenius equation ($V_{max} = Ae^{(-Ea/RT)}$) is obtained by taking the natural log of both sides of the equation. The result is $\ln V_{max} = -Ea/RT + \ln A$, where R is the gas constant and A is a constant (Eisenberg and Crothers, 1979). Over a narrow temperature range, a plot of $\ln V_{max}$ versus 1/T (K^{-1}) results in a straight line with a slope of –Ea/R. Figure 8 shows Arrhenius plots for *C. aceratus* and rabbit MMCK. The linear regressions of these plots have excellent coefficients of determination (R^2; Havilcek and Crain, 1988), which are greater-than 0.99. The slope of these lines gives the Eas for *C. aceratus* and rabbit MMCK of 10,870 cal/mol and 18,235 cal/mol respectively. Table 3 lists the thermodynamic activation parameters for *C. aceratus* and rabbit MMCK and the equations used to calculate them (Low and Somero, 1976). Table 3 indicates that *C. aceratus* MMCK has an *estimated* activation enthalpy ($\Delta H^{\ddagger}$) that is about 7000 cal/mol lower than rabbit MMCK's $\Delta H^{\ddagger}$. On the other hand, *C. aceratus* MMCK has an unfavorable activation entropy ($\Delta S^{\ddagger}$) of –11 cal/mol/K while the $\Delta S^{\ddagger}$ for rabbit MMCK of 12 cal/mol/K is favorable (Table 3). Table 3 shows that $\Delta G^{\ddagger}$ for *C. aceratus* MMCK is 1000 cal/mol lower than $\Delta G^{\ddagger}$ for rabbit MMCK. Similar changes in these parameters have been reported for other homologous enzyme comparisons (Hochachka and Somero,

1984; Somero, 1995; Fields and Somero, 1998; Ciardiello *et al.*, 2000; Lonhienne *et al.*, 2000). These results help to explain *C. aceratus* MMCK's temperature compensation, which largely mediated by a lowering of the reactions $\Delta H^{\ddagger}$.

3.3.2. Estimates of average apparent K_ms of ADP and phosphocreatine.

An enzyme's affinity for its substrate(s) determines its level of activity at constant and fluctuating substrate concentrations (Hochachka and Somero, 1984; Somero, 1995; Fields and Somero, 1998). The apparent Michaelis-Menton constant(s) (K_m(s)) reflects the appropriate substrate concentrations that satisfy an enzyme's rate and regulatory requirements (Hochachka and Somero, 1984; Fields and Somero, 1998). Furthermore, the ratio of k_{cat}/K_m gives an estimate of activity at physiological substrate concentrations (Somero, 1995). Thus, it was important to obtain an estimate of the average apparent K_ms of ADP and PCr for *C. aceratus* MMCKs. Figure 9 shows Hanes plots (Hammes, 1982; Cornish-Bowden, 1995) used to estimate these apparent K_ms, obtained from initial velocity versus substrate concentration data. The equation for these lines is $[S]/v_o = [S]/V_{max} + K_m/V_{max}$, where v_o is the initial velocity and [S] is the substrate concentration. It is seen that the slope of these lines is $1/V_{max}$ and the y-intercept is V_{max}/K_m. Linear regression fitting of these data resulted in excellent coefficients of determination, which in both cases is 0.993. From these plots an estimate of the average apparent K_m of ADP is 0.06 mM and for PCr is 17 mM for *C. aceratus* MMCKs at 0° C. Table 4 shows a comparison of apparent K_ms for *C. aceratus* MMCKs with those reported for other teleosts, chicken, and mammals. Table 4 indicates that when appropriate body

temperatures are taken into account these K_ms are similar, which is consistent to what has been found for other cold- and warm-adapted enzyme comparisons (Hochachka and Somero, 1984; Somero, 1995; Fields and Somero, 1998). This is exemplified by the range K_m values reported from different laboratories for rabbit MMCK, all of which fall within the overall range of K_m values. Table 4 shows that K_ms for ADP are between 0.04 and 0.75 mM while K_ms for PCr are between 0.7 and 23 mM. Therefore, *C. aceratus* MMCKs operate with K_ms that are within the known range of MMCK K_ms.

3.4. Unlike rabbit MMCK, muscle CK from *C. aceratus* has a pH optimum similar to the pH of its resting white muscle.

At 0°-to-1° C the resting intracellular pH (pH_i) of Antarctic teleost white muscle is pH_i 7.40-to-7.45 (Moerland and Eggington, 1998; van Dijk *et al.*, 1999). It has been shown that the white muscle of several Notothenioids exhibit a relatively low glycolytic capacity (Walesby and Johnston, 1979; Dunn and Johnston, 1986; Johnston, 1987; Dunn *et al.*, 1989; Sidell and Crockett, 1989; Crockett and Sidell, 1990). Because of this, during burst swimming the amount of lactic acid accumulated in the white muscle of these fishes is relatively low (Dunn and Johnston, 1986; Johnston, 1989). Thus, it is unlikely that *C. aceratus* white muscle is subjected to extreme acidosis (Egginton, 1997). In contrast, in mammals and eurythermal teleosts the second phase of a burst response relies primarily on glycolysis for ATP, which results in a rapid increase in intracellular lactic acid (Dobson *et al.*, 1987; Dobson and Hochacka, 1987; Parkhouse *et al.*, 1988; Arthur *et al.*, 1991). Accordingly, the resting intracellular pH 7.10 of mammalian

skeletal muscle after exercise can decrease to pH 6.50-to-pH 6.20 (Adams *et al.*, 1991; Pate *et al.*, 1995). These differences between the resting pH_i and post-exercise pH_i of mammalian and *C. aceratus* skeletal muscle indicate that the pH optimum of mammal MMCK and *C. aceratus* MMCK might differ. A comparison between the pH optimum of MMCK from *C. aceratus* and rabbit MMCK was undertaken, to deterimine if this is the case. Egginton (1997) noted that such comparisons have often been overlooked and enzyme activities measurements on enzymes prepared from ectothermic organisms have often been carried out at inappropriate pHs because the selected pHs at which the measurements were made were based on mammalian data. Figure 10 shows that at 30° C rabbit MMCK has a pH optimum of pH 6.00-to-6.30, which at 38° C was between pH 6.20-to-6.50 (data not show). Contrary to this, Figure 10 indicates that at 0.5° C the pH optimum of *C. aceratus* MMCK is pH 7.50-to-7.65. These rabbit results are in excellent agreement with the previously reported optimum pH evaluations for rabbit MMCK at 30° C (Kuby *et al.*, 1954; Nihei *et al.*, 1961). These results indicate that rabbit MMCK's pH optimum is about 0.6-to-1.0 pH unit below resting muscle pH while *C. aceratus* MMCK has a pH optimum similar to resting muscle pH.

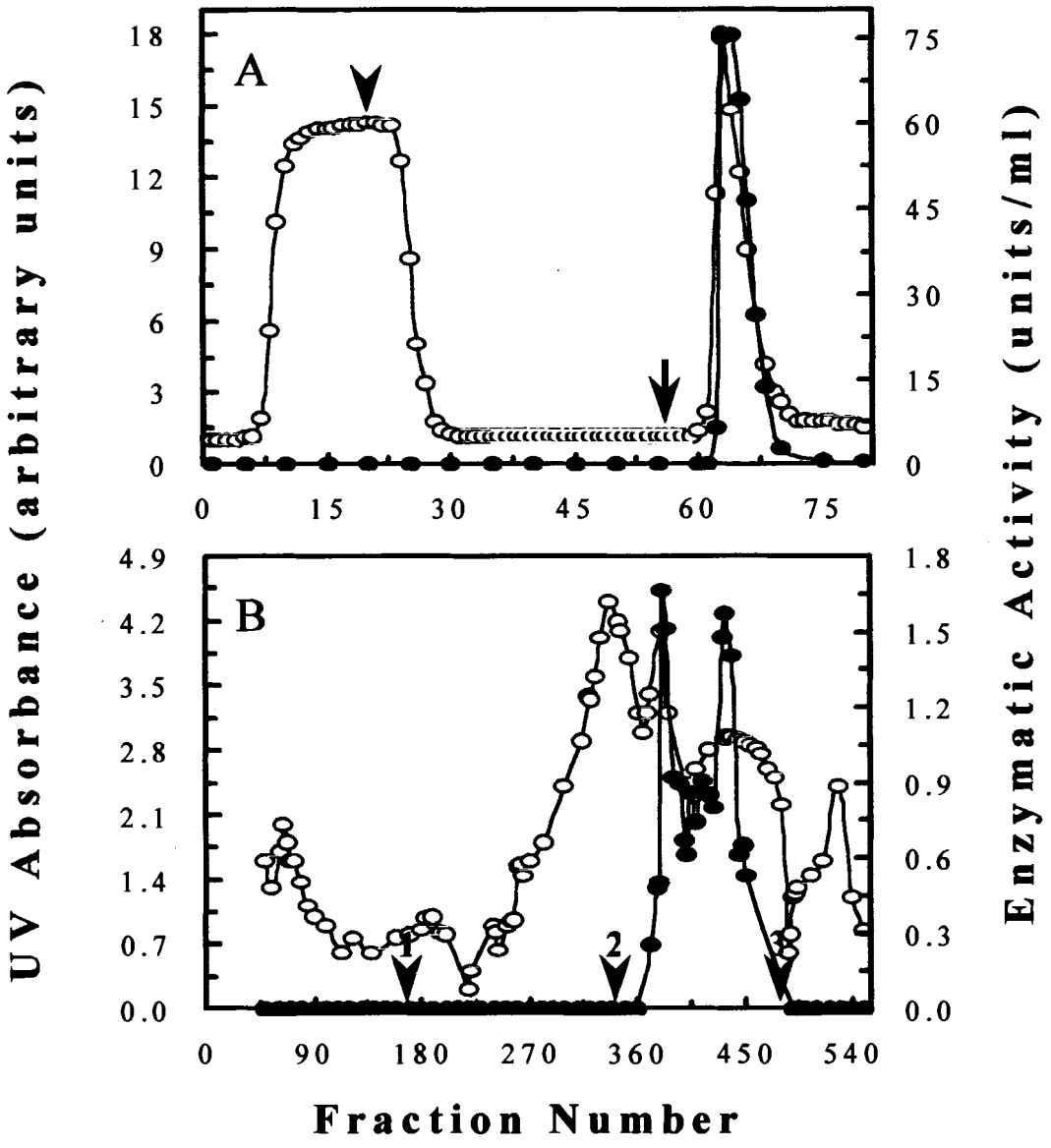

Figure 4. MMCK purification from *C. aceratus* white muscle. Plots are of fraction number versus UV absorbance (left ordinate, open symbols) and enzymatic activity (right ordinate, closed symbols). Panel A: Affinity column purification step. The arrowhead at fraction 19 indicates when wash buffer solution was applied to the column. The arrow at fraction 56 indicates when elution buffer solution was applied to the column. Data-points representing enzyme activity are means of duplicate determinations. Panel B: DEAE column purification step. The numbered arrowheads (1-3) near the abscissa indicate where the linear gradient of KCl was applied to the column. At arrowhead 1 (fraction 162) the gradient was 0-to-30 mM KCl, at arrowhead 2 (fraction 337) it was 30-to-65 mM KCl, and at arrowhead 3 (fraction 481) it was 65-to-100 mM KCl. An explanation of the use of these narrow KCl gradients is given in the text. Each data-point representing enzyme activity was obtained from a single activity measurement.

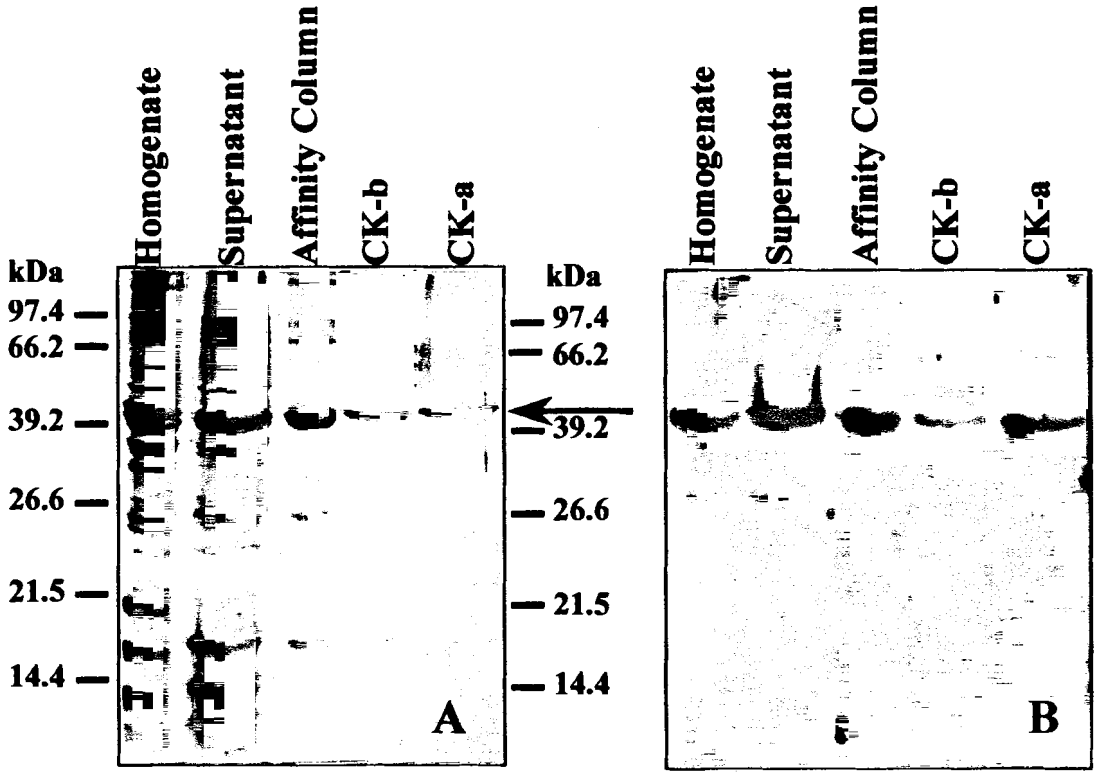

Figure 5. Denaturing PAGE and immunblot evaluation of the purification of MMCKs from *C. aceratus* white muscle. Panel A: A denaturing SDS-PAGE gel where protein bands were visualized with Coomassie blue G-250 staining. Molecular weight markers at either side of the panel are given in kilodaltons (kDa). The lane designed affinity column shows the polypeptide composition of the CK enriched preparation obtained from Cibracon 3GA blue affinity column chromatography. The lanes designated CK-b, and CK-a show the polypeptide composition from the DEAE column eluant (CK-b: fractions 379-387 and CK-a: fractions 430-442, see Fig. 4). The arrow at the right of the panel indicates CK's position in the gel. Panel B: The corresponding immunoblot of the gel shown in Panel A. The blot was probed with a goat antihuman MMCK antibody, which was detected with a horseradish peroxidase conjugated rabbit antigoat antibody and a chemiluminescence substrate. Fifteen micrograms of homogenate and supernatant, 2.0 μg of affinity column eluant, and 0.5 μg of CK-b, and CK-a were loaded onto these gel.

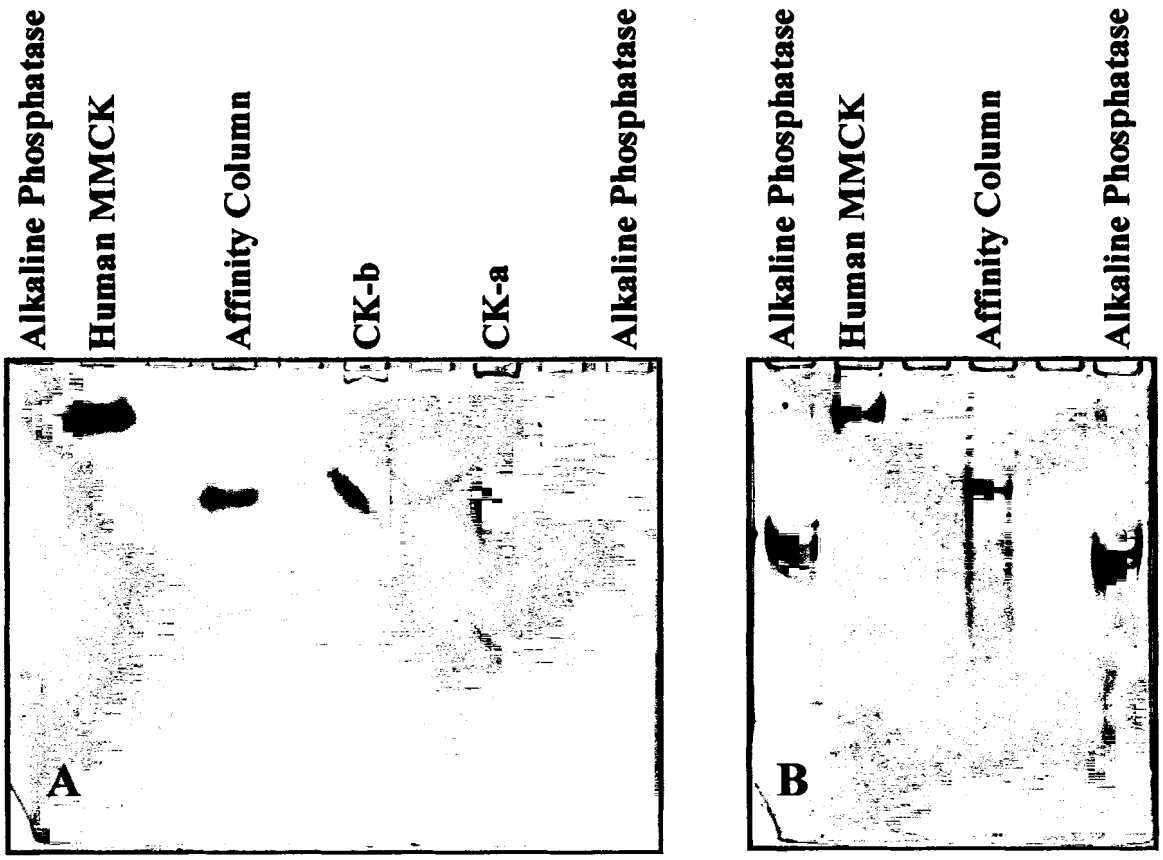

Figure 6. Native PAGE of MMCKs purified from *C. aceratus* white muscle. Panel A: Activity-stained gel where color development is based on the use of PCr, which is a specific substrate for CK. Panel B: Coomassie blue G-250 stained gel. Lanes designated affinity column were loaded with the CK enriched preparation obtained from Cibracon 3GA blue affinity column chromatography (see Fig. 4). Lanes designated CK-b and CK-a were loaded with CKs obtained from DEAE Sepharose CL-6B anion exchange chromatography (CK-b: fractions 379-387 and CK-a: fractions 430-442, see Fig. 4). In all cases 1 μg of total protein was loaded per lane. In lanes CK-b and CK-a the fine band of activity seen just below or in the well is evidence that irreversible aggregation occurs when these preparations are concentrated during electrophoresis. Activity-stained gels swell during development and the activity patterns are diffuse. However, the ratio of human MMCK R_f values/*C. aceratus* affinity column CK R_f values were estimated to be 1.92 in the activity-stained gel and 1.91 in the Coomassie blue G-250 stained gel.

Table 1. Purification of MMCK from *C. aceratus* white muscle.

A. Individual-1 Trial-1[a]

	Total ml	Activity (U[b]/ml)	Specific Activity (U/mg of protein)	Total[c] Units	Yield (%)	Fold Purification
Hom.[d]	37.0	18.2 ± 1.2[g] (4)[h]	3.3 ± 0.2 (4)	672 ± 44	100	1.0
Sup.[e]	33.5	20.7 ± 2.3 (3)	13.4 ± 1.5 (3)	694 ± 76	103	4.1
B.A.C.[f]	12.5	91.8 ± 2.9 (4)	76.5 ± 2.4 (4)	1148 ± 35	171	23.2

B. Individual-1 Trial-2

Hom.	33.0	37.7 ± 3.5 (9)	12.2 ● 1.2 (9)	1244 ● 122	100	1.0
Sup.	30.0	32.5 ± 3.4 (8)	29.5 ± 3.1 (8)	974 ± 102	78.3	2.4
B.A.C.	29.3	30.1 ± 1.3 (9)	94.1 ± 4.1 (9)	809 ± 35	65.0	7.7

C. Individual-2 Trial-3

Hom.	20.0	31.0 ± 1.3 (3)	12.2 ± 0.5 (3)	620 ± 25	100	1.0
Sup.	18.5	21.5 ± 3.0 (6)	19.9 ± 2.8 (6)	398 ± 56	74	1.6
B.A.C.	7.0	36.9 ● 3.0 (3)	59.6 ± 4.8 (3)	258 ± 21	48	4.9

D. Individual-2 Trial-4

Hom.	15.0	41.0 ± 1.7 (3)	8.9 ± 2.0 (3)	615 ± 26	100	1.0
Sup.	13.2	44.1 ± 4.1 (3)	27.7 ± 2.8 (3)	581 ± 58	94	3.1
B.A.C.	6.0	51.8 ± 3.8 (3)	74.2 ± 5.0 (3)	311 ± 21	51	8.3

[a] Muscle samples came from two individuals: Individual-1 and Individual-2. Four separate purifications were carried out: Trials-1 and -2 for Individual-1 and Trials-3 and -4 for Individual 2. [b] U = units = μmole ATP/min; [c] Total units were calculated from specific activities and the protein concentrations of the various samples. [d] Hom. denotes homogenate preparations; [e] Sup. denotes supernatant preparations; [f] B.A.C. denotes Cibracon 3GA blue affinity column eluants. [g] values are means ± 1 standard deviation; [h] number of trials.

Total units/g of frozen tissue were for Trial-1: 300 U/g, for Trial-2: 640 U/g, for Trial-3: 620 U/g. and for Trial-4: 615 U/g.

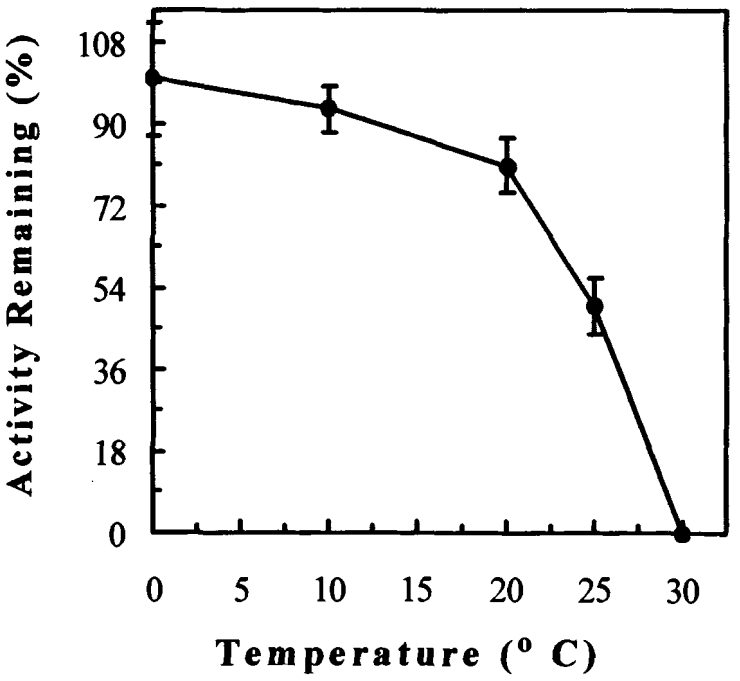

Figure 7. Thermal stability of MMCK from *C. aceratus* white muscle. Plot of temperature versus percent of activity remaining. Samples were incubated for 30 min at the indicated temperatures and then placed on ice prior to activity measurements. Data-points are means of n = 4 (0° C), n = 3 (10° C & 25° C), and n = 5 (20° C & 30° C) determinations ± 1 S.D.

Table 2. MMCK's specific activity (U[a]/mg) as a function of temperature.

		Temperature (°C)							
		0	**5**	**7.5**	**10**	**20**	**25**	**30**	**38**
C. aceratus[b]		94 ± 4[c] (9)[d]	120 ± 3 (3)	151 ± 2 (3)	182 ± 9 (3)	—	—	—	—
Rabbit[b]		11 ± 0.9 (4)	—	—	45 ± 2 (3)	139 ± 14 (5)	—	465 ± 29 (3)	568 ± 8 (3)
Sunfish[e] (*Lepomis cyanellus*)		—	—	—	—	—	60	—	—
Cod[f] (*Gadus morhua*)		—	80 (6)	—	155 (6)	198 (6)	—	315 (6)	252 (6)
Carp[g]	1[h]	—	—	—	12	36	—	53	64
(*Cyprinus carpio*)	2	—	—	—	18	42	—	54	63
	3	—	—	—	6	19	—	19	9

[a] U denotes units = μmol ATP/min, [c] ±1 standard deviation, and [d] number trials.

Data from: [b] this research, [e] Fisher and Whitt (1979), [f] Petrova *et al.* (1987), [g] Sun *et al.* (1998), and [h] 1, 2, & 3 designate the three isoforms

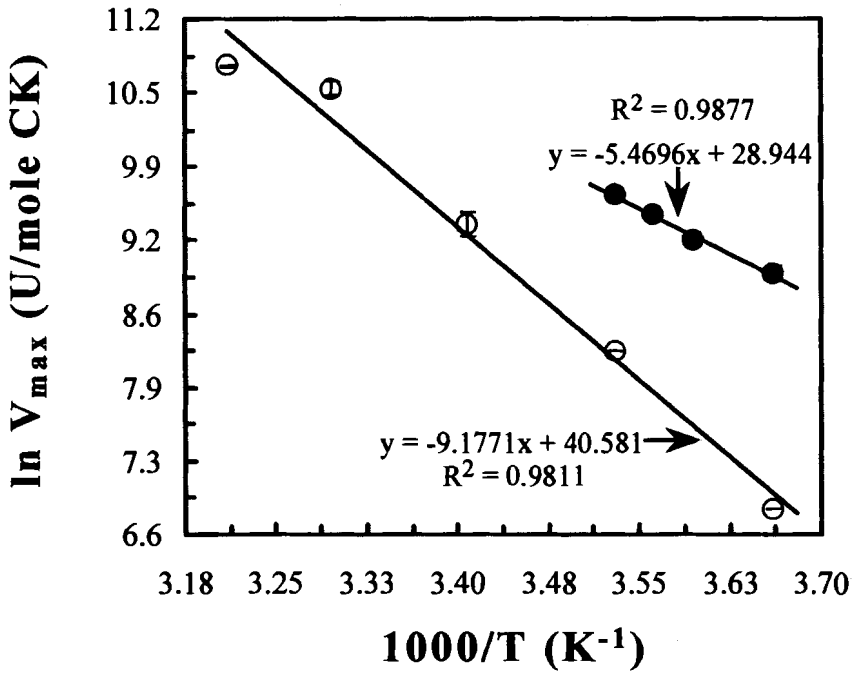

Figure 8. Arrhenius plots for MMCK's reverse reaction. Plots are of the inverse of absolute temperature (x1000) versus the natural log of apparent V_{max} (U = mole ATP/min). Rabbit MMCK data-points (open symbols) represent means of n = 3 (0°, 20°, and 30° C), n = 4 (at 38° C), and n = 5 (10° C) ±1 S.D. *C. aceratus* MMCK data-points (solid symbols) represent means of n = 3 ±1 S.D. Lines were fitted by linear regression analysis and the goodness of fit evaluated by the square of the correlation coefficient (r), which gives the coefficient of determination (R^2). Each linear equation is linked to its line by an arrow. The slopes of these lines are –5470 for the *C. aceratus* MMCK data and –9177 for the rabbit MMCK data. These slopes are equal to $-E_a/R$, where R is the universal gas constant and Ea is the activation energy of the reaction. (Low and Somero, 1976; Longienne *et al.*, 2000).

Table 3. Thermodynamic activation parameters of MMCKs calculated at 0° C

MMCK	Ea[a] (cal/mol)	$\Delta H^{\ddagger}$[b] (cal/mol)	$\Delta S^{\ddagger}$[c] (cal/mol/K)	$\Delta G^{\ddagger}$[d] (cal/mol)
C. aceratus	10,870	10,330	-11	13,300
Rabbit	18,235	17,690	12	14,450

[a] Calculated from the slope of the Arrhenius plot (see Fig. 8).

[b] $\Delta H^{\ddagger} = Ea - RT$; where T is absolute temperature.

[c] $\Delta S^{\ddagger} = (\Delta H^{\ddagger} - \Delta G^{\ddagger})/T$.

[d] $\Delta G^{\ddagger} = 4.756\ T\ (10.3188 - \log(K/T))$ where

$K = V_{max} \times 1.4167$ and V_{max}s were from 0° C measurements.

The use of these equations was described by Low and Someo, 1976 and Lonhienne *et al.*, 2000.

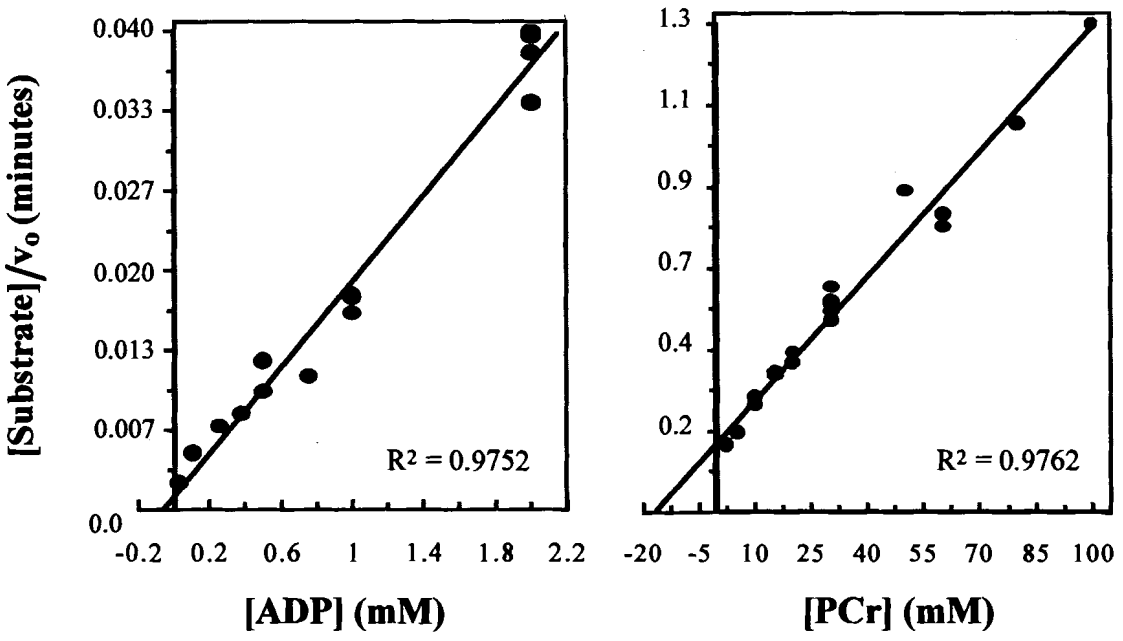

Figure 9. Determination of K_ms of ADP and PCr for *C. aceratus* MMCK at 0° C. Hanes plots of substrate concentration ([ADP] or [PCr]) versus substrate concentration ([substrate]) divided-by initial velocity (v_o) are shown. Lines were fitted by linear regression analysis with the goodness of fit evaluated by the square of the correlation coefficient (r), which gives the coefficient of determination (R^2). The reciprocal of the slopes of these lines gives V_{max} and the y-intercept divided by V_{max} gives K_m. From these plots the estimated K_ms are 0.06 mM for ADP and 17 mM for PCr. These values are averages for the two MMCKs in the affinity eluant, which was the enzyme preparation used in these experiments.

Table 4. Comparison of kinetic constants (K_ms and V_{max}s) for MMCK's reverse reaction*.

MMCK	MgADP (mM)	PCr (mM)	V_{max}[a] (U^b/mg)
C. aceratus[c]	**0.06**	**17**	**130**
Cod[d]	0.75	15	80
Carp-1[e]	—	1.4	45 - 103
Carp-2[e]	—	0.8	54 - 103
Carp-3[e]	—	3	21 - 71
Chicken[f]	0.5	4.8	—
Rabbit[d]	0.6	3.9	—
Rabbit[g]	0.18	0.8	1400
Rabbit[h]	0.05	2.9	—
Ox[h]	0.09	23	—
Monkey[i]	0.04	3.5	—
Human[j]	0.05	0.7	304

* Measurements for *C. aceratus* were at 0.5° ± 0.5° C for cod 5° C, for carp 25° C, and for birds and mammals at 30° C. [a] at saturating substrate concentrations; [b] μmol ATP/min; [c] this research; [d] Petrova *et al.*, 1988; [e] Sun *et al.*, 1998; [f] Eppenberger *et al.*, 1967; [g] Nihei *et al.*, 1961; [h] Watts, 1973; [i] Chegwidden and Watts, 1975; [j] Cantwell et al., 2001.

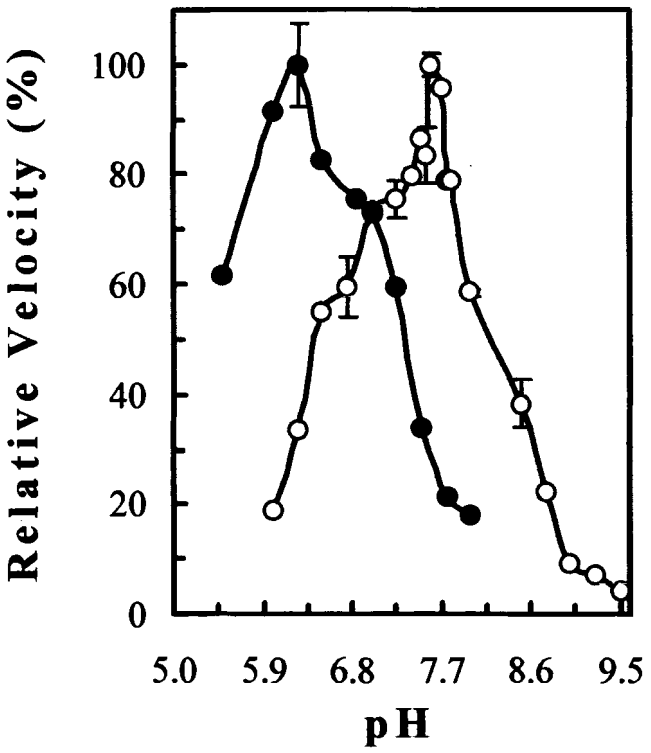

Figure 10. pH optimum of the reverse reaction of MMCKs. Plots are of pH versus percent of maximum velocity. pH profiles for *C. aceratus* MMCK at 0° C (open symbols) and rabbit MMCK at 30° C (closed symbols) are shown. *C. aceratus* MMCK data-points with error bars represent means of n = 3 or 4 ± 1 S.D. or represent means of n = 2, except for pH 7.40, 7.50, 7.70, and 9.50 where n = 1. Rabbit MMCK data-points represent n = 1, except for pH 6.25 where n = 3 ± 1 S.D.

Chapter 4

CK cDNA SEQUENCES FROM *C. ACERATUS*: TISSUE EXPRESSION OF mRNA AND DEDUCED AMINO ACID SEQUENCES

As described above, DEAE purification revealed that CK activity in affinity column eluants was the average of two CK activities (CK-b and CK-a). Denaturing and native gel electrophoresis provided strong evidence that these activities are due solely to muscle isoforms of CK. cDNA cloning and sequencing verified that two different gene products that encode two distinct muscle isoform monomers of CK were present in *C. aceratus* white muscle. The cDNAs and protein monomeric subunits that they encode have been designated MCK-b and MCK-a, which means that the protein homodimers are designed MMCK-b and MMCK-a.

4.1. *C. aceratus* white muscle expresses two distinct muscle isoforms of CK mRNA: MCK-b and MCK-a.

mRNA purified from white muscle provided the starting material for the preparation of white muscle specific double-stranded cDNAs (ds-cDNA). Short adaptors of known sequence were ligated to the 5′- and 3′-ends of these ds-cDNAs. This provided the means for cloning and subsequently sequencing the cDNA's 5′ and 3′ untranslated regions (UTR) with RACE (rapid amplification of cDNA ends). These ds-cDNA preparations were screened for CK cDNA using the polymerase chain reaction (PCR). Initially, degenerate PCR primers were used. Amino acid sequence alignment of homologous CKs (Muhlebach *et al.*, 1994) was the basis of degenerate primer design, which was based on conserved regions of the MCK sequences.

4.1.1. Sequencing of full-length MCK-b.

At the top of Figure 11 is a schematic representation of the full-length cDNA sequence of MCK-b where the 5′, 3′ UTRs, and open reading frame (ORF) are depicted. Below this are representations of PCR products (1-13) with primer names at each end. PCR primer sequences are given in Table 5. The numbered PCR products illustrate the sequencing strategy used to establish and confirm MCK-b's full-length cDNA sequence. PCR product 1 was obtained with degenerate primers that bracketed those nucleotides that encode amino acids at CK's active-site. Subsequently, PCR products were generated from sequence specific primers, which were designed on the basis of the sequence of PCR product 1. Sequencing of PCR products 2 and 3 established the 5′ portion of the MCK-b cDNA sequence, including its 5′ UTR. Sequencing of PCR products 4-to-7 verified the 5′ portion of the MCK-b cDNA sequence. Sequencing of PCR product 8 established the 3′ portion of the MCK-b cDNA sequence, including its 3′ UTR. The 3′ portion of the MCK-b cDNA sequence was confirmed with the sequencing of PCR products 9-to-11. Sequencing of PCR products 12 and 13 confirmed the composite sequence that was obtained from sequence alignment of the sequences of PCR products 1-to-10. In addition, PCR product 5 was generated from a ds-cDNA preparation that was obtained from the white muscle of a second individual. The sequence of PCR product 5 proved to be identical to the sequence of PCR product 4. This is strong evidence that this portion of MCK-b's cDNA sequence is correct. Furthermore, PCR primers used to generate PCR products 9 and 10 were designed to be highly specific for MCK-b. These primers coupled with stringent PCR conditions ensured that MCK-b cDNA specific sequences were obtained and not the corresponding

sequences of MCK-a cDNA (see Fig. 17). It can be seen in Figure 11 that a large degree of overlap exists between the 13 sequences used to establish and confirm the full-length cDNA sequence. This ensured that unambiguous alignments were obtained. Figure 11 illustrates that confirmation of MCK-b's full-length cDNA sequence is based on the sequencing and alignment of 13 PCR products.

4.1.2. Sequencing of MCK-a's full-length cDNA.

Figure 12 shows a schematic representation of the full-length cDNA sequence of MCK-a where the 5′, 3′ UTRs, and ORF are depicted. Below this are representations of PCR products (1-8) with primer names at each end. PCR primer sequences are given in Table 6. The numbered PCR products illustrate the strategy used to establish and confirm MCK-a's full-length cDNA sequence. Sequence alignment of PCR product 1 and 2 with MCK-b's cDNA sequence indicated that a second MCK cDNA was present in *C. aceratus* white muscle. A highly specific PCR primer was designed from the sequence obtained from alignment of the sequences of PCR products 1 and 2. This was used to generated PCR product 3, its sequence established the 5′ portion of MCK-2, including its 5′ UTR. Further highly specific PCR primers were than designed from the sequence that resulted from sequence alignment of PCR products 1-to-3. Sequencing of PCR products 4 and 5, obtained using these primers, confirmed the 5′ portion of MCK-a and proved that it was distinct from the corresponding 5′ end of MCK-b (see Fig. 17). Sequencing of PCR product 6 established the 3′ portion of MCK-a, including its 3′ UTR. Sequencing of PCR products 7 and 8 confirmed the composite sequence that was obtained from alignment of the sequences of PCR products 1-to-6. It can be seen in Figure 12 that a large degree of overlap exists between the 8 sequences used to establish

and confirm the full-length cDNA. This ensured that unambiguous alignments were obtained. Figure 12 illustrates that assessment of MCK-a's full-length cDNA sequence is based on the sequencing and alignment of 8 PCR products.

4.2. MCK-b and MCK-a are not BCK or MtCK cDNAs.

Mammals and birds have four CK genes: muscle (MCK), brain (BCK), sarcomeric mitochondrial (sMtCK), and ubiquitous mitochondrial (uMtCK) (Muhlebach *et al.*, 1994; Qin et al., 1998). These genes have a high degree of identity. The status of fish MtCKs genes is not known. However, MCK and BCK cDNA sequences from teleosts have been reported (Garber *et al.*, 1990; White *et al.*, 1992; Sun *et al.*, 1998). Therefore, the unambiguous identification of MCK cDNAs from *C. aceratus* required that BCK and MtCK cDNA be sequenced as well. This would dispel the possibility that one of the designated MCK cDNA sequences was a BCK or MtCK cDNA sequence and cDNAs for these isoforms were also isolated and sequenced from notothenid white muscle. BCK cDNA from *C. aceratus* is a partial sequence (see below). This sequence was obtained after *Gobionotothen gibberfrons*' BCK full-length cDNA sequence was confirmed.

4.2.1. Sequencing of BCK's full-length cDNA.

Figure 13 shows a schematic representation of the full-length cDNA sequence of BCK from *G. gibberfrons* where the 5′, 3′ UTRs, and ORF are depicted. Below this are representations of PCR products (1-11) with primer names at each end. PCR primer sequences are given in Table 7. The numbered PCR products illustrate the strategy used to establish and confirm BCK's full-length sequence. PCR product 1 was obtained with

degenerate PCR primers. Design of a gene specific primer from this sequence was than used to obtain PCR product 2. Sequencing of PCR product 2 established the 5′ portion of the BCK cDNA sequence, including its 5′ UTR. Sequencing of PCR products 3-to-5 confirmed the 5′ portion of the BCK cDNA sequence. Sequencing of PCR product 6 established the 3′ portion of the BCK cDNA sequence, including its 3′ UTR. This was confirmed with the sequencing of PCR products 7-to-10. Figure 13 shows that the composite sequence that was obtained from alignment of the sequences of PCR products 1-to-10 was confirmed with the sequencing of PCR product 11. It can be seen in Figure 13 that a large degree of overlap exists between the 11 sequences used to establish and confirm BCK's full-length cDNA sequence. This ensured that unambiguous alignments were obtained. Figure 13 illustrates that assessment of BCK's full-length cDNA sequence is based on the sequencing and alignment of 11 PCR products.

Figure 14 shows a schematic representation of a partial BCK cDNA from *C. aceratus* where the 3′ UTR and ORF are depicted. Below this are representations of PCR products (1-2) with primer names at each end. PCR primer sequences are given in Table 8. Figure 14 shows that duplicate sequencing of similar PCR products was used to confirm this partial BCK sequence. *C. aceratus* BCK cDNA is missing only the first 12 nucleotides of the ORF and includes the complete 3′ UTR. There is 96% sequence identity between *G. gibberfrons* and *C. aceratus* BCK and 98% sequence identity between the two ORFs.

4.2.2. Sequencing of MtCK's full-length cDNA.

Figure 15 shows a schematic representation of the full-length cDNA sequence of MtCK from *C. aceratus* where the 5′, 3′ UTRs, and ORF are depicted. Below this are

representations of PCR products (1-14) with primer names at each end. PCR primer sequences are given in Table 9. The numbered PCR products illustrate the strategy used to establish and confirm full-length MtCK. PCR product 1 was obtained with degenerate PCR primers. Design of a gene specific primer from this sequence was than used to obtain PCR product 2. Sequencing of PCR product 2 established the 5′ portion of the MtCK cDNA sequence, including its 5′ UTR. Sequencing of PCR products 3-to-7 confirmed the 5′ portion of the MtCK cDNA sequence. Sequencing of PCR product 8 established the 3′ portion of the MtCK cDNA sequence, including its 3′ UTR. This was confirmed with the sequencing of PCR products 9-to-12. Figure 15 shows that the composite sequence that was obtained from sequence alignment of PCR products 1-to-12 was confirmed with the sequencing and alignment of PCR products 13 and 14. It can be seen in Figure 15 that a large degree of overlap exists between the 14 sequences used to establish and confirm MtCK's full-length cDNA sequence. This ensured that unambiguous alignments were obtained. Figure 15 illustrates that assessment of MtCK's full-length cDNA sequence is based on the sequencing and alignment of 14 PCR products.

4.2.3. Assignment of *C. aceratus* CK cDNAs to specific isoform groups.

Accurate assignment of *C. aceratus* CK cDNAs to their correct isoform groups was obtained by aligning their ORF sequences with several of the CK ORF sequences found in GeneBank. Alignment and maximum parsimony analyses were done using the DAMBE computer package (Xia and Xie, 2001). Much of DAMBE's programming is derived from earlier alignment and phylogentic analysis programs including Felsenstein's Phylip package (Felsenstein, 1984) and Clustal W (Higgins and Gibson, 1994). The

maximum parsimony program used here is based on the established assumptions of Phylip's unrooted parsimony analysis (Felsenstein, 1979; Felsenstein, 1988). Analyses were performed on CK ORF sequences and the portion of the MtCK ORF sequences that encode the transit-sequence (see Fig. 17) were removed prior to analyses. In these analyses polycheate (*Chaetopterus variopedatus*, Pineda *et al.*, 1999; Graber and Ellington, 2001) or torpedo (Giraudat *et al.*, 1984) MCK ORF sequences were used as the outgroup and 1000 resamplings (Bootstraps) were applied. This analysis was performed solely for the purpose of assigning the CK cDNA sequences to appropriate homologous categories and was not done to determine evolutionary distances.

Figure 16 shows the majority-rule and strict consensus tree that was constructed from this analysis. In Figure 16 the number of times that each node was reproduced during resampling is shown. In Figure 16 *C. aceratus* CK isoforms are highlighted in red. It can be seen that MCK-b and MCK-a sequences group with other teleost MCK sequences and that these group with MCK sequences from chicken and mammals. Similarly, the BCK sequence from *C. aceratus* groups with trout and mammal BCK sequences. The MtCK sequence from *C. aceratus* groups with sMtCK sequences, which are a part of the larger group of MtCK sequences that includes the uMtCK sequences of chicken and mammals. A similar tree was obtained when a maximum likelihood analysis (1000 Bootstraps) was applied with torpedo MCK cDNA as the outgroup. In addition, the same groupings were obtained when maximum parsimony analyses (Phylip package) of amino acid sequences were done, except the *C. aceratus* MtCK sequence became the sister group of the other MtCK sequences. These analyses provided strong evidence that

MCK-b and MCK-a sequences from *C. aceratus* encode distinct muscle isoforms of CK and not brain or mitochondrial isoforms of CK.

4.2.4. Comparison of MCK-b, MCK-a, BCK and MtCK cDNAs from *C. aceratus*.

The distinction between the MCK transcripts and those of BCK and MtCK is readily seen in a sequence alignment. Figure 17 shows the alignment of MCK-b, MCK-a, BCK, and MtCK cDNA sequences. The bold-type and underlined nucleotides at the 5′-end of the MtCK transcript encode the mitochondrial transit-sequence. This is a hallmark of the MtCK isoform and is missing from the other isoform cDNA sequences. From Figure 17 it can be seen that distinct 5′ and 3′ UTRs occur in the different isoforms. Figure 17 indicates that the distinction between MCK-b and MCK-a is most evident in the 5′ terminal half of these sequences. The 5' UTR sequences are only 59% identical. The distinction between MCK-b and MCK-a is also apparent throughout the first 650 nucleotides of the ORFs but only minor variation between nucleotides 650 and 1050 of the coding regions, is seen. Figure 17 shows that the last 92 nucleotides of these coding regions and their 3′ UTRs are identical. Overall, there is only 88% identity between MCK-b and MCK-a. Differences seen between these two sequences indicate that two separate genes encoding two MCK monomer polypeptides are found in *C. aceratus* white muscle. An overall analysis indicates that there is only 76% identity between the coding regions of BCK and MCKs and only 64 % identity between the coding regions of MtCK and MCKs while the coding regions BCK and MtCK are 66% identitcal. Therefore, *C. aceratus* has distinct MCK-b, MCK-a, BCK, and MtCK genes.

4.3. MCK mRNA tissue expression is distinct from BCK and MtCK mRNA.

CK isozymes have characteristic expression patterns in adult tissues (Schafer and Perriard, 1988; Trask and Billadello, 1990; Wilson *et al.*, 1995; Qin *et al.*, 1998). Mammalian MCK mRNA is the most abundant CK expressed in adult skeletal and cardiac muscle. Mammalian BCK is the predominant isoform of adult brain, smooth muscle, and sperm, but is also expressed in adult cardiac muscle and to a much lesser extent in adult skeletal muscle (Qin *et al.*, 1998). In birds MCK mRNA is found only in skeletal muscle while only BCK is expressed in heart tissue (Qin *et al.*, 1998). Sarcomaric MtCK is found in heart and skeletal muscle while ubiquitous MtCK has an expression pattern similar to that of BCK (Qin *et al.*, 1998). Determining the tissue distribution MCK mRNA in *C. aceratus* tissue can thus be used as a verification of isozyme type.

The northern blots shown in Figure 18 indicate that MCK is expressed in white muscle and to lesser extent in pectoral muscle (Fig. 18A). The approximately 16 kb MCK transcript is not seen in heart, brain, or testis. These tissues instead expressed the BCK transcript (Fig. 18C). This expression pattern is also distinct from that of the mitochondrial isoform, which is expressed in white muscle, heart, and pectoral muscle (Fig. 18B). This data shows unambiguous distinctions in tissue distribution of CK isozymes from *C. aceratus* and that MCK-b and MCK-a are found only in skeletal muscle.

4.4. Differences between the deduced amino acid sequences of *C. aceratus* MCKs and rabbit MCK.

To determine differences and conserved motifs in monomer peptide sequences, amino acid sequences were deduced from MCK-b and MCK-a cDNAs. These have been compared to the well-characterized rabbit sequence. In Figure 19 the rabbit MCK sequence shows a number of conserved motifs (Muhlebach *et al.*, 1994). These include isoform-specific, CK family-specific, active-site residues, a putative adenine binding motif, and catalytically important residues (Clarke and Price, 1979; Rosevear *et al.*, 1981; Lin *et al.*, 1994; Clottes and Vial, 1996; Chen *et al.*, 1996; Wood *et al.*, 1998; Eder *et al.*, 2000; Edmiston *et al.*, 2001; Cantwell *et al.*, 2001). The deduced monomer molecular weights are 42.4 and 42.7 kDa for MCK-b and MCK-a polypeptide respectively, which are in good agreement with the monomer molecular weight determined from SDS-PAGE experiments of 43 kDa (Chap. 3, Fig. 5), and with CK's known monomer molecular weights (Muhlebach *et al.*, 1994). In addition, deduced amino acid sequences indicate that these MCK monomers have different isoelectric points (pIs) of 6.61 (MCK-1) and 6.74 (MCK-2). The predicted charge on the monomers is –2.74 for MCK-1 and –1.68 for MCK-2, at pH 7.0. This charge difference is consistent with the resolution of the affinity column eluant into two activity peaks during DEAE anion exchange chromatography. Figure 19 shows that MCK-b and MCK-a differ at their amino-terminal segments. That is, 14 of their first 130 amino acids and 12 of the next 190 amino acids have different physio-chemical properties. All but one of their last 68 amino acids are identical. Several amino acid residues of *C. aceratus* MCKs are also found in carp (Sun *et al.*, 1998) or zebrafish (GenBank) MCKs. The teleost specific residues shown in Figure 19

are: K4, C6, D9, V16, K36, G40, Q46, S46, S108, F112, N124, N147, T159, A182, N278, N189, Q242, H277, T304, V304, and G332. Other differences shown in Figure 19 between rabbit and *C. aceratus* MCK amino acid sequences are not unique. Thus, E83 of is found in other mammalian MCKs, A163, S177, and N221 are found in electric ray MCKs, P300 and K258 are found in chicken MCK, and E371 is in a Xenopus MCK (Walliman et al., 1994). Table 10 lists distinct differences between *C. aceratus* MCK and rabbit MCK amino acid sequences. Overall, MCK-b and MCK-a are 92% similar and 87% identical, MCK-b and rabbit MCK are 87% similar and 81% identical while MCK-a and rabbit MCK are 92% similar and 85% identical. The 81%-to-85% identity between the deduced amino sequences of *C. aceratus* MCKs and the amino sequence of rabbit MCK is consistent to what has been observed when other known MCK amino sequences are compared (Muhlebach *et al.*, 1994). On the other hand, comparisons between known MCK and BCK amino acid sequences or MCK and MtCK amino acid sequences shows only 77%-to-82% and 60%-to-65% identity respectively (Muhlebach *et al.*, 1994). The difference between MCK-b and MCK-a deduced amino acid sequences reflects the distinction observed in their cDNAs.

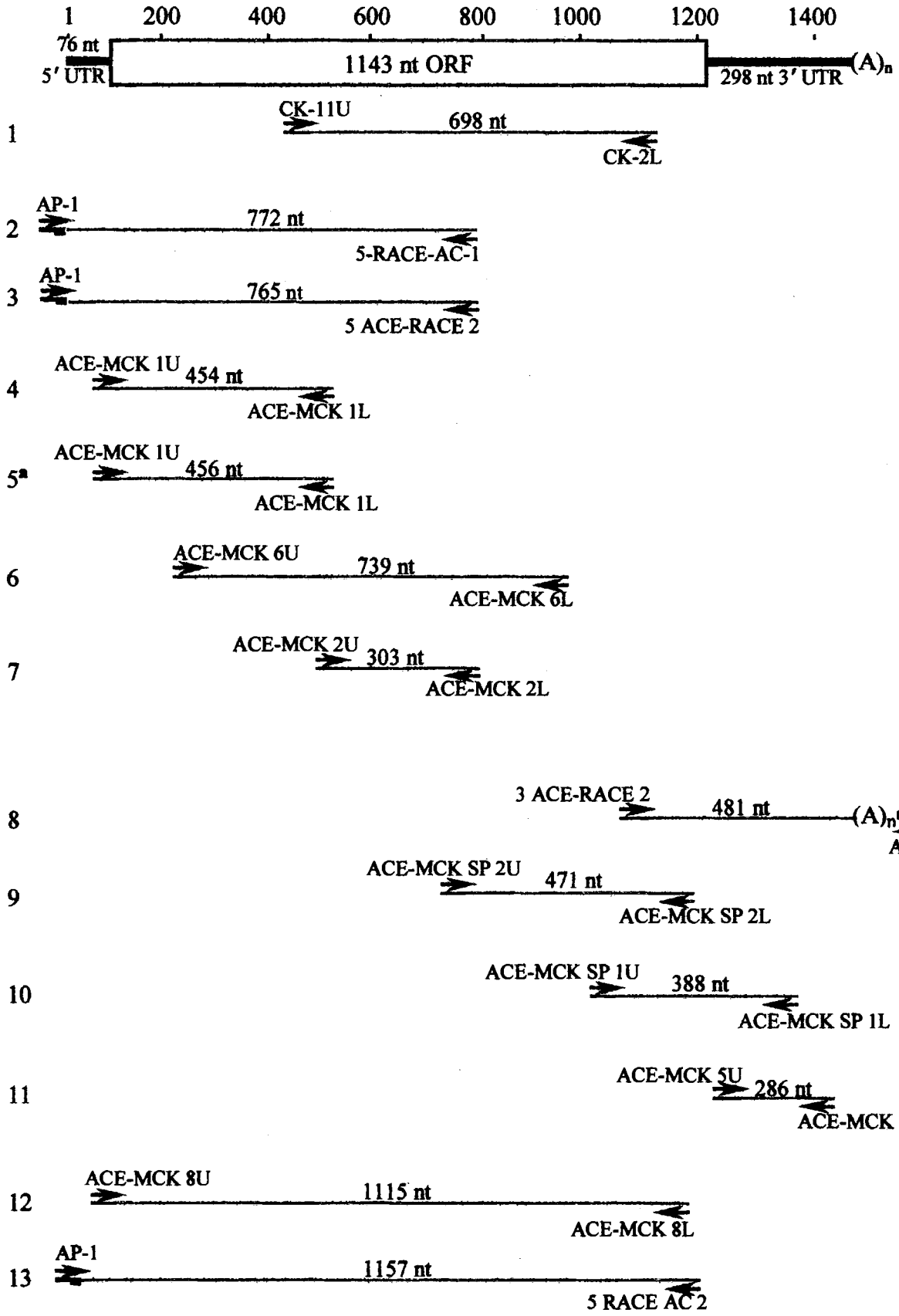
1
200
400
600
800
1000
1200
1400
76 nt
5′ UTR
1143 nt ORF
298 nt 3′ UTR
(A)n
1
CK-11U
698 nt
CK-2L
2
AP-1
772 nt
5-RACE-AC-1
3
AP-1
765 nt
5 ACE-RACE 2
4
ACE-MCK 1U
454 nt
ACE-MCK 1L
5a
ACE-MCK 1U
456 nt
ACE-MCK 1L
6
ACE-MCK 6U
739 nt
ACE-MCK 6L
7
ACE-MCK 2U
303 nt
ACE-MCK 2L
8
3 ACE-RACE 2
481 nt
(A)n
AP-1
9
ACE-MCK SP 2U
471 nt
ACE-MCK SP 2L
10
ACE-MCK SP 1U
388 nt
ACE-MCK SP 1L
11
ACE-MCK 5U
286 nt
ACE-MCK 5L
12
ACE-MCK 8U
1115 nt
ACE-MCK 8L
13
AP-1
1157 nt
5 RACE AC 2

Figure 11

Table 5. Sequences of PCR primers for MCK-b cDNA from *C. aceratus.*

Primer Name	Sequence	Location[a]	T_m (°C)[b]	T_{anneal} (°C)[c]
CK-11U	5'-d(MCG RCG GAY CTG GAY)-3'	425 -> 439	40.0[d]	50.0
CK-2L	5'-d(ATY TGS ACC WGY TCC ACC TC)-3'	1109 <- 1128	49.0[d]	
AP-1[e]	5'-d(CCA TCC TAA TAC GAC TCA CTA TAG GGC)-3'	adaptor ->	71.0[f]	64->62->60
5-RACE-AC1	5'-d(ACT CTG GTG TGG TCC TCC TCA TTC ACC)-3'	757 <- 783	60.0	
AP-1	5'-d(CCA TCC TAA TAC GAC TCA CTA TAG GGC)-3'	adaptor ->	71.0[f]	57->55->53
5 ACE-RACE 2	5'-d(ACT CTG GTG TGG TCC TCC TCA TTC A)-3'	759 <- 783	59.8	
ACE-MCK 1U	5'-d(AAG CAG GTG GAG CAA GAA)-3'	51 -> 68	47.8	56.0
ACE-MCK 1L	5'-d(GGG GGC AGG GTG ATT C)-3'	489 <- 504	50.0	
ACE-MCK 6U	5'-d(GGA GAT CTA TGC CAA GCT GAG GGG AAA GTC)-3'	181 -> 210	66.4	63.0
ACE-MCK 6L	5'-d(CAG GTT GGA GGG GCA GGT CAG GAT GTA)-3'	908 <- 934	67.3	
ACE-MCK 2U	5'-d(GTA CCG GAC GCA GCA TCA AG)-3'	468 -> 487	55.5	62.0
ACE-MCK 2L	5'-d(CCT CCT CGT TCA CCC AGA CC)-3'	751 <- 770	55.6	
3-ACE RACE 2	5'-d(TAC ATC CTG ACC TGC CCC TCC AAC CT)-3'	908 -> 933	65.3	62->60->58
AP-1	5'-d(CCA TCC TAA TAC GAC TCA CTA TAG GGC)-3'	<- adaptor	71.0[f]	
ACE-MCK SP 2U	5'-d(GGC ATC TGG CAC AAC AAC AAC AAG ACC TTC CT)-3'	719 -> 750	70.1	70->68->66
ACE-MCK SP 2L	5'-d(GCC TCT CCC TTC TCC AGC TTC TTC TCC ATC TCA A)-3'	1155 <- 1188	71.1	
ACE-MCK SP 1U	5'-d(CAG CAC ACA CGC CAA GTT CGA GGA GAT TCT GAC)-3'	979 -> 1011	72.2	70->68->66
ACE-MCK SP 1L	5'-d(GGA AGG ATG TGA ACC ACA AAG CTG GAA GGA AGA CA)-3'	1330 <- 1364	71.8	
ACE-MCK 5U	5'-d(CCG CCC AGA AGT AAA G)-3'	1206 -> 1221	42.9	55.0
ACE-MCK 5L	5'-d(GAA CAG CGT CAA TAA TCA T)-3'	1473 <- 1491	42.0	
AP-1	5'-d(CCA TCC TAA TAC GAC TCA CTA TAG GGC)-3'	adaptor ->	71.0[f]	57->55->53
5-RACE-AC2[g]	5'-d(TCT CTT CAT GTT GCC TCC CTT CTC CAT G)-3'	1171 <- 1198	64.0	

ACE-MCK 8U	5'-d(TGA TCC CAG GAC TGT TAC TTC TTT CTT TTC)-3'	17 -> 46	60.4	62.0
ACE-MCK 8L	5'-d(GCC TCT CCC TTC TCC AGC TTC TTC TC)-3'	1163 <- 1188	62.0	

In the degenerate primer-pair (CK-11U // CK-2L) the M, R, S, W, and Y designations indicate ambiguous positions, which means that these sequences are of mixed base composition where M = a + c, R = g + a, S = c + g W = a + t, and Y = c + t.

[a] Location indicates the nucleotide position on the transcript where a primer hybridizes. Numbering of the full-length cDNA sequence begins at the first nucleotide. [b] Unless otherwise indicated, melting temperatures as determined by PrimerSelect of Dnastar (see Material and Methods). [c] Annealing temperaures were empirically determined starting with those given by PrimerSelect. Touchdown conditions (see Materials and Methods) are indicated by decreasing temperatures that are separated by arrows. [d] Melting temperature estimates provided with GIBCO BRL's "Certificate of Analysis" for primers in 50 mM NaCl. [e] AP-1 designates Adaptor Primer 1. This is supplied with CLONTECH's Marathon Kit and is designed to hybridize to their adaptor sequence (see Material and Methods). [f] Melting temperatures provided by CLONTECH. [g] The extension temperature used in PCR with this primer-pair was 68° C rather than the 72° C used in all other cases.

-> denotes a sense-strand primer and <- an antisense-strand primer.

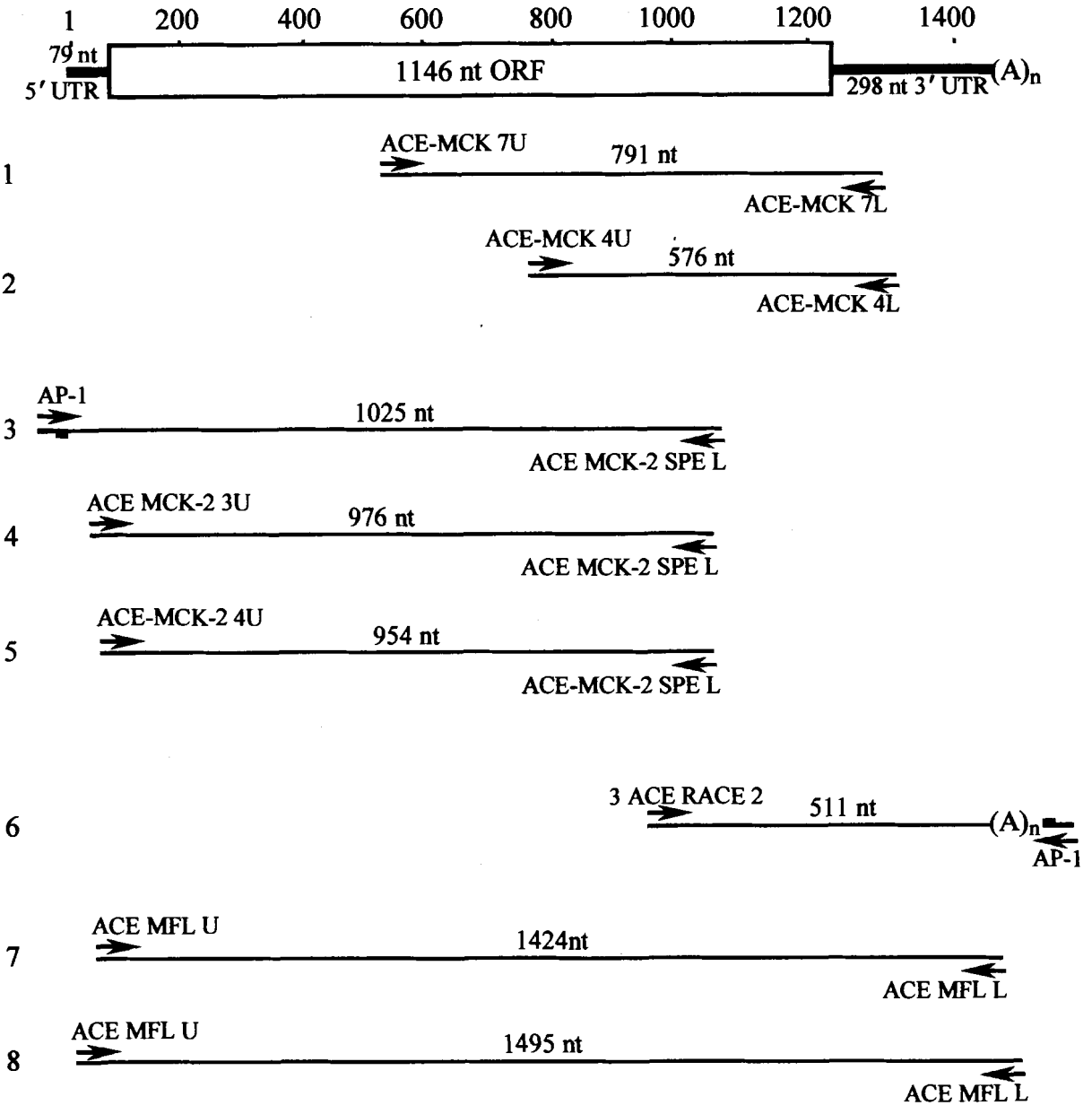
1
200
400
600
800
1000
1200
1400
79 nt
5′ UTR
1146 nt ORF
298 nt 3′ UTR
(A)n
1
ACE-MCK 7U
791 nt
ACE-MCK 7L
2
ACE-MCK 4U
576 nt
ACE-MCK 4L
3
AP-1
1025 nt
ACE MCK-2 SPE L
4
ACE MCK-2 3U
976 nt
ACE MCK-2 SPE L
5
ACE-MCK-2 4U
954 nt
ACE-MCK-2 SPE L
6
3 ACE RACE 2
511 nt
(A)n
AP-1
7
ACE MFL U
1424nt
ACE MFL L
8
ACE MFL U
1495 nt
ACE MFL L

Figure 12

Table 6. Sequences of PCR primers for MCK-a cDNA from *C. aceratus.*

Primer Name	Sequence	Location[a]	T_m (°C)[b]	T_{anneal} (°C)[c]
ACE MCK 7U	5'-d(CGT GGC GAG CGC AGA GGC ATT GAG AAG C)-3'	521 -> 548	74.2	63.0
ACE MCK 7L	5'-d(TGG AAG GAA GAC ACA GGC GAG CAG AGT)-3'	1322 <- 1348	65.9	
ACE MCK 4U	5'-d(TGG GTG AAC GAG GAG GAT)-3'	761 -> 778	49.6	58.0
ACE MCK 4L	5'-d(CAC AGG CGA GCA GAG TCA)-3'	1320 <- 1337	49.9	
AP-1[d]	5'-d(CCA TCC TAA TAC GAC TCA CTA TAG GGC)-3'	adaptor ->	71.0[e]	72->70->68->66
ACE MCK-2 SPE L	5'-d(CAG CCT GCT GAG GAT CTC GTC G)-3'	1003 <- 1024	60.8	
ACE MCK-2 SPE 3U	5'-d(TTG TCG GCT GTG AAG TGT TAG AAA G)-3'	50 ->74	56.6	72->70->68->66
ACE MCK-2 SPE L	5'-d(CAG CCT GCT GAG GAT CTC GTC G)-3'	1003 <- 1024	60.8	
ACE MCK-2 SPE 4U	5'-d(CCA TCC TAA TAC GAC TCA CTA TAG GGC)-3'	71 ->96	60.1	72->70->68->66
ACE MCK-2 SPE L	5'-d(CAG CCT GCT GAG GAT CTC GTC G)-3'	1003 <- 1024	60.8	
3-ACE RACE 2	5'-d(TAC ATC CTG ACC TGC CCC TCC AAC CT)-3'	914 -> 939	65.3	62->60->58
AP-1	5'-d(CCA TCC TAA TAC GAC TCA CTA TAG GGC)-3'	<- adaptor	71.0[e]	
ACE MFL U	5'-d(GAA CAG GTT CTG ATC CCA GGA CTG TTA CTT CTT TC)-3'	14 -> 36	66.3	60
ACE MFL L	5'-d(TTG AGC AAT ATG AAC AGC GTC AAT AAT CAT TAC TT)-3'	1474 <- 1508	63.5	

[a] Location indicates the nucleotide position on the transcript where a primer hybridizes. Numbering of the full-length cDNA sequence begins at the first nucleotide. [b] Unless otherwise indicated, melting temperatures as determined by PrimerSelect of Dnastar (see Material and Methods). [c] Annealing temperaures were empirically determined starting with those given by PrimerSelect. Touchdown conditions (see Materials and Methods) are indicated by decreasing temperatures that are separated by arrows. [d] AP-1 designates Adaptor Primer 1. This is supplied with CLONTECH's Marathon Kit and is designed to hybridize to their adaptor sequence (see Material and Methods). [e] Melting temperature estimates provided with GIBCO BRL's "Certificate of Analysis" for primers in 50 mM NaCl.

-> denotes a sense-strand primer and <- an antisense-strand primer.

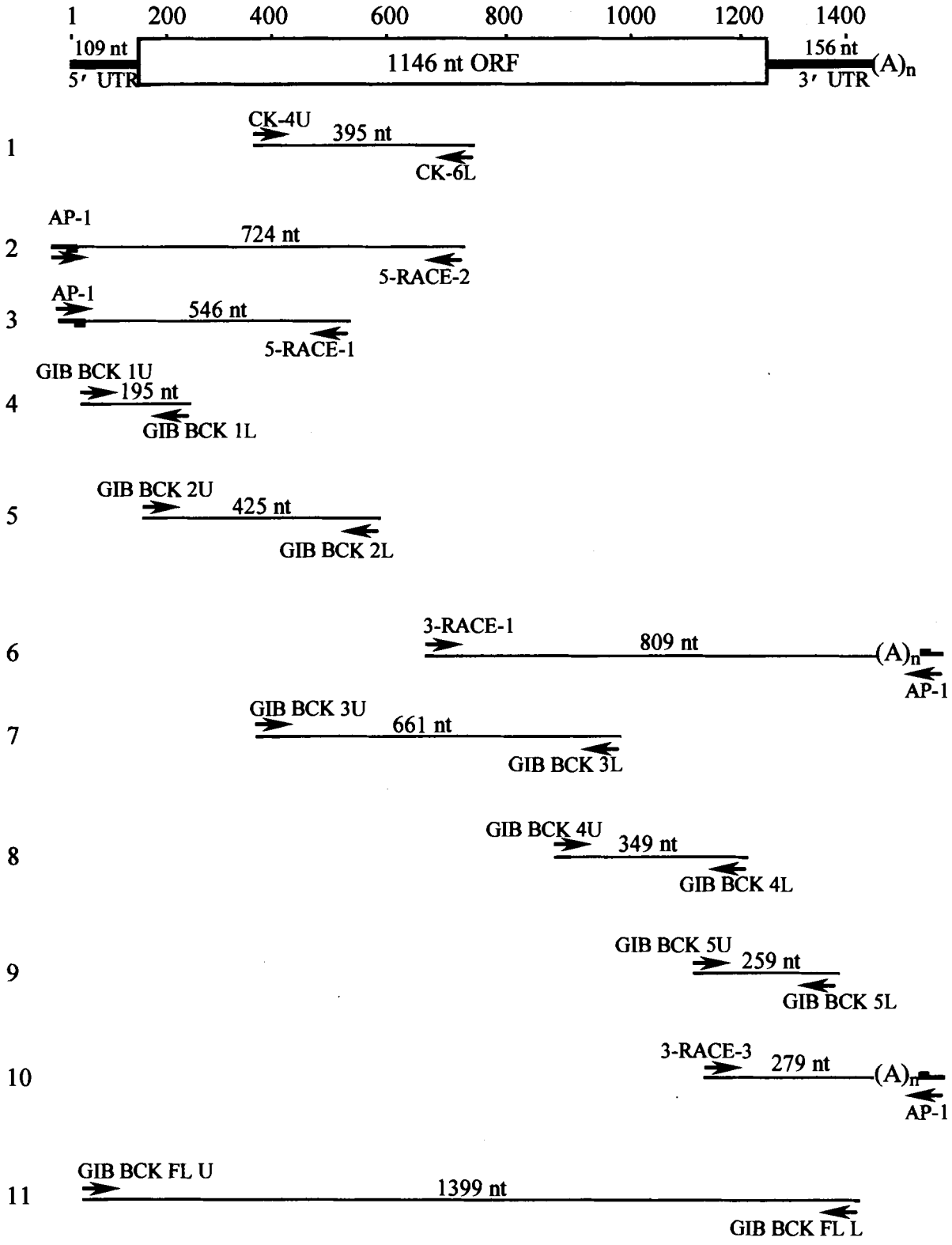
1
200
400
600
800
1000
1200
1400
109 nt
1146 nt ORF
156 nt
5′ UTR
3′ UTR
(A)n
1
CK-4U
395 nt
CK-6L
2
AP-1
724 nt
5-RACE-2
3
AP-1
546 nt
5-RACE-1
4
GIB BCK 1U
195 nt
GIB BCK 1L
5
GIB BCK 2U
425 nt
GIB BCK 2L
6
3-RACE-1
809 nt
(A)n
AP-1
7
GIB BCK 3U
661 nt
GIB BCK 3L
8
GIB BCK 4U
349 nt
GIB BCK 4L
9
GIB BCK 5U
259 nt
GIB BCK 5L
10
3-RACE-3
279 nt
(A)n
AP-1
11
GIB BCK FL U
1399 nt
GIB BCK FL L

Figure 13

Table 7. Sequences of PCR primers for BCK cDNA from *G. gibberifrons.*

Primer Name	Sequence	Location[a]	T_m (°C)[b]	T_{anneal} (°C)[c]
CK-4U	5'-d(CGT GGC NGG CGA NGA GGA)-3'	377 -> 394	52.0[d]	55.5
CK-6L	5'-d(CCN GAG GCN ANN AGC AGN GGA)-3'	752 <- 772	54.0[d]	
AP-1[e]	5'-d(CCA TCC TAA TAC GAC TCA CTA TAG GGC)-3'	adaptor ->	71.0[f]	71->69->67
5-RACE-2	5'-d(CAG AGG CCA GCA GCA GAG GAG ACA CT)-3'	699 <- 724	67.3	
AP-1A[g]	5'-d(ATC CTA ATA CGA CTC ACT ATA)-3'	adaptor ->	41.0[d]	50.0
5-RACE-1	5'-d(GCA GTG AGG TGG CAG GCA GGC AGA AGC CAC)-3'	521 <- 546	75.0[h]	
GIB BCK 1U	5'-d(CGC ATA CTG TTC GTT TGT GAG C)-3'	9 -> 30	55.0	57.0
GIB BCK 1L	5'-d(CTT GGC CAT ATG ATT GTT GTG TTT)-3'	181 <- 204	54.8	
GIB BCK 2U	5'-d(AAC ACG CAC AAC ACG ATG AAG ATG)-3'	121 -> 144	58.6	62.0
GIB BCK 2L	5'-d(GCA GTG AGG TGG CAG GCA GAA)-3'	526 <- 546	59.8	
3-RACE-1	5'-d(TGA GTG GAG ACC TGC AGG GGA AGT ACT C)-3'	602 -> 629	72.0[h]	70->68->66
AP-1	5'-d(CCA TCC TAA TAC GAC TCA CTA TAG GGC)-3'	<- adaptor	71.0[f]	
GIB BCK 3U	5'-d(CGC CGG AGA CGA GGA GAC ATA)-3'	333 ->353	58.8	62.0
GIB BCK 3L	5'-d(GCA CAC CGG CAC GCA GAC)-3'	977 <- 994	58.2	
GIB BCK 4U	5'-d(CGC TTC TGC ACC GGA CTC ACC AA)-3'	862 -> 884	65.0	62.0
GIB BCK 4L	5'-d(TCC AGC TTC TTC TCC ATC TCC ACC ATC A)-3'	1184 <- 1211	65.6	
GIB BCK 5U	5'-d(CGA CAT CTC TAA CGC CGA CAG)-3'	1110 -> 1130	54.9	50.0
GIB BCK 5L	5'-d(TTC ATC TTA AAT ACC CAA CCA AAA TC)-3'	1344 <- 1369	54.0	
3-RACE-3	5'-d(CTG GGC TTC TCC GAG GTG GA)-3'	1132 -> 1151	53.0[d]	55.0
AP-1	5'-d(CCA TCC TAA TAC GAC TCA CTA TAG GGC)-3'	<- adaptor	71.0[f]	
GIB BCK FL U	5'-d(GCA TAC TGT TCG TTT GTG AGC TCC TCG TTT G)-3'	10 -> 40	66.9	55.0
GIB BCK FL L	5'-d(AAC CAG AAC ATG TTT TTA TTT CAT TGC CAT CCT C)-3'	1376 <- 1409	65.9	

In the degenerate primer-pair (CK-4U // CK-6L) the N designation indicates ambiguous positions, which means that these sequences are of mixed base composition where N = a + c + g + t.

[a] Location indicates the nucleotide position on the transcript where a primer hybridizes. Numbering of the full-length cDNA sequence begins at the first nucleotide. [b] Unless otherwise indicated, melting temperatures as determined by PrimerSelect of Dnastar (see Material and Methods). [c] Annealing temperaures were empirically determined starting with those given by PrimerSelect. Touchdown conditions (see Materials and Methods) are indicated by decreasing temperatures that are separated by arrows. [d] Melting temperature estimates provided with GIBCO BRL's "Certificate of Analysis" for primers in 50 mM NaCl. [e] AP-1 designates Adaptor Primer 1. This is supplied with CLONTECH's Marathon Kit and is designed to hybridize to their adaptor sequence (see Material and Methods). [f] Melting temperatures provided by CLONTECH. [g] AP-1A is a truncated version of AP-1 designed for use at lower annealing temperatures. [h] Melting temperatures estimated according to Rychlik *et al.*, 1990.
-> denotes a sense-strand primer and <- an antisense-strand primer.

Table 8. Sequences of PCR primers for BCK cDNA from *C. aceratus.*

Primer Name	Sequence	Location[a]	T_m (°C)[b]	T_{anneal} (°C)[c]
GIB BCK 2U	5'-d(AAC ACG CAC AAC ACG ATG AAG ATG)-3'	1 -> 24	58.6	60.0
AP-1[d]	5'-d(CCA TCC TAA TAC GAC TCA CTA TAG GGC)-3'	<- adaptor	71.0[e]	

[a] Location indicates the nucleotide position on the transcript where a primer hybridizes. Numbering of the full-length cDNA sequence begins at the first nucleotide. [b] Unless otherwise indicated, melting temperatures as determined by PrimerSelect of Dnastar (see Material and Methods). [c] Annealing temperaures were empirically determined starting with those given by PrimerSelect. Touchdown conditions (see Materials and Methods) are indicated by decreasing temperatures that are separated by arrows. [d] AP-1 designates Adaptor Primer 1. This is supplied with CLONTECH's Marathon Kit and is designed to hybridize to their adaptor sequence (see Material and Methods). [e] Melting temperatures provided by CLONTECH.

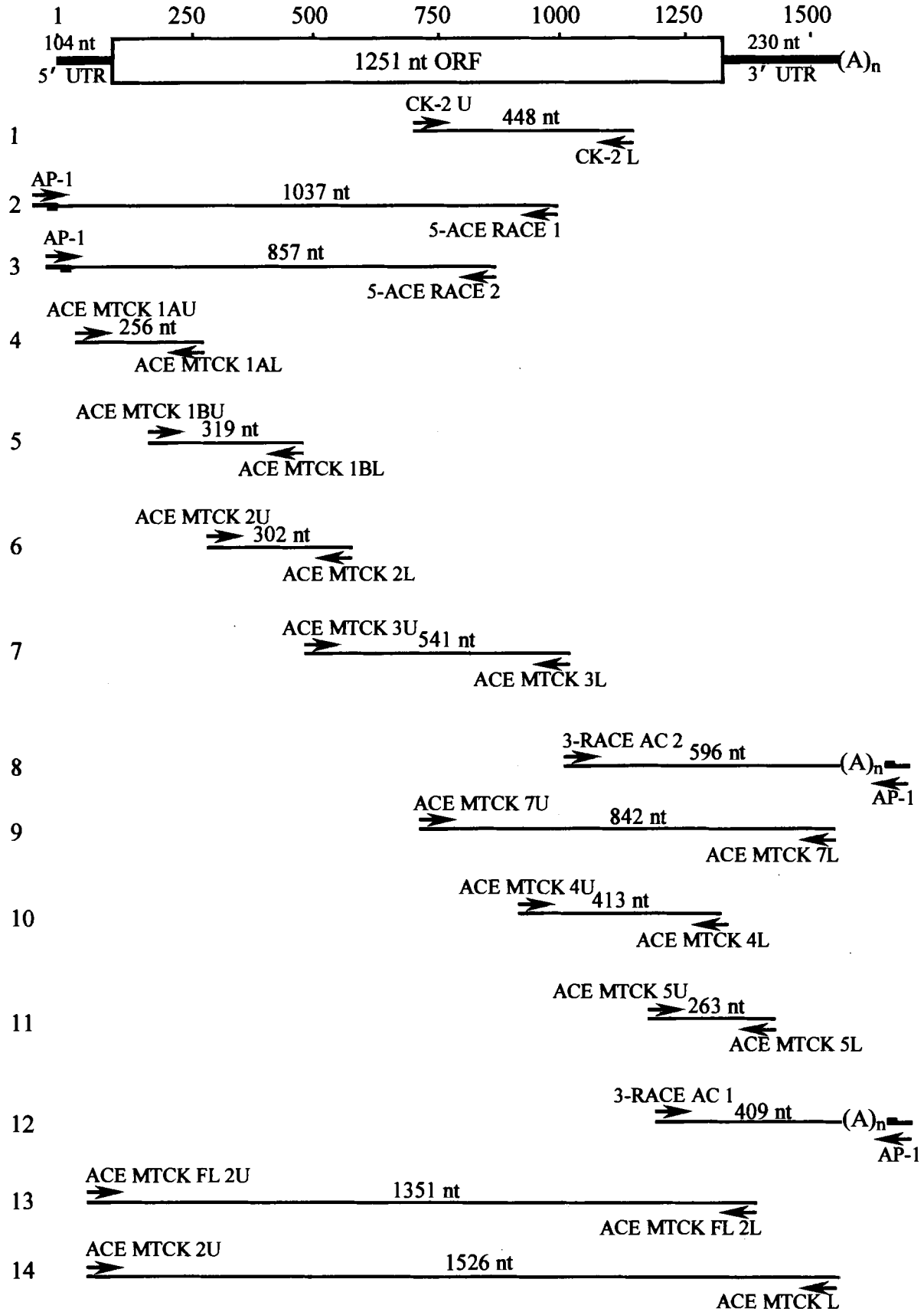
1
250
500
750
1000
1250
1500
104 nt
5′ UTR
1251 nt ORF
230 nt
3′ UTR
(A)n
CK-2 U
448 nt
CK-2 L
AP-1
1037 nt
5-ACE RACE 1
AP-1
857 nt
5-ACE RACE 2
ACE MTCK 1AU
256 nt
ACE MTCK 1AL
ACE MTCK 1BU
319 nt
ACE MTCK 1BL
ACE MTCK 2U
302 nt
ACE MTCK 2L
ACE MTCK 3U
541 nt
ACE MTCK 3L
3-RACE AC 2
596 nt
(A)n
AP-1
ACE MTCK 7U
842 nt
ACE MTCK 7L
ACE MTCK 4U
413 nt
ACE MTCK 4L
ACE MTCK 5U
263 nt
ACE MTCK 5L
3-RACE AC 1
409 nt
(A)n
AP-1
ACE MTCK FL 2U
1351 nt
ACE MTCK FL 2L
ACE MTCK 2U
1526 nt
ACE MTCK L

Figure 15

Table 9. Sequences of PCR primers for a MtCK cDNA from *C. aceratus.*

Primer Name	Sequence	Location[a]	T_m (°C)[b]	T_{anneal} (°C)[c]
CK-2U	5'-d(CAG CAG CTN ATY GAY GAC CA)-3'	753 -> 772	48.0[d]	53.0
CK-2L	5'-d(ATY TGS ACC WGY TCC ACC TC)-3'	1236 <- 1255	49.0[d]	
AP-1[e]	5'-d(CCA TCC TAA TAC GAC TCA CTA TAG GGC)-3'	adaptor ->	71.0[f]	57->55->53
5 ACE-RACE 1	5'-d(GTA TCC CAG GCG TTC GTT CCA CA)-3'	1015 <- 1037	61.7	
AP-1	5'-d(CCA TCC TAA TAC GAC TCA CTA TAG GGC)-3'	adaptor ->	71.0[f]	57->55->53
5 ACE-RACE 2	5'-d(ACT CTG GTG TGG TCC TCC TCA TTC A)-3'	886 <- 910	59.8	
ACE MTCK 1AU	5'-d(CCC GGG CAG GTG AAG)-3'	39 -> 53	49.5	54.0
ACE MTCK 1AL	5'-d(GCC ATG CAG TTG TTG TGT)-3'	275 <- 292	46.6	
ACE MTCK 1BU	5'-d(TGG CGA CTG GTT TCC TGA TG)-3'	181 -> 200	55.7	59.0
ACE MTCK 1BL	5'-d(AGC CGT TGT GCC TGT CTT TG)-3'	479 <- 498	55.1	
ACE MTCK 2U	5'-d(GCT CTG ACT CCG GCC ATT TAC G)-3'	297 -> 317	59.6	62.0
ACE MTCK 2L	5'-d(TGC GGA CAC GGG ACG ACA G)-3'	579 <- 597	60.0	
ACE MTCK 3U	5'-d(GGC TAC GAC CCC ACC ACC AT)-3'	495 -> 514	58.1	62.0
ACE MTCK 3L	5'-d(CCC AGG CGT TCG TTC CAC AT)-3'	1014 <- 1033	59.3	
3-RACE-AC2	5'-d(GTG GAA CGA ACG CCT GGG ATA CAT C)-3'	1016 -> 1040	63.3	68->66->64
AP-1	5'-d(CCA TCC TAA TAC GAC TCA CTA TAG GGC)-3'	<- adaptor	71.0[f]	
ACE MTCK 7U	5'-d(GAC CTG GCC GGA CGC TAC TAC)-3'	702 -> 722	57.4	54.0
ACE MTCK 7L	5'-d(TTT TGC TTA TTG TCG TTG TTT TTA TTG A)-3'	1566 <- 1589	56.7	
ACE MTCK 4U	5'-d(CAT GGA GAA GGG AGG CAA CA)-3'	917 -> 939	54.8	59.0
ACE MTCK 4L	5'-d(GTG ACG GGA GAC GGG ACT TT)-3'	1320 <- 1339	55.2	
ACE MTCK 5U	5'-d(CTG CCA CTG GAG ACA CC)-3'	1183 -> 1199	45.4	58.0
ACE MTCK 5L	5'-d(GTA GCA GCG GAC AGA CG)-3'	1427 <- 1443	45.6	

3-RACE-AC1	5'-d(AGC TGC CAC TGG AGA ACA CTT TGA CAT T)-3'	1181 -> 1208	64.8	68->66->64
AP-1	5'-d(CCA TCC TAA TAC GAC TCA CTA TAG GGC)-3'	<- adaptor	71.0[f]	
ACE MTCK FL 2U	5'-d(GCT TTC CTA CAG CTC ATT TGT TTC TTT TAA AGA GTT ACC)-3'	53 -> 91	65.4	62.0
ACE MTCK FL 2L	5'-d(CGG AGC AGA GAG CCC CCC CAC TA)-3'	1384 <- 1406	66.0	
ACE MTCK FL 2U	5'-d(GCT TTC CTA CAG CTC ATT TGT TTC TTT TAA AGA GTT ACC)-3'	53 -> 91	65.4	62.0
ACE MTCK FL L	5'-d(GTC GTT GTT TTT ATT GAA GTC AGG AAT AGT GAT GA)-3'	1544 <- 1578	63.3	

In the degenerate primer pair (CK-2U // CK-2L) the N, S, W, and Y designations indicate ambiguous positions, which means that these sequences are of mixed base composition where N = a + c + g + t, S = c + g, W = a + t, and Y = c + t.

[a] Location indicates the nucleotide position on the transcript where a primer hybridizes. Numbering of the full-length cDNA sequence begins at the first nucleotide. [b] Unless otherwise indicated, melting temperatures as determined by PrimerSelect of Dnastar (see Material and Methods). [c] Annealing temperaures were empirically determined starting with those given by PrimerSelect. Touchdown conditions (see Materials and Methods) are indicated by decreasing temperatures that are separated by arrows. [d] Melting temperature estimates provided with GIBCO BRL's "Certificate of Analysis" for primers in 50 mM NaCl. [e] AP-1 designates Adaptor Primer 1. This is supplied with CLONTECH's Marathon Kit and is designed to hybridize to their adaptor sequence (see Material and Methods). [f] Melting temperatures provided by CLONTECH.
-> denotes a sense-strand primer and <- an antisense-strand primer.

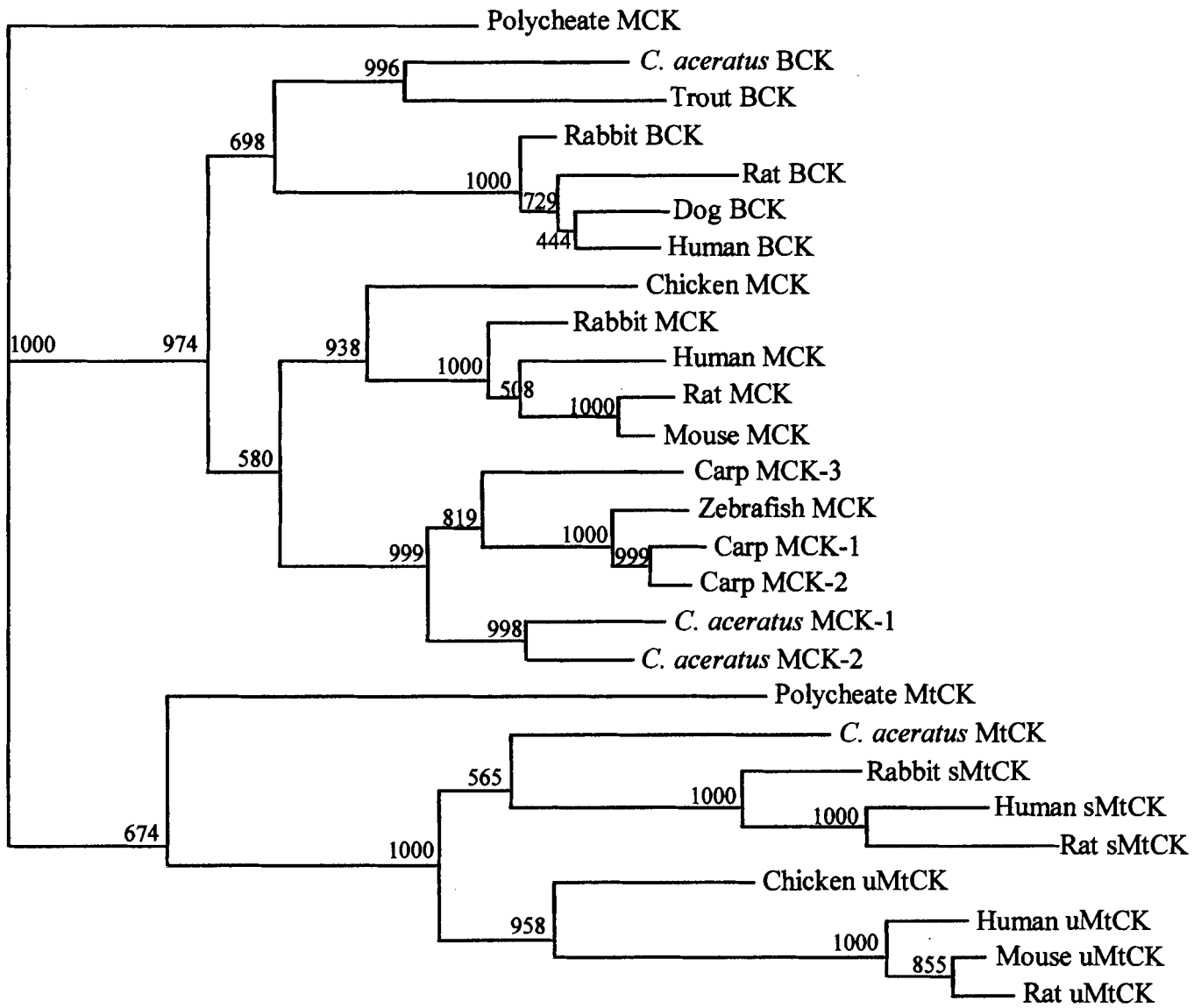
Polycheate MCK
C. aceratus BCK
Trout BCK
Rabbit BCK
Rat BCK
Dog BCK
Human BCK
Chicken MCK
Rabbit MCK
Human MCK
Rat MCK
Mouse MCK
Carp MCK-3
Zebrafish MCK
Carp MCK-1
Carp MCK-2
C. aceratus MCK-1
C. aceratus MCK-2
Polycheate MtCK
C. aceratus MtCK
Rabbit sMtCK
Human sMtCK
Rat sMtCK
Chicken uMtCK
Human uMtCK
Mouse uMtCK
Rat uMtCK
996
698
1000
729
444
1000
974
938
1000
508
1000
580
819
1000
999
999
998
565
1000
1000
674
1000
958
1000
855

Figure 17. Alignment of MCK-b, MCK-a, BCK, and MtCK cDNA sequences from *C. aceratus*. MCK-b, MCK-a, BCK, and MtCK denote muscle-b, muscle-a, brain, and mitochondrial isoforms respectively. Differences between these sequences are shown. Identities are indicated by dots and gaps are indicated by dashes. Lower-case letters indicate 5′ and 3′ UTRs while ORFs are shown by upper-case letters. Residues 108-to-218 of the MtCK sequence encodes MtCK's transit-sequence and is shown in bold-type and underlined. ATG start and TAA termination codons are shown in bold-type with a double underline. The putative poly(A) signal sequence is shown in bold-type and underlined. These sequences are found 18-to-23 nucleotides from the last nucleotide of each 3′ UTR.

```
MCK-b                      a- -ttggtgaac aggttctgat ccc-----ag  25
MCK-a                  ttttg.c t......... ...a...... ...a----..  33
BCK                       -- ---------- ---------- ----------  0
MtCK        ccatcctaa tacgactc.c ta.a.g.--. tc.ag.g.cc g..cgggc..  47

MCK-b       gactgtta-- ---------- ----cttctt tcttttctcc t---aagcag  56
MCK-a       ..t.....-- ---------- ----.c.... ....g..gg. .gtg...t-.  66
BCK         ---------- ---------- ---------- ---------- ----------  0
MtCK        .--..a-.gc tttcctacag ctcat..g.. ......---- ----..ag..  86

MCK-b       gtggag-c-a --agaatcgc aaccATG--- ---------- ----------  79
MCK-a       t.-------- --....agca .t.-...--- ---------- ----------  82
BCK         ---------- ---------- ---------- ---------- ----------  0
MtCK        t.accta.t. tc....ag-- ----...GCT GGCTCTTTCA CACGTATGAT  130

MCK-b       ---------- ---------- ---------- ---------- ----------  79
MCK-a       ---------- ---------- ---------- ---------- ----------  82
BCK         ---------- ---------- ---------- ---------- ----------  0
MtCK        CGGCGGACGC AACGGGGCTG TGCTGTTGGC CAGCCTGGGC GCGGGAACCA  180

MCK-b       ---------- ---------- ---------- --------GC GAAG---AAT  88
MCK-a       ---------- ---------- ---------- --------C. TTTCGGT..C  94
BCK         ---------- ---------- ---------- ---------- -------..C  3
MtCK        TGGCGACTGG TTTCCTGATG AGTGATAACC CCCTAGCT-- ----------  218

MCK-b       TGTCATAACG ACTACAAGAT GAAGTTCTCA GGGGACGAGG AGTTCCCCGA  138
MCK-a       ACC..C...A .C.T...AC. C..C.A.AAG .TT..G..T. ..........  144
BCK         ACG..CC..A CGATG..... ...A.A.G.T TCG..TC... ...AT..T..  53
MtCK        GC.G.GGT.A GGACA...C. C---.A.C.C CCCAGCTCT. .T........  265

MCK-b       CCTGTCGCTG CACAACAACC ATATGGCTAA GGTGCTGACC AAGGAGATCT  188
MCK-a       T......AA. .......... .......G.. .......... .....AC.G.  194
BCK         ...CAGCAAA ........T. .......C.. .A.C.....T CCT.CC..G.  103
MtCK        ....AGGAAA .........T GC.....C.. ..CT.....T CC..CC..T.  315

MCK-b       ATGCCAAGCT GAGGGGAAAG TCTACCCCCA GCGGCTTCAC CGTGGATGAT  238
MCK-a       .C.G....A. T..A.AC.G. CAG..A..T. .T....A... .C.......C  244
BCK         .C.AG..T.. ....A.C..A GAG..G.... ....A..T.. TC........  153
MtCK        .C.G..GA.. .....AC... ATC.....   A.AA..GG.. .C....CC.G  365
```

Figure 17 (continued)

```
MCK-b     GTCATCCAGA CTGGTGTTGA CAACCCTGGT CACCCCTTCA TCATGACTGT  288
MCK-a     .......... .......G.. ......C... .......... ..........  294
BCK       .....T.... ....GA.... T.....A..C .......... ..........  203
MtCK      TG......A. .C..A..G.. ......C..A .......... ...A...C..  415

MCK-b     TGGTTGCGTT GCTGGTGACG AGGAGTGCTA TGAAGCCTTC AAGGAGCTGC  338
MCK-a     ...C...... ........T. ......C... C..G.T.... .....T...T  344
BCK       G..C.....C ..C..A.... .....GCA.. C..G.T.... ..........  253
MtCK      G..C..T..G ........T. .....AG... C..G..G... TCT..A..CT  465

MCK-1     TGGACCCCAT CATCTCTGAC CGTCATAGTG GATACAAGCC CACCGACAAG  388
MCK-2     .......... ......A... ......G... .......... ...T......  394
BCK       ........G. ....GAG... A.G...G.A. .C.....A.. .T.A......  303
MtCK      .T........ ....AAA... A.G..CAAC. .C...G.C.. ...CAC..T.  515

MCK-1     ---CATTCGA CCGACCTGAA CTTCGAGAAC CTGAAGGGAG GTGACGACCT  435
MCK-2     ---..CGT.. .A........ .......... ........C. ..........  441
BCK       ---..CAA.. .T...A.C.. .CCA..T... ........A. ..........  350
MtCK      ACT..CCCC. .T......G. .GC.TCC..- --..TAACCA A..G..TGT.  562

MCK-b     GGACCCCAAC TACGTGCTGT CCAGCCGCGT GCGTACCGGA CGCAGCATCA  485
MCK-a     .......GC. .....T.... .......... ......T..C ..........  491
BCK       T...T.AG.. .....C...A G.TCT..... ...A..A..C ......G..C  400
MtCK      T...GA...A .....C.... .GTC...T.. C..C..T..G .....T...C  612

MCK-b     AGGGATTCAC CCTGCCCCCC CACAACAGCC GTGGCGAGCG CAGAGGCATT  535
MCK-a     ....C..... .......... .......... .......... .........C  541
BCK       GT..C...TG ......A..T ...TG..... .A..A...A. GC.T.CTG.G  450
MtCK      GC..GC.G.G ...C...... GC.TG.TC.A .G.CG..... .C.T.AGG.G  662

MCK-b     GAGAAGCTGT CCATTGAAGC TCTGGCCAGC CTGGATGGGG AGTTCAAGGG  585
MCK-a     .......... ..G....G.. ....A..... ........C. ..........  591
BCK       ...C....C. ....C..G.. .....A.TCT ...AG...A. .CC.GC....  500
MtCK      ...CG.G..G TGG.GATG.. C......G.. ...A.G..A. .CC.GGCC..  712

MCK-b     AAAGTACTAC CCCCTGAGCG GCATGACCGA CGCCGAGCAG GACCTGCTGA  635
MCK-a     .......... .......AGT C......T.. T..G...... ....A.....  641
BCK       G......... G......AGA A....T.A.. T..T...... C.G.A...C.  550
MtCK      .CGC...... GG....C.AG A.C....A.. .AAG...... C.G.A...C.  762

MCK-b     TCAACGATCA CTTCTTGTTT GACAAGCCCG TGTCCCCCCC GCTGACCTGC  685
MCK-a     .......... ....C....C .......... .C..T....T ..........  691
BCK       ..G....C.. ....C..... ........A. ....T..T.T ....CTGGC.  600
MtCK      .TG....C.. ....C..... ........T. .C..T..T.T .T....A..T  812

MCK-b     GCCGGAATGG CCCGTGACTG GCCCGACGGC AGAGGCATCT GGCACAACAA  735
MCK-a     ..T....... .......... .......... .........A T.......G.  741
BCK       T......... G......... ........C. ..G....... ........G.  650
MtCK      ...TTT.... ..A.A..... ...T....C. .......... ..........  862
```

Figure 17 (continued)

```
MCK-b     CAACAAGACC TTCCTGGTCT GGGTGAACGA GGAGGATCAT CTGCGTGTCA  785
MCK-a     .......... .......... .......... .......... ..........  791
BCK       .......... .....T..G. .......T.. ......C... ........T.  700
MtCK      TG.G...... ......A... .......T.. ......C..C ACCA.A....  912

MCK-b     TCTCCATGCA GCAGGGCGGC AACATGAAGG AGGTCTTCAG ACGCTTCTGC  835
MCK-a     .......... .......... .......G.. ..........A G.........  841
BCK       .......... .A.A..T... ....C..... .A..G....A C.........  750
MtCK      ........G. .A....A... .........A GA..G..TG. GA.A......  962

MCK-b     GTTGGTCTGC AGAACATTGA GGGCATCTTC AAGAAGCACA ACCATGGCTT  885
MCK-a     .....C...A ....G..... ..AG...... .........G GA..C.....  891
BCK       ACC..A..C. CC..G..... .ACCC.G... ...G..AGG. .A....AA..  800
MtCK      AGA..A..CA .AC.GG.G.. ACAGC.GA.. C..G..AGAG GCTGG.AG..  1012

MCK-b     CATGTGGAAC GAGCATCTGG GCTACATCCT GACCTGCCCC TCCAACCTGG  935
MCK-a     .......... ........C. .......... .......... ..........  941
BCK       .......... .....C.... .....G.... C........A ..........  850
MtCK      .......... ..A.GC.... .A........ C..A..T... ..........  1062

MCK-b     GAACCGGCCT GCGCGGTGGA GTGCACGTCA AGCTGCCCAA GCTCAGCACA  985
MCK-a     .......... ...T...... ..C....... ....C..... ...G...GT.  991
BCK       .C..T..T.. .....CC..T ........G. .........A CT.G....AA  900
MtCK      .C..T..A.. CA.G.C...C ........GC GC.....A.. T..C....AG  1112

MCK-b     CACGCCAAGT TCGAGGAGAT TCTGACCAGA CTGCGTCTGC AGAAGCGTGG  1035
MCK-a     .......... ....C..... C..C.G.... .......... .......C..  1041
BCK       A.T....... .T.....T.. ...C.AG.AG ...A.G..C. ..........  950
MtCK      G..ATACGT. ..TCCA.... C..CGA..AC .....G.... .....A.A..  1162

MCK-b     AACAGGTGGT GTGGACACAG CCTCCGTGGG TGGTGTGTTC GACATCTCCA  1085
MCK-a     C......... .......... .......... .......... ..........  1091
BCK       ...C.....C .......... ..G.T..... C..A...... ..........  1000
MtCK      C........A .......... .TG..ACT.. A.ACACC..T .....T....  1212

MCK-b     ACGCTGACCG TCTGGGCTCC TCCGAGGTGG CCCAGGTGCA GATGGTGGTT  1135
MCK-a     .......... .......... .......... .......... .C........  1141
BCK       ....C...A. G.......T. .......... AG.T...... .........G  1050
MtCK      ..AAC..... .......AAA ..T....... AG.TT..C.. ....T....G  1262

MCK-b     GATGGTGTCA AGCTGATGGT TGAGATGGAG AAGAAGCTGG AGAAGGGAGA  1185
MCK-a     .......... .......... .......... .......... ..........  1191
BCK       .....C.... G......... G......... .......... .......CC.  1100
MtCK      .....C.... .CTACC..A. ...ATGT... ......A... .........C.  1312

MCK-b     GGCTATCGAC AGCATGATCC CCGCCCAGAA G--------- TAAagaggga  1226
MCK-a     .......... .......... .......... .--------- ..........  1232
BCK       .T.C.....T .A.G.C..G. .......... .--------- ....------  1135
MtCK      ..AC...A.A GT.CC.TCT. ...T.ACCC. .TACAGGAAG ....a..---  1359
```

Figure 17 (continued)

```
MCK-b     caatcttgca tttacctcac gaccattcat gtgcaatgga accagctgac  1276
MCK-a     .......... .......... .......... .......... ..........  1282
BCK       ------ca.. .---...g.. .c....---- --------a. ...t-.ac..  1163
MtCK      -----c..a. c.c.t.--.. ag.-.ccgg. ..-t.g...g gg-g...ct.  1399

MCK-b     gggcgtgcag aggagacaga agctcaccag agactattga ctctgctcgc  1326
MCK-a     .......... .......... .......... .......... ..........  1332
BCK       ..c.c.c.-- ---------- --.c.t..t. .-.tg..... .....-..-.  1196
MtCK      t.ctcc---- ---------g .....c..cc .a..ctca.. .---.tct.t  1434

MCK-b     ctgtgtcttc cttccagctt tgtggttcac atccttcctt ttgttctcgt  1376
MCK-a     .......... .......... .......... .......... ..........  1382
BCK       ...aa.---- ------..a. .c..ta.... .g------g. ..ggat.ttg  1230
MtCK      .c.------- ..g.t.---- -------..g gagg..t... .-------ac  1458

MCK-b     tctcctgtgt tggttggtaa catcctggga tcagcctcca ctgagctggg  1426
MCK-a     .......... .......... .......... .......... ..........  1432
BCK       .-.--..... --a..--... -.a....--- ---------- -....-----  1253
MtCK      .t...aacaa a.a...-c.. atctt.at.. .-.a..a.at t.t..tca--  1504

MCK-b     ctcgcctagc agacgtggta tcacctactt ttttttatga aaagtaatga  1476
MCK-a     .......... .......... .......... .......... ..........  1482
BCK       ---------- -..--...c. --------- -------.... ----------  1264
MtCK      -.g.a..-.. ..ttag..gg gatt....c. caag..ccag gtca.c.ct.  1552

MCK-b     ttattgacgc tgttcatatt gct**caataaa** aaaagtacc- ----gc       1517
MCK-a     .......... .......... .......... .........- ----..       1523
BCK       ---------- ---------- ----...... ...t..tctg gt--a.       1282
MtCK      ..cc....-- --..------ ---..... ..c.acga.a ataa..       1585
```

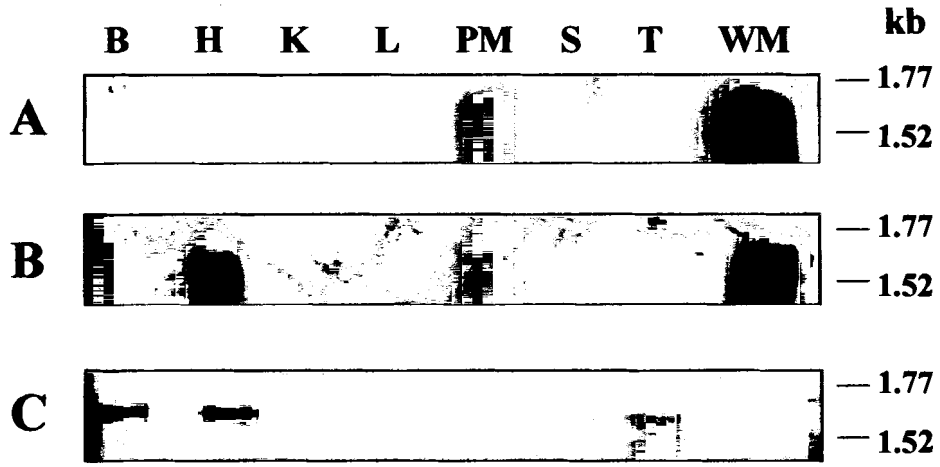

Figure 18. Northern blots of total RNA from *C. aceratus* tissues. As indicated at the top of the figure, RNA was from the following tissues: B, brain; H, heart; K, kidney; L, liver; PM, pectoral muscle; S, spleen; T, testis; WM, white muscle. Panel A: this northern was screened with a ^{32}P-labeled MCK specific probe. Panel B: this northern was screened with a ^{32}P-labeled MtCK specific probe. Panel C: this northern was screened with a DIG-labeled BCK specific probe was used. Molecular size markers given at the right of each panel are in kilobases (kb).

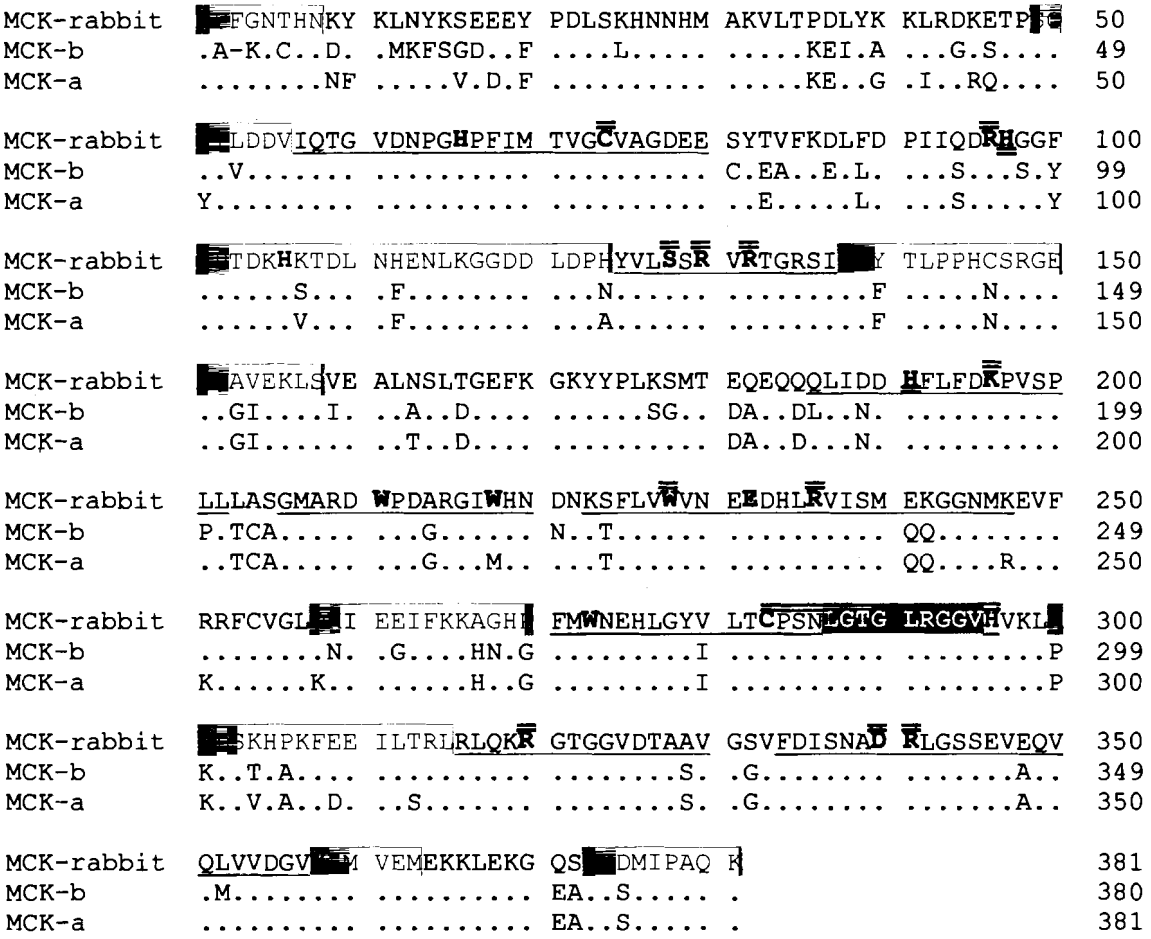

Figure 19. Alignment of cytosolic muscle CK monomer amino acid sequences. *C. aceratus* CK deduced monomer sequences are designated MCK-b and MCK-a and are compared to the rabbit MCK monomer sequence. Differences between *C. aceratus* sequences and rabbit MCK are shown. Dots indicate identities between *C. aceratus* sequences and the rabbit sequence. According to Muhlebach *et al.* (1994), gray blocks indicate "signature" cytosolic muscle CK isoform residues. Residues with a single underline are conserved in all CK isoforms. Residues with a double-line above them are *at* the active-site. Residues shown in the black box are the putative adenine-binding site. In the folded protein, residues found *near* the active-site are shown in bold-type with a double-line above them. The arginines found in this group of residues are involved with nucleotide binding and interact with phosphate groups of ADP or ATP (Wood *et al.*, 1998; Edmiston *et al.*, 2001). The glutamate at position 232 might function as an acid-base catalyst at the guanidino group of PCr or Cr (Cantwell *et al.*, 2001). Histidine residues shown in bold-type and with a double-line below them contribute to enhanced substrate binding (synergism) (Chen *et al.*, 1996). Conserved tryptophans (Clottes and Christian, 1996) and histidines (Chen *et al.*, 1996; Forstner *et al.*, 1997) are shown in bold-type.

Table 10. Summary of amino acid differences between *C.aceratus* MCKs and rabbit MCK

Residue #[1]	*C. aceratus* MCK-b	Rabbit MCK
40	Aln	Lys
44	Gly	Asp
98	Ser	Gly
178	Gly	Ser
186	Leu	Gln
259	Asn	Lys
262	Gly	Glu
	MCK-a	
107	Val	Lys
124	Aln	His
163	Thr	Asn
218	Met	Trp
	MCK-b & MCK-a	
203	Thr	Leu
204	Cys	Aln
205	Aln	Ser
329	Ser	Aln
348	Aln	Glu
372	Aln	Ser
375	Ser	Asp

[1] Residue number is based on the rabbit MCK sequence.

Chapter 5

DISCUSSION

The results of this work have revealed several interesting characteristics of *C. aceratus* muscle-specific CKs that may have important implications with respect to physiological adaptation to the chronically cold Antarctic environment and the inability of their glycolytic enzymes to function efficiently under these conditions. This research has demonstrated: (1) Two distinct MMCK isoforms are present in *C. aceratus* white skeletal muscle (Fig. 4). cDNA sequences confirms the existence of these two forms (Fig. 17). (2) One or both of these MMCKs is cold-temperature adapted. On average, these MMCKs function very efficiently at the physiological temperature of *C. aceratus*, displaying an apparent V_{max} at 0° C that is greater-than that of eurythermal fish at 25° C and, when taking into account Q_{10} analysis, comparable to rabbit MMCK at 38° C (Tables 2 and 4). (3) These MMCKs display pH optimums appropriate for the higher intracellular pH of *C. aceratus* sarcoplasm (Fig. 10). (4) Average apparent K_ms of these MMCKs at 0° C are similar to those of fish, mammalian, and bird MMCKs at their body temperatures (Table 4). The highly efficient activity of MMCK at cold temperature could contribute to efficient burst activity of Antarctic *C. aceratus* and may supplement or overcome the deficiency of their glyoclytic capacity.

5.1. *C. aceratus* MMCK's enzymatic efficiency is mediated by its activation free energy.

The purpose of this section is to first describe the validity of using V_{max} as a measure of enzyme efficiency. Then, that one or both *C. aceratus* MMCKs have undergone temperature compensation is discussed. Finally, a discussion of how thermodynamic activation parameters help us to understand how this higher efficiency can occur is presented.

The Michaelis-Menten equation is $v = k_{cat}[E]_T[S]/(K_m + [S])$, where v is the velocity, k_{cat} is the catalytic constant, $[E]_T$ is the total enzyme concentration, [S] is the substrate concentration, and K_m is the Michaelis-Menten constant (Cornish-Bowden, 1995). It is apparent from the Michaelis-Menten equation that when [S] is much greater-then K_m that $v = k_{cat}[E]_T$. The right side of this equation is referred to as the limiting velocity or V_{max} (Cornish-Bowden, 1995). Under the Briggs-Haldane assumptions of steady-state, k_{cat} has properties of a first-order rate constant and directly indicates how competent the enzyme is at forming product once the enzyme-substrate complex has formed (Cornish-Bowden, 1995). Thus, apparent V_{max} measurements can be used to indicate whether or not an enzyme is efficient at converting substrate to product.

An enzyme is considered to have undergone cold-temperature adaptation if its specific activity (V_{max}/mg) at low temperature is close to that predicted by a Q_{10} analysis (Clarke, 1991). Thus, it is significant to find that *C. aceratus* MMCKs have a mean specific activity that is 2-to-4 times higher than that predicted from a Q_{10} analysis of rabbit MMCK data. Between 0° and 38° C rabbit MMCK's specific activity increased

about 60 fold (Table 2), under the conditions used here. Over this temperature range increases in specific activity are not linear and range from 4-to-1.2 fold for every 10° C increase in temperature. Thus, the average Q_{10} for rabbit MMCK is estimated to be 2.0-to-3.0. This analysis indicates that one would anticipate that at 0° C *C. aceratus* MMCK might have a specific activity of 20-to-35 U/mg. However, one or both of *C. aceratus* MMCKs have high enzyme efficiency (at least 75-to-90 U/mg). In addition, this high specific activity matches or exceeds that of other eurythermal and cold-temperate teleost MMCKs (Table 2). These findings are consistent with the definition of cold-temperature adaptation.

According to Erying's transition-state theory, we can suggest that a cold-adapted enzyme is as efficient or more efficient than its warm-adapted counterpart at forming a stable transition-state or activated enzyme-subtrate complex ($[ES]^{\ddagger}$). Erying's equation ($k = (RT/N_Ah)e^{-\Delta G\ddagger/RT}$) defines the second-order rate constant (k) for the dissociation of $[ES]^{\ddagger}$ into [E] and [S] (Cornish-Bowden, 1995). In this equation R is the gas constant, T is the temperature, N_A is the Avogadro constant, h is Plank's constant, and $\Delta G^{\ddagger}$ is the activation free energy (Cornish-Bowden, 1995). Erying's equation is derived by assuming that the *activated* ES complex is in thermodynamic equilibrium with E and S and therefore, can also be written as $k = (RT/N_Ah)K^{\ddagger}$, where $K^{\ddagger}$ is the equilibrium constant (Eisenberg and Corthers, 1979). This is because, $-RTlnK^{\ddagger} = \Delta G^{\ddagger} = \Delta H^{\ddagger} - T\Delta S^{\ddagger}$, where $\Delta H^{\ddagger}$ is the activation enthalpy and $\Delta S^{\ddagger}$ is the activation entropy. From this

it can be shown that Erying's equation can be linked to the Arrhenuis equation ($k = Ae^{-Ea/RT}$) where, A is a constant at a given temperature and from Erying's equation $A = (RT/N_Ah)e^{\Delta S‡/R}$ while Ea is the activation energy and from Erying's equation $Ea = \Delta H‡ + RT$ (Cornish-Bowden,1995). In the present study, Arrhenuis plots provided Ea data and this allowed for an estimation of rabbit and *C. aceratus* MMCKs' thermodynamic activation parameters (Low and Somero, 1976; Hochachka and Somero, 1984; Ciardiello *et al.*, 2000; Lonhienne et al., 2000). This showed that *C. aceratus* MMCK has a $\Delta G‡$ similar to that of rabbit MMCK (Table 3). As just pointed out both $\Delta H‡$ and $\Delta S‡$ contribute to $\Delta G‡$. The probability of forming the transition-state is evaluated by measuring the activation entropy (Cornish-Bowden, 1995), which provides a measure of the relative degrees of freedom available to the reacting molecules (Eisenberg and Crothers, 1979). Activation enthalpy gives a measure of the bond-breaking or bond-forming energies that participate in the transition-state (Cornish-Bowden, 1995). Formation of the transition-state is an endergonic process because an input of energy is required for the formation of partially broken bonds (Eisenberg and Crothers, 1979). Generally, the number of bonds involved in maintaining the conformation of a warm-adapted enzyme is thought to be larger than that of a flexible cold-adapted enzyme (Hochachka and Somero, 1984; Fields and Somero, 1998). Thus, relative to cold-adapted enzymes, conformational changes of warm-adapted enzymes may require disruption of a larger number of bonds. If such conformational changes involve formation of the transition-state then the result is an increase in $\Delta H‡$ and thus $\Delta G‡$. This may explain the finding that MMCK from *C. aceratus* has a $\Delta H‡$ that is about 7 kcal/mol lower than the

$\Delta H^{\ddagger}$ of rabbit MMCK (Table 3). Other homologous enzyme comparisons have obtained activation enthalpy data that differ in a manner similar to that shown here (Johnston and Goldsplink, 1975; Hochachka and Somero, 1984; Ciardiello *et al.*, 2000). On the other hand, the free entropy of activation for *C. aceratus* MMCK is negative. From the classical perspective of entropy this is unfavorable while that of rabbit MMCK is favorable (Table 3). A possible explanation for this difference is that the relatively rigid rabbit MMCK is more efficient at holding the substrates close together while the flexible *C. aceratus* MMCK has a tendency to "flop about". This latter property would be disruptive to proper substrate-substrate orientation. That is, the collision frequency of properly oriented substrates is lower in the case of the *C. aceratus* MMCK reaction. Fields and Somero (1998) and Ciardiello *et al.* (2000) have pointed out that the greater flexibility (entropy) that is an inherent property of a cold-adapted enzyme requires less energy (enthalpy) to bring about conformational changes, as explained above. Lower activation entropies have been observed for other homologous enzyme comparisons as well (Hochachka and Somero, 1985; Ciardiello *et al.*, 2000). The resulting $\Delta G^{\ddagger}$s for these rabbit and icefish MMCKs differ by about 1 kcal/mol, which is comparable to what has been previously reported (Hochachka and Somero, 1985; Ciardiello *et al.*, 2000). The apparent modest changes in $\Delta G^{\ddagger}$ between cold-adapted and warm-adapted enzymes can be interpreted from two perspectives. One is the logarithmic relationship between $\Delta G^{\ddagger}$ and velocity. This means that at a given temperature a decrease of 1 kcal/mol (less-than the energy of one H-bond; Habermann and Murphy, 1996) translates into a 5 fold increase in velocity (Eisenberg and Crothers, 1979; Hagelauer and Faust, 1982). The second is that for the attainment of temperature adaptation the evolutionary pressure may

be on the attainment of an optimal $\Delta G^{\ddagger}$ (Low *et al.*, 1973; Low and Somero, 1976). The offsetting contributions from $\Delta H^{\ddagger}$ and $\Delta S^{\ddagger}$ are what bring about the relatively small differences between $\Delta G^{\ddagger}$s observed between cold- and warm-adapted enzymes (Hochachka and Somero, 1984; Lonhienne *et al.*, 2000).

5.2. Physiological significance of conserved K_ms.

Comparative studies have revealed that cold-adapted and warm-adapted enzymes have similar K_ms, when measured at the organisms body temperature (Hochachka and Somero, 1984; Fields and Somero, 1998; Ciardiello *et al.*, 2000). Such data implies that cells from different vertebrates maintain similar intracellular substrate concentrations (Hochachka and Somero, 1984; Fields and Somero, 1998). For mammals, the concentration of PCr in resting muscle has been reported to be in the range of 20-to-35 mM while the free ADP concentration is about 1-to-20 μM (Wallimann *et al.*, 1992). The concentration of PCr found in fish white muscle tissue examined to date is similar to that reported for mammalian muscle (Hunter, 1929; Danulat and Hochachka, 1989; Schulte *et al.*, 1992; Arthur *et al.*, 1992). As pointed out by Arthur *et al.* (1992), measurements of PCr concentrations are subjected to errors due to acid hydrolysis of PCr during the extraction process. Those authors suggest that a good estimate of PCr concentration can be obtained if one considers that about 80% of the total creatine concentration in the cell is in the form of PCr. Thus, Dunn and Johnston's (1986) data indicate that the PCr concentration of Antarctic fish white muscle is about 30 mM. No data are available on the free ADP concentration in fish muscle. However, the total ADP concentration in fish muscle is similar to that found in mammalian muscle (Danulat and

Hochachka, 1989; Schulte *et al.*, 1992; Arthur *et al.*, 1992). Consequently, the free ADP concentration is likely to be similar as well. Therefore, during cold- or warm-adaptation, changes in enzyme structure are constrained by a need to minimize any changes to K_m(s) (Hochachka and Somero, 1984; Fields and Somero, 1998). This is apparent when one considers that *in vivo* enzymes function at substrate concentrations that are near their K_ms, which ensures that an enzyme maintains the ability to respond to changes in substrate concentration. For example, a decrease in substrate concentration results in a decrease in rate while an increase results in a rate increase (Hochachka and Somero, 1984). In broad terms, the data collected in Table 4 shows that K_ms for the MMCKs is consistent with this model and it is apparent that average apparent K_ms for *C. aceratus* MMCKs are the same as those found for other vertebrate MMCKs. However, the average apparent K_m of *C. aceratus* MMCK for PCr is roughly fives times and prehaps as much as twenty times higher (see Table 4: rabbit[g], human, carp-2) than that for the warm-adapted MMCKs, except for Ox. This may reflect that a higher concentration of PCr exists in *C. aceratus* white muscle when compared to these other vertebrate muscle PCr concentrations. Moreover, this higher K_m would be predicted if one considers that *C. aceratus* MMCK's higher apparent V_{max} at 0° C is governed to some extend by an increase in its flexibility (Fields and Somero, 1998). That is, its number of conformational states increases and this cold-adapted enzyme will exhibit a larger number of conformations that interact inefficiently or not at all with PCr (Fields and Somero, 1998). Therefore, although the K_ms of C. aceratus MMCK for ADP and PCr are

similar the observed differences may be significant and correlated its high efficiency at 0° C.

5.3. *C. aceratus* MMCK's cold-adaptation is a reflection of its structure.

Increased flexibility, that is, fewer H-bonds and ionic interactions, may allow enzymes to function efficiently at low temperatures because necessary conformational changes that often occur upon substrate binding should be less constrained (Somero, 1975, Hochachka and Somero, 1984; Sidell and Moerland, 1989; Fields and Somero, 1998; Lonhienne *et al.*, 2000). Conformational changes occur when rabbit MMCK combines with substrate (Forstner *et al.*, 1998; Shen *et al.*, 2001). Such substrate binding induced conformational changes are characteristic of many enzymes (Hochachka and Somero, 1968, Hochachka and Somero, 1984; Fields and Somero, 1998). However, such changes in protein structure may make cold-temperature adapted enzymes less stable and more susceptible to thermal denaturation (Fields and Somero, 1998). MMCK from *C. aceratus* white muscle appears to fit this paradigm. Thus, *C. aceratus* MMCKs have only 50% of its activity after a 30 minute incubation at 25° C. In contrast, shark, mammalian, and bird MMCKs are 50% inactivated after incubation at temperatures above 50° C (Dawson *et al.*, 1967; Grossmann and Mollo, 1979; Gray *et al.*, 1986). Therefore, *C. aceratus* MMCKs apparently have tertiary and quaternary interactions that are capable of maintaining a native structure only at cold temperatures (≤ 10° C) and are disrupted at relatively low temperatures (20°-to-30° C).

Comparisons between primary structures of homologous proteins from endotherms and ectotherms is often used as a way to predict those amino acid residues

that most likely contribute to tertiary and quaternary structural changes that bring about differences in thermal stability (Watts *et al.*, 1980). Two perspectives can be taken when this rationale is applied to a comparison between the amino acid sequences of *C. aceratus* MCKs and the amino acid sequence the rabbit MCK. First, it has been established that thermal denaturation of rabbit MMCK's active-site precedes its global thermal denaturation (Bai *et al.*, 1998; Lyubarev *et al.*, 1999; Cao *et al.*, 1999). Hence, amino acid composition at or near MMCK's active-site may participate in active-site stability. Thus, differences between rabbit and *C. aceratus* MCK sequences at amino acid residue positions 98, 124, and 186 are predicted to affect the thermal stability at the active-site of *C. aceratus* MMCKs (Fig. 19). This is because these three residues are within 2-to-5 residues of known active-site residues. Second, from a global perspective the differences identified in Table 10 might contribute to thermal stability. For example, differences between rabbit and *C. aceratus* MCK sequences at positions 40, 44, 107, 124, 186, 259, 262, 348, and 375 indicates the loss of a charged amino acid residue in *C. aceratus* MCKs. When found at the proteins surface, such charged residues usually participate in salt-bridges. Relative to H-bonds, such electrostatic interactions are capable of absorbing more heat before breaking and therefore, are more effective at stabilizing protein structure (Hochachka and Somero, 1984). These are replaced in *C. aceratus* MCKs by either polar residues or by hydrophobic residues. Polar residues participate in weaker H-bond interactions and hydrophobic interactions are weaker at cold temperatures (Hochachka and Somero, 1984; Habermann and Murphy, 1996; Schellman, 1997). Another consideration is dimer-dimer interactions that involve residues N8-K9, Y14, E18-D22, K25, S49, D54, H145-R152, K177, and R209-D210 (Rao *et al.*, 1998; Shen *et*

al., 2001). In *C. aceratus* MCK-b phenalanine replaces tyrosine at position 14, leucine replaces lysine at position 25, and serine replaces lysine at position 177 (Fig. 19). Thus, intermolecular interactions between MCK-b monomers may be weakened. Only a more thorough 3-D computer model analysis or site-directed mutagenesis studies can determine whether or not these predictions are valid. However, what is shown by this comparative data is that apparently few amino acid residues mediate the lower thermal stability of *C. aceratus* MMCK as well as its necessary functional flexibility, which is consistent with what has been found in other cold-adapted enzymes (Fields and Somero, 1998).

5.4. Physiological significance of *C. aceratus* MMCK pH optimum.

Under the conditions used here *C. aceratus* MMCKs have maximum activity between pH 7.50 and pH 7.60 at 0.5° C (Fig. 2), which is consistent with earlier results (Walesby and Johnston, 1979; Dunn and Johnston, 1986; Johnston, 1987). The pH optimum found here is similar to the physiological pH of *C. aceratus* white muscle, which is about pH 7.5 (Hardewig *et al.*, 1998; van Dijk *et al.*, 1999). This pH value is consistent with measurements of intracellular white muscle pHs of fish acclimated to temperatures ≤ 5° C (Cameron, 1984; Portner *et al.*, 1990; Lehoux and Guderley, 1997; Arthur *et al.*, 1997). Further support for the contention that pH 7.5 is the resting pH of *C. aceratus* white muscle comes from measurements of resting blood pH. Resting blood pH for *C. aceratus* is pH 7.9-to-8.0 at 1° C (Hemmingsen and Douglas, 1972; Egginton, 1997) and is similar to what has been reported for other Antarctic fish (Qvist *et al.*, 1977; Egginton *et al.*, 1991; Egginton, 1997). What appears to be elevated pH values actually

fit the trend reported for cold-adapted ectotherms (Howell *et al.*, 1970; Rahn and Baumgardner, 1972). Drawing upon this type of data, Hochachka and Somero (1984) predicted that the intracellular pH of Antarctic fish should fall into the range of pH 7.3-to-7.5. Furthermore, Antarctic fish with low glycolytic capacity do not generate large amounts of lactate during burst swimming and their intracellular muscle pH is unlikely to decrease much from pH 7.5 (Dunn and Johnston, 1986; Johnston, 1987). On the other hand, mammalian intracellular muscle pH's range from pH 6.30 (strenuous exercise)-to-7.15 (at rest) (Adams *et al.*, 1991; Pate *et al.*, 1995; Chin and Allen, 1998) and rabbit MMCK has a pH optimum of 6.10-to-6.50 at 30°-to-38° C (Kuby *et al.* 1954; Nihei *et al.* 1961; present research).

The alphastat buffer theory purports that histidine residues in proteins and in small peptides contribute to the buffer capacity of cold-blooded vertebrate tissue (Howell *et al.*, 1970; Rahn and Baumgardner, 1972; Abe, 1981; Abe *et al.*, 1985; Rahn et al., 1975; 1985; Suzuki *et al.*, 1987; Hitzig *et al.*, 1994). This is because as temperature changes the charge of imidazole-histidine remains constant. Yancey and Somero (1978) pointed out that the sensitivity of enzyme function to changes in its charged-state is offset by this property of histidine residues. That is, the proportion of imidazol-histidine ionized remains constant when temperature changes and thus, so does the associated charge (Somero, 1981; Somero, 1986). In the case of MMCK the protonated state of histidine residues affects catalysis (Clarke and Price, 1979; Rosevear *et al.*, 1981; Chen *et al.*, 1996; Forstner *et al.*, 1998). It has been shown that three evolutionarily conserved histidine residues (H96, H190, and H295) participate in MMCK's efficient interaction with substrates (Rosevear *et al.*, 1981; Chen *et al.*, 1996). H96 and H190 appear to be

involved in conformational changes that enhance substrate binding through a synergistic affect. This increases the affinity for second substrate once the first substrate binds (Chen *et al.*, 1996). H295 is essential and mutating it to an asparagine inactivates rabbit MMCK (Chen *et al.*, 1996). These four histidines are conserved in *C. aceratus* MMCKs. Thus, at 0° C and pH 7.50 one would predict that the charge-state of these histidines in *C. aceratus* MMCK would be similar to what occurs in their mammalian homologues at 37° C pH 6.80. Therefore, this property of histidine may contribute to how efficiently *C. aceratus* MMCK's binds its substrates at cold temperature.

5.5. Why does *C. aceratus* express two MMCKs ?

Finding two MCK genes is unusual and birds and mammals carry only one (Muhlebach *et al.*, 1994). Data on other teleosts is sparse, only one MCK cDNA has been reported for zebrafish (GenBank) and electric eel (Batista e Silva *et al.*, 2000). A single MMCK has been isolated from sunfish (Fisher and Whitt, 1979) and cod white muscle (Petrova *et al.*, 1987). Moreover, the ancestral condition appears to be the expression of a single MCK gene. For example, only one MCK sequence has been reported from the cartilogenous skates (West *et al.*, 1984; Giraudat *et al.*, 1984) and only a single MMCK was isolated from shark muscle (Simonarson and Watts, 1972; Gray *et al.*, 1986). Carp are capable of expressing three MMCKs (Sun *et al.*, 1998). Carp are polypoid and have been shown to be capable of expressing different isoforms of enzymes. For example, carp can express a variety of myosin ATPases. These enzymes have different catalytic properties that apparently provide survival advantages when habitat conditions change (Goldspink *et al.*, 1992). In contrast, *C. aceratus* is diploid

(Morescalchi *et al.*, 1992; Capriglione *et al.*, 1994; Prirodina, 1994; Eastman, 1993), stenothermic, and thrives in a habitat where O_2 content is relatively high and constant (Eastman, 1993). Thus, *C. aceratus* is not faced with a variety of habitat conditions. From this perspective there is no obvious selection pressure driving the expression of two MMCK's. One possibility is that the differences in amino-terminus sequences (Fig. 19) between MMCK-b and MMCK-a might direct each isoform to a different subcellular microcomparment. Distinct sequence differences between mammalian BBCK and MMCK are important. Thus, MMCK is the only CK dimer that can bind to the M-line of a sarcomer. This binding is brought about by two 'lysine-charge clamps' that are located within the amino-terminus of the MCK monomer but missing from the BCK monomer (Hornemann *et al.*, 2000). Location at the M-line is physiologically important because it allows MMCK to be directly coupled to myosin ATPase activity (Wallimann and Eppenberger, 1985). For mammals, it has been demonstrated that the amount of MMCK at the M-line is capable of supplying all the necessary ATP to this location (Wallimann and Eppenberger, 1985). This may be an important consideration for fish muscle, as well (Hochachka *et al.*, 1983). Thus, an important difference between MMCK-b and MMCK-a may be the complete loss of the first lysine-charge clamp from MMCK-b. This difference is quite distinct and in MMCK-b at this site a reversal of net charge has occurred. That is, lysine at position 8 in mammalian MCK is an asparate in icefish MCK-b while the lysine a position 24 in mammalian MCK is a leucine in *C. aceratus* MCK-b (Fig. 19). In contrast, in MCK-a lysine at position 8 is replaced by a polar glutamate and lysine at position 24 is conserved (Fig. 19). Thus, *C. aceratus* MMCK-a may have a higher propensity to bind at the M-line while MMCK-b may be found at a

different subcellular location (Kraft *et al.*, 2000). Other considerations that explain the existence of two isforms are less supported by the present data. At this time our data on any kinetic differences between MMCK-b and MMCK-a is equivocal. Further investigation may reveal that these isoforms have different kinetic properties. If this proves to be the case, it may be that *C. aceratus* utilizes one MMCK during the initial phase of a burst response, when substrates are at high concentrations, and rely on the other as subtrate concentrations fall. We have reported average apparent K_ms, but this suggestion implies that these two MMCKs would have different K_ms for ADP or PCr or both. For example, as PCr becomes depleted the rate of one of these MMCKs could remain high because it would continue to be nearly saturated with substrate. This would extend the reserve energy capacity available to *C. aceratus*. Alternatively this type of gene duplication may be a trait of nototheniid genome evolution. For example, nototheniids have two metallothionein genes (Carginale *et al.*, 1998; Bargelloni *et al.*, 1999) while a single metallothionein gene is found in other vertebrates including fishes. The metallothionein genes of *Notothenia coriiceps* are of particular interest because they have identical 3′ UTRs but different 5′ UTRs, which is similar to what was found here for the MCK genes of *C. aceratus*.

REFERENCES

Abe H. (1981) Determination of L-histidine-related compounds in fish muscles using high-performance liquid chromatography. Bull. Jap. Soc. Scient. Fisheries, 47:139.

Abe H., Dobson G.P., Hoeger U., and Parkhouse W.S. (1985) Role of histidine-related compounds to intracellular buffering in fish skeletal muscle. Am. J. Physiol., 249:R449-R454.

Adams G.R., Fisher M.J., and Meyer R.A. (1991) Hypercapnic acidosis and increased $H^2PO_4^-$ concentration do not decrease force in cat skeletal muscle. Am. J. Physiol., 260:C805-C815.

Amicon (1980) Dye-ligand chromatography. Amicon Corporation, Lexington, MA.

Anido V., Conn R.B., Mengole H.F., and Anido G. (1974) Diagnostic efficacy of myocardial creatine phosphokinase using polyacrylamide disk gel electrophoresis. Am. J. Clin. Pathol., 61:599-605.

Appukuttan P.S. and Basu D. (1992) Human brain creatine kinase binding to immobilized cibracron blue F3GA: Characterization and use in purification of the enzyme. Indian J. Biochem. Biophysics, 29:346-349.

Arthur P.G., West T.G., Brill R.W., Schulte P.M., and Hochachka P.W. (1992) Recovery metabolism of skipjack tuna (*Katsuwonus pelamis*) white muscle: rapid and parallel changes in lactate and phosphocreatine after exercise. Can. J. Zool., 70:1230-1239.

Atkinson D.E. (1970) Adenine nucleotides as universal stoichiometric metabolic coupling agents. Adv. Enzyme Regulation, 9:207-219.

Baba N., Kim S., and Farrell E.C. (1976) Histochemistry of creatine phosphokinase. J. Mol. Cell. Cardio., 8:599-617.

Bai J.-H., Zheng S.-Y., and Zhou H.-M. (1998) Inactivation of creatine kinase is due to the conformational changes of the active sites during thermal denaturation. Biochem. Mol. Biol. Int., 45:941-951.

Bargelloni L., Scudiero R., Parisi E., Carginale V., Capasso C., and Pararnello T. (1999) Metallothioneins in Antarctic fish: Evidence for independent duplication and gene conversion. Mol. Biol. Evol., 16:885-897.

Barrantes F.J., Braceras A., Caldironi H.A., Miesdes G., Moser H., Toren Jr. E.C., Roque M.E., Wallimann T., and Zechel A. (1985) Isolation and characterization of acetylcholine receptor membrane-associated (nonreceptor v_2-protein) and soluble electrocyte creatine kinase. J. Biol. Chem., 260:3024-3034.

Batista e Silva C.M., Nunes T.N., Giovanni-De-Simone S., Nery da Matta A., and Hasson-Voloch A. (2000) Purification and partial characterization of creatine kinase from electric organ of *Electrophorus electricus* (L). Int. J. Biochem. Cell Biol., 32:427-433.

Beissner R.S. and Rudolph F.B. (1978) Interaction of cibracon blue 3G-A and related dyes with nucleotide-requiring enzymes. Arch. Biochem. Biophys., 189:76-80.

Bessman S.P. and Geiger P.J. (1981) Transport of energy in muscle: The phosphorylcreatine shuttle. Science, 211:448-452.

Biellmann, J.-F., Samama J.-P., Branden C.I., and Eklund H. (1979) X-ray studies of the binding of cibracon blue F3GA to liver alcohol dehydrogenase. Eur. J. Biochem., 102:107-110.

Bohme H.-J., Kopperschlager G., and Hofmann E. (1972) Affinity chromatography of phosphofructokinase using cibracon blue F3G-A. J. Chromatogr., 69:209-214.

Cameron J.N. (1984) Acid-base status of fish at different temperatures. Am. J. Physiol., 246:R452-R459.

Cantwell J.S., Novak W.R., Wang P.-F., McLeisch M.J., Kenyon G.L., and Babbit P.C. (2001) Mutagenesis of two acidic active site residues in human muscle creatine kinase: Implications for the catalytic mechanism. Biochemistry, 40:3056-3061.

Cao Z.-F., Luo W., and Zhou H.-M. (1999) Effect of Mg^{2+} on the thermal inactivation and unfolding of creatine kinase. Int. J. Biochem. Cell Biol., 31:1307-1313.

Capriglione T., Morescalchi A., Olmo E., Rocco L., Stingo V., and Manzo S. (1994) Satellite DNAs, heterochromatin and sex chromosomes in *Chionodraco hamatus* (Channichthyidae, Perciformes). Polar Biology, 14:285-290.

Carginale V., Scudiero R., Capasso C., Capasso A., Kille P., di Prisco G., and Parisi E. (1998) Cadmium-induced differential accumulation of metallothionein isoforms in the Antarctic icefish, which exhibits no basal metallothionein protein but high endogenous mRNA levels. Biochem. J., 332:475-481.

Chegwidden W.R. and Watts D.C. (1975) Kinetic studies and effects of anions on creatine phosphokinase from skeletal muscle of rehesus monkey (*Macaca mulatta*). Biochem. Biophys. Acta, 410:99-114.

Chen L.H., Borders Jr. C.L., Vasquez J.R., and Kenyon G.L. (1996) Rabbit muscle creatine kinase: Consequences of the mutagenesis of conserved histidine residues. Biochemistry, 35: 7895-7902.

Chin E.R. and Allen D.G. (1998) The contribution of pH-dependent mechanisms to fatigue at different intensities in mammalian single muscle fibers. J. Physiol., 512:831-840.

Ciardiello M.A., Camardella L., Carratore V., and di Prisco G. (2000) L-Glutamate dehydrogenase from the Antarctic fish *Chaenocephalus aceratus* Primary structure, function and thermodynamic characterization: Relationship with cold adaptation. Biochim. Biophys. Acta, 1543:11-23.

Clarke A. (1991) What is cold adaptation and how should we measure it? Amer. Zool., 31:81-92.

Clarke A. and Johnston I.A. (1996) Evolution and adaptive radiation of Antarctic fishes. Trends Ecol. Evol., 8:212-217.

Clarke D.E. and Price N.C. (1979) The reaction of rabbit muscle creatine kinase with diethyl pyrocarbonate. Biochem. J., 181:467-475.

Clottes E. and Vial C. (1996) Discrimination between the four tryptophan residues of MM-creatine kinase on the basis of the effect of N-bromosuccinimide on activity and spectral properties. Arch. Biochem. Biophys., 329:97-103.

Cornish-Bowden A. (1995) Fundamentals of enzyme kinetics. Portland Press Ltd., London, UK.

Crockett E.L. and Sidell B.D. (1990) Some pathways of energy metabolism are cold adapted in Antarctic fishes. Physiol. Zool., 63:472-488.

Danulet E. and Hochachka P.W. (1989) Creatine turnover in the starry flounder, Platichthys stellatus. Fish Physiol. Biochem., 6:1-9.

Dawson D.M., Eppenberger H.M., and Kaplan N.O. (1967) The comparative enzymology of creatine kinase. J. Biol. Chem., 242:210-217.

Dobson G.P., Parkhouse W.S., and Hochachka P.W. (1987) Regulation of anaerobic ATP-generating pathways in trout fast-twitch skeletal muscle. Am. J. Physiol., 253:R186-R194.

Dobson G.P. and Hochachka P.W. (1987) Role of glycolysis in adenylate depletion and repletion during work and recovery in teleost white muscle. J. Exp. Biol., 129:125-140.

Dunn J.F. and Johnston I.A. (1986) Metabolic constraints on burst-swimming in the Antarctic teleost *Notothenia neglecta*. Marine Biology, 91:433-440.

Dunn J.F. (1988) Muscle metabolism in Antarctic fish. Comp. Biochem. Physiol., 90B:539-545.

Dunn J.F., Archer S.D., and Johnston I.A. (1989) Muscle fibre types and metabolism in post-larval and adult stages of Notothenioid fish. Polar Biology, 9:213-223.

Eastman J.T. (1993) Antarctic fish biology. Academic Press, Inc., San Diego, CA.

Eastman J.T. (1995) The evolution of antarctic fishes: Questions for consideration and avenues for research. Cybium, 19:371-389.

Eder M., Stolz M., Wallimann T., and Schlattner U. (2000) A conserved negatively charged cluster in the active site of creatine kinase is critical for enzymatic activity. J. Biol. Chem., 275:27094-27099.

Edmiston P.L., Schavolt K.L., Kersteen E.A., Moore N.R., and Borders Jr. C.L. (2001) Creatine kinase: a role for arginine-95 in creatine binding and active site organization. Biochim. Biophys. Acta, 1546:291-298.

Egginton S. (1997) A comparison of the response to induced exercise in red- and white-blooded Antarctic fishes. J. Comp. Physiol. B, 167:129-134.

Egginton S. and Rankin J.C. (1998) Vascular adaptations for a low pressure/high flow blood supply to locomotory muscles of Antarctic icefish. In: Fishes of Antarctica. A biological overview. di Prisco G., Pisano E., and Clarke A. (eds), Springer-Verlag, Italia.

Egginton S. and Sidell B.D. (1989) Thermal acclimation induces changes in subcellular structure of fish skeletal muscle. Am. J. Physiol., 256:R1-R9.

Eisenberg D. and Crothers D. (1979) Physical chemistry with applications to the life sciences. The Benjamin/Cummings Publishing Co., Inc., Menlo Park, CA.

Eppenberger H.M., Dawson D.M., and Kaplan N.O. (1967) The comparative enzymology of creatine kinase. I. Isolation and characterization from chicken and rabbit tissue. J. Biol. Chem., 242:204-209.

Felsenstein J. (1979) Alternative methods of phylogenetic inference and their interrelationship. Syst. Zool., 28:49-62.

Felsenstein J. (1984) The statistical approach to inferring evolutionary trees and what it tells us about parsimony and compatibility. In: Cladistics: Perspectives on the reconstruction of evolutionary history. Duncan T. and Stuessy T.F. (eds), Columbia University Press, New York.

Felsenstein J. (1988) Phylogenies from molecular sequences: Inference and reliability. Annu. Rev. Genet., 22:521-565.

Fields P.A. and Somero G.N. (1998) Hot spots in cold adaptation: Localization increases in conformational fexibility in lactate dehydrogenase A_4 orthologs of Antarctic notothenioid fishes. Proc. Natl. Acad. Sci. USA, 95:11476-11481.

Fisher S.E. and Whitt G.S. (1979) Purification of the creatine kinase isozymes of the green sunfish (*Lepomis cyanellus*) with blue Sepharose CL-6B. Anal. Biochem., 94:89-95.

Fitch N.A., Johnston I.A., and Wood R.E. (1984) Skeletal muscle capillary supply in a fish that lacks respiratory pigments. Respiration Physiol., 57:201-211.

Forstner M., Muller A., Stolz M., and Wallimann T. (1997) The active site histidines of creatine kinase. A critical role of His 61 situated on a flexible loop. Protein Sci., 6:331-339.

Garber A.T., Winkfein R.J., and Dixon G.H. (1990) A novel creatine kinase cDNA whose transcript shows enhanced testicular expression. Biochim Biophys. Acta, 23:256-258.

Gekko K. and Timasheff S.N. (1981) Mechanism of protein stabilization by glycerol: Preferential hydration in glycerol-water mixtures. Biochemistry, 20:4667-4676.

German Society for Clinical Chemistry (1977) Standard method for the determination of creatine kinase activity. J. Clin. Chem. Biochem., 15:255-260.

Giraudat J., Devillers-Thiery A., Perriard J.-C., and Changeux J.-P. (1984) Complete nucleotide sequence of Torpedo marmorata mRNA coding for the 43,000-dalton v_2 protein: Muscle-specific creatine kinase. Proc. Natl. Acad. Sci. USA, 81:7313-7317.

Goldspink G., Turay L., Hansen E., Ennion S., and Gerlach G. (1992) Switches in fish myosin genes induced by environment temperature in muscle of the carp. Symp. Soc. Exp. Biol., 46:139-149.

Graber N.A. and Ellington W.R. (2001) Gene duplication events producing muscle (M) and brain (B) isoforms of cytoplasmic creatine kinase: cDNA and deduced amino acid sequences from two lower chordates. Mol. Biol. Evol., 18:1305-1314.

Gray K.A., Grossman S.H., and Summers D.D. (1986) Purification and characterization of creatine kinase isozymes from the nurse shark *Ginglymostoma cirratum*. Comp. Biochem. Physiol., 83B:613-620.

Grossman S.H. and Mollo E. (1979) Physical and serological comparison and hybridization of isozymes of creatine kinase from primates. Int. J. Biochem., 10:367-381.

Habermann S.M. and Murphy K.P. (1996) Energetics of hydrogen bonding in proteins: A model compound study. Protein Sci., 5:12291239.

Hagelauer U. And Faust U. (1982) The catalytic activity and activation energy of creatine kinase isoenzymes. J. Clin. Chem. Clin. Biochem., 20:633-638.

Hall T.A. (1999) BioEdit: a user-friendly biological sequence alignment editor and analysis programs for Windows 95/98/NT. Nucl. Acids Symp. Ser. 41:95-98.

Hammes G.G. (1982) Enzyme catalysis and regulation. Academic Press, Inc., Orlando, FL.

Hardewig I., van Dijk P.L.M., and Portner H.O. (1998) High-energy turnover at low temperatures: recovery from exhaustive exercise in Antarctic and temperate eelpouts. Am. J. Physiol., 274:R1789-R1796.

Hemmingsen E.A. and Douglas E.L. (1972) Respiratory and circulatory responses in a hemoglobin-free fish, *Chaenocephalus aceratus*, to change in temperature and oxygen tension. Comp. Biochem. Physiol., 43A:1031-1043.

Hess J.W., Murdock K.J., and Natho G.J.W. (1968) Creatine Phosphokinase: A spectrophotometric method with improved sensitivity. Am. J. Clin. Path., 50:89-97.

Hitzig B.M., Perng W.-C., Burt T., Okunieff P., and Johnson D.C. (1994) ^{1}H-NMR measurement of fractional dissociation of imidazole in intact animals. Am. J. Physiol., 266:R1008-R1015.

Hochachka P.W. and Somero G.N. (1968) The adaptation of enzymes to temperature. Comp. Biochem. Physiol., 27:659-668.

Hochachka P.W., Dobson G.P., and Mommsen T.P. (1983) Role of isozymes in metabolic regulation during exercise: Insights from comparative studies. In: Isozymes: Current topics in biology and medical research. Vol. 8: Cellular localization, metabolism, and physiology. Alan R. Liss, Inc., New York, N. Y.

Hochachka P.W. (1985) Fuels and pathways as designated systems for support of muscle work. J. Exp. Biol., 115:149-164.

Hochachka P.W. and Somero G.N. (1984) Biochemical Adaptation Chp. 11. Princeton University Press, Princeton, NJ.

Horder M., Magid E., Pitkanen E., Harkonen M., Stromme J.H., Theodorsen L., Gerhardt W., and Waldenstrom J. (1979) Recommended method for the determination of creatine kinase in blood modified by the inclusion of EDTA. Scand. J. Clin. Lab. Invest., 39:1-5.

Hornemann T., Stolz M., and Wallimann T. (2000) Isoenzyme-specific interaction of muscle-type creatine kinase with the sarcomeric M-line is mediated by NH2-terminal lysine charge-clamps. J. Cell Biol., 149:1225-1234.

Howell B.J., Baumgardner F.W., Bondi K., and Rahn H. (1970) Acid-base balance in cold-blooded vertebrates as a function of body temperature. Am. J. Physiol., 218:600-606.

Hunter A. (1929) The creatine content of the muscles and some other tissues in fishes. J. Biol. Chem., 81:513-523.

Johnston I.A. (1985) Temperature adaptation of enzyme function in fish muscle. Symp. Soc. Exp. Biol., 39:95-122.

Johnston I.A. (1987) Respiratory characteristics of muscle fibres in a fish (*Chaenocephalus aceratus*) that lacks haem pigments. J. Exp. Biol., 133:415-428.

Johnston I.A. (1989) Antarctic fish – structure, function and physiology. Antarctic Science, 1:97-108.

Johnston I.A. and Goldspink G. (1975) Thermodynamic activation parameters of fish myofibrillar ATPase enzyme and evolutionary adaptations to temperature. Nature, 257:620-622.

Johnston I.A. and Camm J.-P. (1987) Muscle structure and differentiation in pelagic and demersal stages of the Antarctic teleost *Notothenia neglecta*. Marine Biology, 94:183-190.

Jovin T.M. (1973) Multiphasic zone electrophoresis I. Steady-state moving-boundary systems formed by different electrolyte combinations. Biochemistry, 12:871-879.

Khan L.A., Raj M., and Amin M. (1989) Coupling of the enzymic activities of myosin ATPase and creatine kinase and its role in muscular contraction. Indian J. Biochem. Biophysics, 26:148-152.

Kim E.E. and Wyckoff H.W. (1991) Reaction mechanism of alkaline phosphatase based on crystal structures. Mol. Biol., 218:449-464.

Kraft T., Hornman T., Stolz M., Nier V., and Wallimann T. (2000) Coupling of creatine kinase to glycolytic enzymes at the sarcomeric I-band of skeletal muscle: a biochemical study in situ. J. Muscle Res. Cell Motil., 21:691-703.

Kuby S.A., Noda L., and Lardy H.A. (1954) Adenosinetriphosphate-creatine transphosphorylase III. Kinetic studies. J. Biol. Chem., 210:65-82.

Kyhse-Andersen J. (1988) Semidry electroblotting – Transfer using equipment without buffer vessel. In: CRC Handbook of immunoblotting of proteins, I:79-85, Bjerrum O.J. and Heegaard N.H.H. (eds), CRC Press, Boca Raton, FL.

Lehoux E.A. and Guderley H.E. (1997) Thermally induced changes in intracellular pH and modulators of phosphofructokinase in trout white muscle. J. Exp. Biol., 200:931-939.

Lin L., Perryman B., Friedman D., Roberts R., and Ma T.S. (1994) Determination of the catalytic state of creatine kinase by site-direction mutagenesis. Biochim. Biophys. Acta, 1206:97-104.

Londraville R.L. and Sidell B.D. (1990) Ultrastructure of aerobic muscle in Antarctic fishes may contribute to maintenance of diffusive fluxes. J. Exp. Biol., 150:205-220.

Lonhienne T., Gerday C., and Feller G. (2000) Psychrophilic enzymes: revisiting the thermodynamic parameters of activation may explain local flexibility. Biochim. Biophys. Acta, 1543:1-10.

Low P.S., Bada J.L., and Somero G.N. (1973) Temperature adaptation of enzymes: role of the free energy, the enthalpy, and the entropy of activation. Proc. Natl. Acad. Sci. USA, 70:430-432.

Low P.S. and Somero G.N. (1976) Adaptation of muscle pyruvate kinases to environmental temperatures and pressures. J. Exp. Zool., 198:1-12.

Lyubarev A.E., Kurganov B.I., Orlov V.N., and Zhou H.-M. (1999) Two-state irreversible thermal denaturation of muscle creatine kinase. Biophys. Chem., 79:199-204.

Mickelson J.K., Carlson C.J., Kaysen G.A., and Rapport E. (1985) Creatine kinase: purification, characterization, and tissue distribution of the MM subtypes. Clin. Chim. Acta, 153:181-190.

Miller J., Johnson M., and Wei R. (1982) Preparation of creatine kinase-MM isoenzymes from canine and human tissues. Clin. Chim. Acta, 118:67-76.

Moerland T.S. and Egginton S. (1998) Intracellular pH of muscle and temperature insight from *in vivo* ^{31}P NMR measurements in a stenothermal Antarctic teleost (*Harpagifer antarcticus*). J. Therm. Biol., 23:275-282.

Morescalchi A., Hureau J.C., Olmo E., Ozouf-Costaz C., Pisano E., and Stanyon R. (1992) A multiple sex-chromosome system in Antarctic ice-fishes. Polar Biol., 11:655-661.

Muhlebach S.M., Gross M., Wirz T., Wallimann T., Perriad J.-C., and Wyss M. (1994) IV-2 Sequence homology and structure predictions of the creatine kinase isoenzymes. Mol. Cell. Biochem., 133/134:245-262.

Neuhoff V., Arold N., Taube D., and Ehrhardt W. (1988) Improved staining of proteins in polyacrylamide gels including isoelectric focusing gels with clear background at nanogram sensitivity using Coomassie Brilliant Blue G-250 and R-250. Electrophoresis, 9:255-262.

Nicholas K.B., Nicholas H.B. Jr., and Deerfield D.W. II (1997) GeneDoc: Analysis and visualization of genetic variation. Embnew. News, 4:14.

Nielsen L. and Ludvigsen B. (1963) Improved method for the determination of creatine kinase. J. Lab. Clin. Med., 62:159-168.

Nihei T., Noda L., and Morales M.F. (1961) Kinetic properties and equilibrium constant of the adenosine triphosphate-creatine transphosphorylase-catalyzed reaction. J. Biol. Chem., 236:3203-3209.

Oliver I.T. (1955) A spectrophotometric method for the determination of creatine phosphokinase and myokinase. Biochem. J., 61:116-122.

Page R.D.M. (1996) TreeView: an application to display phylogenetic trees on personal computers. Comput. Appl. Biosci., 12:357-358.

Parkhouse W.S., Dobson G.P., and Hochachka P.W. (1988) Organization of energy provision in rainbow trout during exercise. Am. J. Physiol., 254:R302-R309.

Pate E., Bhimani M., Franks-Skiba K., and Cooke R. (1995) Reduced effect of pH on skinned rabbit psoas muscle mechanics at high temperatures: implications for fatigue. J. Physiol., 486:689-694.

Petrova T.A., Shamova O.V., and Lyzlova S.N. (1988) Comparative enzymatic analysis of creatine kinases from skeletal muscles of the cod, frog, and rabbit. Zh. Evol. Biokhim. Fiziol., 24:489-496.

Pineda Jr. A.O. and Ellington W.R. (1999) Structural and functional implications of the amino acid sequences of dimeric, cytoplasmic and octameric mitochondrial creatine kinases from a protostome invertebrate. Eur. J. Biochem., 264:67-73.

Portner H.O., Boutilier R.G., Tang Y., and Toews D.P. (1990) Determination of inracellular pH and P_{CO_2} after metabolic inhibition by fluoride and nitrilotriacetic acid. Respir. Physiol., 81:255-274.

Prirodina V.P. (1994) Review of karyotypes and taxonomic diversity in the suborder Notothenioidei (Perciformes). J. Ichthy., 34:180-186.

Qin W., Khuchua Z., Cheng J., Boero J., Payne R.M., and Strauss A.W. (1998) Molecular characterization of the creatine kinases and some historical perspectives. Mol. Cell. Biochem., 184:153-167.

Quest A.F.G., Eppenberger H.M., Wallimann T. (1989) Purification of brain-type creatine kinase (B-CK) from several tissues of the chicken: B-CK subspecies. Enzyme, 41:33-42.

Rahn H. and Baumgardner F.W. (1972) Temperature and acid-base regulation in fish. Respir. Physiol., 14:171-182.

Rahn H., Reeves R.B., and Howell B.J. (1975) Hydrogen ion regulation, temperature, and evolution. Am. Rev. Respir. Dis., 112:165-172.

Raibeks A. and Massey V. (1996) Glycerol-induced development of catalytically active conformation of *Crotalus adamanteus* L-amino acid oxidase *in vitro*. Proc. Natl. Acad. Sci. USA, 93:7546-7551.

Rao J.K.M., Bujacz G., and Wlodawer A. (1998) Crystal structure of rabbit muscle creatine kinase. FEBS Lett., 439:133-137.

Rosalki S.B. (1967) An improved procedure for serum creatine phosphokinase determination. J. Lab. Clin. Med., 69:696-705.

Rosevear P.R., Desmeules P., Kenyon G.L., and Mildvan A.S. (1981) Nuclear magnetic resonance studies of the role of histidines at the active site rabbit muscle creatine kinase. Biochemistry, 20:6155-6164.

Rychlik W., Spencer W.J., and Rhoads R.E. (1990) Optimization of the annealing temperature for DNA amplification in vitro. Nucleic Acid Res., 18:6409-6412.

Sambrook J., Fritsch E.F., and Maniatas T. (1989) Molecular Cloning. Cold Spring Harbor Laboratory Press, N.Y.

Schafer B.W. and Perriard J.-C. (1988) Intracellular targeting of isoproteins in muscle cytoarchitecture. J. Cell Biol., 106:1161-1170.

Schellman J.A. (1997) Temperature, stability, and the hydrophobic. Biophys. J., 73:2960-2964.

Scholl A. And Eppenberger H.M. (1972) Patterns of the isoenzymes of creatine kinase in teleostean fish. Comp. Biochem. Physiol., *42B*:221-226.

Schulte P.M., Moyes C.D., and Hochachka P.W. (1992) Integrating metabolic pathways in post-exercise recovery of white muscle. J. Exp. Biol., 166:181-195.

Shen Y.-q., Tang L., Zhou H.-m., and Lin Z.-j. (2001) Sructure of human muscle creatine kinase. Acta Cryst., D57:1197-1200.

Sidell B.D. (1988) Diffusion and ultrastructual adaptive responses in ectotherms. In: Microcompartmentation. Jones D.P. (ed.), CRC Press, Boca Raton, FL.

Sidell B.D. and Crockett E.L. (1989) Metabolic characteristics of muscle tissues from Antarctic fishes. Antarctic J. U.S., 23:138-140.

Sidell B.D. and Moerland T.S. (1989) Effects of temperature on muscular function and locomotory performance in teleost fish. In: Adv. Comp. Envir. Physiol., 5:116-156. Springer-Verlag, Berlin Heidelberg.

Simonarson B. and Watts D.C. (1972) Purification and properties of adenosine triphosphate-creatine phophotransferase from muscle of the dogfish *Scylliorhinus canicula*. Biochem. J., 128:1241-1253.

Sjovall K. (1967) A tetrazolium technique for the histochemical localization of ATP: Creatine phosphotransferase. Histochemie, 10:336-340.

Somero G.N. (1975) Temperature as a selective factor in protein evolution: The adaptational strategy of "compromise". J. Exp. Zool., 194:175-188.

Somero G.N. (1981) pH-temperature interactions on proteins: Principles of optimal pH and buffer system design. Marine Biol. Lett., 2:163-178.

Somero G.N. (1986) Protons, osmolytes, and fitness of internal milieu for protein function. Am. J. Physiol., 251:R197-R213.

Somero G.N. (1995) Proteins and temperature. Annu. Rev. Physiol., 57:43-68.

Sun H.-W., Hui C.-F., and Wu J.-L. (1998) Cloning, characterization, and expression *in Escherichia coli* of three creatine kinase muscle isoenzyme cDNAs from carp (*Cyprinus carpio*) striated muscle. J. Biol. Chem., 273:33774-33780.

Surlter C.H. and DeLuca M. (1983) How to prevent losses of protein by adsorption to glass. Anal. Biochem., 135:112-119.

Suzuki T., Hirano T., and Suyama M. (1987) Free imidazole compounds in white and dark muscles of migratory marine fish. Comp. Biochem. Physiol., 87B:615-619.

Sweeney H.L. (1994) The importance of the creatine kinase reaction: the concept of metabolic capacitance. Med. Sci. Sports Exerc., 26:30-36.

Szasz G., Gruber W., and Bernt E. (1976) Creatine kinase in serum: 1. Determination of optimum reaction conditions. Clin. Chem., 22:650-656.

Thompson J.D., Higgins D.G., and Gibson T.J. (1994) CLUSTAL W: improving the sensitivity of progressive multiple sequence alignment through sequence weighting, position-specific, gap penalties and weight matrix choice. Nucleic Acid Res., 22:4673-4680.

Timasheff S.N. (1992) Water as ligand: Preferential binding and exclusion of denaturants in protein unfolding. Biochemistry, 31:9857-9864.

Trask R.V. and Billadello J.J. (1990) Tissue-specific distribution and developmental regulation of M and B creatine kinase mRNAs. Biochim. Biophys. Acta, 1049:182-188.

van Deursen J., Heerschap A., Oerlemans F., Ruitenbeek W., Jap P., ter Laak H., and Wieringa B. (1993) Skeletal muscles of mice deficient in muscle creatine kinase lack burst activity. Cell, 74:621-631.

van Dijik P.L.M., Tesch C., Hardewig I., and Portner H.O. (1999) Physiological disturbances at critically high temperatures: A comparison between stenothermal Antarctic and eurythermal temperate eelpouts (Zoarcidae). J. Exp. Biol., 202:3611-3621.

Walesby N.J. and Johnston I.A. (1979) Activities of some enzymes of energy metabolism in the fast and slow muscles of an Antarctic teleost fish (*Notothenia rossii*). Biochem. Soc. Trans., 7:659-661.

Wallimann T. and Eppenberger H.M. (1985) Localization and function of M-line bound creatine kinase. Cell and Muscle Motil., 6:239-285.

Wallimann T., Wyss M., Brdiczka D., Nicolay K., and Eppenberger H.M. (1992) Intracellular compartmentation, structure and function of creatine kinase isoenzymes in tissues with high and fluctuating energy demands: the 'phosphocreatine circuit' for cellular energy homeostasis. Biochem. J., 281:21-40.

Watts D.C. (1973) Creatine Kinase (adenosine 5'-triphosphate-creatine phosphotransferase. In: The enzymes, 8 (part A), 3rd ed., Boyer P.D. (ed.), Academic Press, N.Y.

Watts D.A., Rice R.H., and Brown W.D. (1980) The primary structure of myoglobin from yellowfin tuna (Thunnus albacares). J. Biol. Chem., 255:10916-10924.

West B.L., Babbitt P.C., Mendez B., and Baxter J.D. (1984) Creatine kinase protein sequence encoded by a cDNA made from Torpedo californica electric organ mRNA. Proc. Natl. Acad. Sci. USA, 81:7007-7011.

White K.C., Babbit P.C., Buechter D.D., and Kenyon G.L. (1992) The principal islet of the coho salmon (*Oncorhyncus kisutch*) contains the BB isoenzyme of creatine kinase. J. Protein Chem., 11:489-494.

Winnard Jr. P.T. (1987) Equilibrium sedimentation of lubrol-solubilized rabbit thrombomodulin. Masters Thesis, University of New Hampshire.

Wison I.A., Brindle K.M., and Fulton A.M. (1995) Differential localization of the mRNA of the M and B isoforms of creatine kinase in myoblasts. Biochem. J., 308:599-605.

Wood T.D., Guan Z., Borders Jr. C.L., Chen L.H., Kenyon G., and McLafferty F.W. (1998) Creatine kinase: Essential arginine residues at the nucleotide binding site identified by chemical modification and high-resolution tandem mass spectrometry. Proc. Natl. Acad. Sci. USA, 95:3362-3365.

Xia X. and Xie Z. (2001) DAMBE: Data analysis in molecular biology and evolution. J. Heredity, 92:371-373.

Yancey P.H. and Somero G.N. (1978) Temperature dependence of intracellular pH: Its role in the conservation of pyruvate apparent K_m values of vertebrate lactate dehydrongenases. J. Comp. Physiol., 125:129-134.

Zhou H.-M., Zhang X.-H., Yin Y., and Tsou C.-L. (1993) Conformational changes at the active site of creatine kinase at low concentrations of guanidinium chloride. Biochem. J., 291:103-107.

Appendix:

MATERIALS and METHODS

Protein Purification

Reagents and labware.

Low-range protein molecular weight marker mixture (14.4-to-97.4 kDa) was from Roche. Human MMCK (7.5 mg/ml) and goat anti-human MMCK (serum) were from Biodesign International. Unless otherwise indicated, all other chemical reagents were from Sigma. Sterile plastic tubes (50 and 15 ml) were from Corning. All glassware, Oakridge centrifuge tubes, and mortar and pestal, were sterilized.

Animals and tissue.

Live specimens of *Chaenocephalus aceratus* and *Gobionotothen gibberifrons* were caught using an otter trawl deployed from the R/V *Polar Duke* during 1991, 1993 and 1999 expeditions to the Antarctic. Tissues were dissected immediately after the fish were killed, frozen in liquid N_2, and stored at –70° C until use.

White muscle homogenization and supernatant preparation.

Preparations were carried out at 0°-to-2° C. Homogenization solution was 10 mM MES, 20 mM KCl, 5 mM creatine, 5mM $MgCl_2$, 1 mM EGTA, 30% glycerol, 10 mM β-mercaptoethanol, 0.5 mM phenylmethylsulfonyl fluoride, 10 μM (5 μg/ml) leupeptin, 1 μM (0.685 μg/ml) pepstatin A pH 6.25 at 1° C. Frozen (-70° C) *C. aceratus* myotomal white muscle was pulverized to a fine powder in a pre-cooled (liquid N_2) mortar and

pestal. The muscle powder was homogenized in 10 volumes of homogenization buffer in a glass-on-glass tissue grinder. Homogenate was centrifuged at 2° C at 39,000x g for 50 minutes. Supernatant was applied directly to the Cibacron 3GA blue affinity column.

Cibacron blue 3GA affinity chromatography.

Affinity columns were equilibrated at 30 ml/hr with 20 volumes of homogenization solution. Five milliliters of packed matrix was used per gram of frozen tissue. The column was loaded with supernatant at 15 ml/hr. The column was washed with 10 volumes of homogenization solution and eluted at 15 ml/hr with 10 volumes of elution buffer solution (10 mM HEPES, 20 mM KCl, 1 mM EGTA, 30% glycerol, 10 mM β-mercaptoethanol pH 8.0 at 1° C). One milliliter fractions were collected and every fifth fraction was assayed for creatine kinase activity using a colorimetric assay (see below). Fractions with the highest activity were determined spectrophotometrically and pooled. The UV monitor was set at 0.2 AUFS (absorbance units full scale) while the chart was run at 2 cm/hr with a full-scale deflection setting of 1.0 V. The column was regenerated by successively washing with 10 volumes of each of the following buffer solutions: (a) 0.1 M borate, 1.0 M NaCl pH 9.8 (Sigma's data sheet recommendation), (b) 0.1 M borate pH 9.8 (Sigma's data sheet recommendation), (c) 0.1 M Tris, 1.0 M NaCl pH 9.0 (Fisher and Watts, 1979), and stored in 2.0 M NaCl-0.02% NaN_3 (Sigma's data sheet recommendation).

Anion exchange on a DEAE column.

DEAE loading buffer solution was 2.5 mM Tris base, 30% glycerol, 1.0 mM Triton X-100, 10 mM β-mercptoethanol, pH 8.5 at 2.0° C. An aliquot of pooled blue affinity column CK was dialyzed in 14 kDa cutoff dialysis tubing (Spectra/Por) for two days against 400 fold excess of DEAE loading buffer solution with a change of buffer solution after the first overnight dialysis. DEAE Sepharose CL-6B beads were suspended in 0.5 M Tris base pH 8.9 at 2° C. A 4.5 ml column of DEAE matrix was equilibrated with 15 volumes 0.5 M Tris base pH 8.9 followed by 30 volumes of DEAE loading buffer solution, at 2.0° C. Flow rate throughout was at 2-to-4 ml/hr. For elution, a linear gradient of 0-to-0.2 M KCl in DEAE loading-buffer solution was applied. It was necessary to apply this as 4 successive narrow linear gradients of 0-to-0.03 M KCl (30 ml), 0.03-to-0.065 M KCl (25 ml), 0.065-to-0.1 M KCl (20 ml), and 0.1-to-0.2 M KCl (30 ml). Fraction size was 0.15-to-0.18 ml. The UV monitor was set at 0.2 AUFS while the chart was run at 1 cm/hr with a full-scale deflection setting of 500 mV. Washing successively with 10 volumes of 2 M NaCl and 0.5 M Tris base pH 8.9 regenerated the column.

Detection of creatine kinase in chromatographic fractions.

At 4° C, 10 µl of affinity or DEAE column fractions was mixed with 10 µl of creatine kinase colorimetric assay solution (100 mM HEPES-100 mM KCl, 36 mM $Mg(Ac)_2$, 60 mM PCr, 40 mM glucose, 10 mM $NADP^+$, 4 mM ADP, 0.7 mM Nitro Blue Tetrazolium, 0.15 mM Phenazine Methosulfate, 50 U/ml HK, 10 U/ml G-6-PDH, final

pH 7.3-to-7.5). In this assay NADPH reduces PMS which transfers an electron to NTB producing a blue-black formazan precipitate (Dewey and Conklin, 1960, Sjovall, 1967, and Kim *et al.*, 1976). Fractions with high CK activity began to show color within 0.5-to-5 minutes and the reaction appeared to be complete in all CK containing tubes in 0.5 hour while longer incubation times (> 1.0 hr) gave false positives.

Protein concentration estimates.

Bicinchoninic acid (BCA, Pierce) assays were used to estimate protein concentrations with standard curves produced using rabbit MMCK. The stock concentration of rabbit MMCK was determined using $E^{1\%}$ = 8.76 ml/mg at 280 nm (Noda *et al.*, 1954, Sigma's data sheet). Prior to BCA analysis protein samples and buffer solution blanks (i.e., MES, HEPES, and Tris) were dialyzed against 10 mM HEPES, 20 mM KCl pH 7.5, at 4^0 C. The 30 minute-60° C assay was carried out according to the supplier's directions followed by 30 minutes of cooling at room temperature. Triplicate determinations were used throughout.

Polyacrylamide gel Eeectrophoresis, denaturing gels.

Denaturing SDS-PAGE was carried out using a modification of the Ornstein-Lammaeli SDS discontinuous buffer system (Jovin, 1973; Winnard Jr., 1987). The stock resolving gel buffer solution was 1.64 M Tris base, 0.21 M HCl pH 9.2. The concentration of Tris base in the resolving gel was 0.465 M. The stock stacking gel buffer solution was 0.585 M Tris base, 0.6 M HCl pH 6.7. Tris base concentration in the stacking gel was 0.116 M. Anode buffer solution was 200 mM Tris base pH 8.4 and cathode buffer solution was 80 mM Tris base, 96 mM Glycine, 0.1% SDS pH 8.9 (Jovin,

1973). Acrylamide stock solution was 30% acrylamide and 1% bisacrylamide, that is, a stock solution of 31% total acrylamide. Five percent total acrylamide stacking and 12.5 % total acrylamide resolving gels were prepared. Prior to loading onto stacking gels, samples were mixed 1:1 with sample treatment buffer (25% glycerol, 40% stacking buffer solution, 2% SDS, 1.25 M β-mercaptoethanol, 0.01% bromophenol blue) and heated at 94° C for 3 minutes. Electrophoresis was run at a constant current of 20 mA per mini-gel. The tracking dye reached the bottom of the gel in about 1.0 hour.

Polyacrylamide gel electrophoresis, native gels.

Native PAGE was a modification of Wang *et al.*'s (1990) procedure. Resolving gels were prepared using a 2x native resolving gel stock buffer solution of 50 mM Tris Base, 36 mM HCl pH 8.3 at 4° C. The electrode buffer solution was 75 mM Glycine, 5 mM Tris Base pH 9.0 at 4° C. Just prior to use, β-mercaptoethanol was added to 1x resolving gel and electrode buffer solutions to a final concentration of 2.5 mM. Prior to loading, samples were mixed 1:1 with 2x native treatment buffer (20% glycerol, 75% 2x native resolving gel stock buffer solution, 5 mM β-mercaptoethanol, 0.01% bromophenol blue). Electrophoresis was run at a constant current of 2 mA per mini-gel.

Polyacrylamide gel electrophoresis, staining.

Protein bands in polyacrylamide gels were stained according to Neuhoff *et al.*, 1988 and required no destaining. The stock Coomassie Brilliant Blue G-250 staining solution was 2% (w/v) phosphoric acid, 10% (w/v) ammonium sulfate, 0.1% Brilliant Blue G-250. The working stain was prepared by diluting 80 ml of stock staining solution into 20 ml of methanol (Neuhoff *et al.*, 1988). Gels were incubated for 30 minutes in 12% TCA (Neuhoff *et al.*, 1988). The working stain was then prepared and added to the

gel. Quantitative staining required an overnight incubation (Neuhoff *et al.*, 1988). The stain was then discarded and, to dissolve excess colloidal particles stuck to the gel and the staining container, 25% methanol was added and shaking continued for 5-to-10 min. This process was repeated until all colloid particles were removed. For best results, gels were than incubated with 25% methanol for 0.5-to-1.0 hour with shaking, which gave a clear background. Stained gels were then stored (indefinitely) in 25% ammonium sulfate.

Activity in native gels was detected using a 1:1 dilution of the colorimetric solution used for activity detection in chromatographic fractions. Prior to staining, gels were equilibrated for 1.0 hr in 10 mM HEPES, 20 mM KCl pH 7.5, at 4° C. Twenty milliliters of activity stain was used per mini-gel. Staining required at least a 4 hr incubation with a change stain after the first 2 hr.

Immunoblot analyses.

Protein was transferred from SDS or native resolving gels to polyvinylidene difluoride (PVDF) membranes (BIO-RAD) using a semi-dry transfer apparatus (Transblot transfer cell, BIO-RAD), according to the procedure of Kyhse-Andersen (1986). Dilution of DIG blocking buffer solution was with phosphate buffered saline pH 7.4 (PBS). Membranes were blocked for 1.0 hour at 4° C with a 10% solution of DIG blocking buffer solution (Roche). Membranes were washed five times for 5-to-10 minutes in PBS at 4° C and then incubated for 2.0 hours at 4° C with a 1:5000 dilution of anti-human MMCK in 10% blocking solution. The washing step was repeated and membranes were then incubated overnight at 4° C with a 1:5000 dilution of horseradish peroxidase conjugated rabbit anti-goat whole IgG in 10% blocking solution. This

incubation was then continued for 15 minutes at room temperature and the washing step was repeated. Immunoreactive protein bands were visualized, after chemiluminescence development (SupersSignal West Pico Kit, Pierce), by exposure (0.5-to-15 min) to Kodak BIOMAX MR film.

Creatine kinase kinetic assay.

In this assay ATP production by CK is coupled to NADPH production (Oliver, 1954). Glucose-6-phosphate dehydragenase (G-6-PDH) (2857 U/ml) from Torula yeast was used because of its high stability (Sigma's data sheet). Sulfate-free hexokinase (HK) was reconstituted at 10,000 U/ml in 0.125 M HEPES-0.125 M KCl pH 7.5 and stored as 50 µl aliquots at –20 ° C. The composition of the standard assay reaction mixture was 50 mM HEPES, 50 mM KCl, 18 mM $Mg(Ac)_2$, 30 mM PCr, 20 mM glucose, 5 mM $NADP^+$, 2 mM ADP, 10 mM AMP pH 7.60 ± 0.03 (at 0.5° ± 0.5° C), 25 U/ml HK, 5 U/ml G-6-PDH. HK and G-6-PDH were added to each cuvette just prior to conducting the assay. AMP was added to inhibit adenylate kinase activity (Oliver, 1954). This was used only when assaying white muscle homogenate and subsequent supernatant preparations. The composition of the final assay was similar to what has been reported previously (Nielsen and Ludvigsen, 1963; Rosalki, 1967; Hess *et al.*, 1968; Szasz *et al.*, 1976; Dunn and Johnston, 1986).

Creatine kinase kinetic assay, pH optimum.

For pH optimum experiments, Bis-Tris propane or MES replaced HEPES as the assay buffer during pH 6.00-to-pH 9.50 or pH 5.50-to-6.50 pH determinations respectively.

Determination of the apparent V_{max}.

A Hewlett Packard spectrophotometer (Model 89532A) equipped with a thermostattable cell holder was used to measure and record absorbances (A) at 340 nm as a function of time. The refrigerated circulating bath was from NESLAB. The temperature before and after every blank and sample run was determined using a TRACEABLE Model NEW 15-078H digital thermometer. Assays were carried out at $0.5^{o} \pm 0.5^{o}$ C. The outside of the cuvettes was kept free of condensation by a stream of cold and dry N_2 gas. Final assay volumes of 1 ml or 1.5 mls were used. Apparent V_{max}s were calculated by subtracting the ΔA_{340}/minute of blank solutions (no enzyme) from the ΔA_{340}/minute of sample solutions (enzyme included). The resulting values were multiplied by a correction factor (1.16), which corrected for the opaqueness of the methlyacrylate cuvette (86% transmitance at 340 nm Fisher Scienitific). After correcting for dilution units per ml (μmoles ATP/min/ml) were calculated by dividing by the micromolar extinction coefficient of NADPH (6.22 ml/μmol). When necessary, conversion to U/(mg of protein) /min were then made.

Estimates of average apparent K_ms of ADP and PCr.

Hanes plots (Hammes, 1982; Cornish-Bowden, 1995) were used to estimate average apparent K_ms. These plots are constructed from the equation: $[S]/v_o = [S]/V_{max} + K_m/V_{max}$, where v_o is the initial velocity and [S] is the substrate concentration. V_{max} is obtained from the slope ($1/V_{max}$) and K_m from the y-intercept (K_m/V_{max}).

Estimates of thermodynamic activation parameters.

Estimates of thermodynamic activation parameters were obtained according to Low and Somero (1976).

Sequencing of *C. acerratus* CK cDNAs and the Tissue Expression of their mRNAs

Reagents and labware.

[α-^{32}P]-deoxycytidine 5$\prime$-triphosphate tetra(triethylammonium) salt (10 mCi/ml) was from Dupont NEN. TRIzol reagent, DNA mass ladders, and RNA molecular size ladders were from Gibco BRL. Taq DNA Polymerase, 100 mM dNTP solutions, 25 mM $MgCl_2$, and 10x PCR buffer solution were from Roche. Advantage-2 DNA polymerase kit was from Clontech. 3-(N-Morpholino)propanesulfonic acid (MOPS) was from United States Biochemical. Unless otherwise indicated, all other chemical reagents were from Sigma. Washed glassware, mortars and pestals, and metal spatulas were baked overnight at 180-200^{o} C while Oakridge tubes were autoclaved. The Mill-Q water used to prepare buffer and salt solutions was treated overnight with diethyl pyrocarbonate (DPEC) using 1 ml DEPC/liter of Milli-Q water and autoclaved. Any labware or equipment that could not be autoclaved or cleaned as described was treated with RnaseZap (Ambion RNA Company), just prior to use.

Total RNA and mRNA preparation.

Total RNA was extracted from *G. gibberifrons* white muscle using either the hot phenol method described by Vayda *et al.* 1997. In all other cases, total RNA was prepared from tissues using TRIzol reagent according to the suppliers directions. Frozen

tissues were pulverized in a pre-cooled (liquid N_2) morter and homogenized (50 mg/ml of TRIzol reagent) in a glass tissue grinder. Yields from white muscle preparations were between 0.3 and 0.8 mg of total RNA per gram of frozen tissue. Total RNA was stored at –70° C.

Messenger RNA (mRNA) was prepared from 0.6-to-1.0 mg of total RNA using Oligotex mRNA Mini kits (QIAGEN) with two modifications (QIAGEN technical support, personal communication). (1) The 3 minute 70° C disruption of secondary structure step was increased to 4 minutes. (2) The suggested 10 minute hybridization to oligo$(dT)_{30}$ beads was increased to 20-to-30 minutes. mRNA was eluted in 20-to-40 µl of elution buffer and stored at –70° C. Total yields of mRNA ranged from 0.9-to-3.2 % of total RNA.

First-strand cDNA preparations.

Single-stranded cDNA preparations were obtained from total RNA from *G. gibberifrons* white muscle using a SuperScript II reverse-transcriptase (RT) kit (Gibco BRL) with a poly(A) specific primer: 5′-d(AAT TCG CGG CCG CTT TTT TTT TTT TTT)-3′. cDNA preparations were stored at –20° C. In all other cases first-strand cDNAs were prepared using Marathon cDNA Amplification kits (Clontech).

Double-stranded cDNA preparations.

Double-stranded (ds) cDNA libraries were prepared from 0.9-1.0 µg of mRNA using Marathon cDNA Amplification kits (Clontech). The final ds-cDNAs had an adaptor (ap) sequence ligated to both ends and were stored at –20° C. These preparations

made cloning and subsequent sequencing of 5′ and 3′ untranslated regions (UTRs), by RACE (rapid amplification of cDNA ends), possible. Prior to use as polymerase chain reaction (PCR) templates, these stock ds-cDNA preparations were diluted 1:250 in 10 mM Tricine, 0.1 mM EDTA pH 8.5 and were stored at –20° C.

Polymerase chain reactions (PCRs).

Oligonucleotide primers were synthesized by Gibco BRL (see Tables 5-to-9 for sequences). Reaction mixtures were 1x PCR buffer, 2.5 units of Tag (or Red-Tag), 1 mM Mg^{2+}, 0.2 mM of each dNTP, and 2 μM of each primer. To this was added either 1 or 2 μl of cDNA or 1 μl of gel-purified PCR product or 5 μl of RACE ds-cDNA template. RACE experiments were identical to other PCRs except 1 μl of Advantage 2 DNA polymerase kit was used, which gave a Mg^{2+} concentration of 3.5 mM. Thermocycling (MJ Research Mini Cycler) protocols always began with a 1-to-5 minute 94° C "hot start", ended with 10 minutes of extension at 72° C and used 35 cycles (or occassionally 50) of melting-annealing-extension of 1 minute each (annealing temperatures are listed in Tables 5-to-9). Touchdown PCRs were used to increase the specificity of the PCR reaction. Most touchdown PCRs were designed for RACE experiments and were carried out according to the directions in the Marathon instruction booklet. Other touchdown PCRs included separate annealing temperatures and extension times. PCR products were analyzed by electrophoresis in 2 % agarose gels (SeaKem LE, FMC BioProducts). Purified PCR products were stored at –20° C.

Plasmid cloning.

Desired inserts were prepared on the day of plasmid cloning. PCR products were purified from agarose gels using QIAquick Gel Extraction kits (QIAGEN). PCR products were eluted from the kit's anion exchange column in 20-to-40 μl of elution buffer. The concentrations of these eluants were determined by electrophoresing 2-to-5 μl in agarose gels alongside a DNA low-mass ladder (Gibco BRL). Plasmid preparation and clonings were then carried out using The Original TA Cloning kit (Invitrogen). Plasmids were purified using QIAprep Spin Miniprep kits (QIAGEN). Roughly 90% of the total amount of plasmid loaded onto the kit's column was eluted in the first 40 μl of elution buffer applied to the column. Aliquots of purified plasmids (500 μg of plasmid) were digested with EcoR I (Gibco BRL) and digestion mixtures analyzed by electrophoresis in 1.5% agarose gels, to determine which plasmids contained the appropriate inserts. Purified plasmid preparations were stored at –20° C.

DNA sequencing.

All sequencing was done with an automated DNA sequencer at the University of Maine sequencing facility. PCR products that were submitted for sequencing had first been purified using QIAquick gel extraction reagents. Appropriate PCR primers were supplied with their PCR products allowing for the sequencing in both directions. Plasmids were sequenced using primers specific to the vector sequence and thus, inserts were sequenced in both directions.

Northern blot analyses.

Electrophoresis of RNA under denaturing conditions followed standard protocols (Sambrook *et al.* 1989). Five micrograms of total RNA from each tissue was analyzed. Samples were resolved in a 1.25 % agarose-formaldehyde gel in 20 mM MOPS, 8 mM Na(Ac), 1 mM EDTA pH 7.0. Prior to loading the samples onto the gel, electrophoresis was run at 60 V for 5 minutes. Samples were then loaded and electrophoresis was run at 80 V for 2.0 hr. and finished at 100 V for 1.5 hr. Transfer to Hybond-N nylon membranes (Amersham Life Science) was carried out with 20x SSPE (3.0 M NaCl, 0.2 M NaH_2PO_4, 20 mM EDTA pH 7.4) as the transfer buffer solution. Transfers started with 2.0 hrs of descending transfer (Chomczynski and Mackey, 1994) followed by an overnight ascending transfer (Sambrook *et al.*, 1989). Immediately after transfer, RNA was crosslinked to the nylon membranes by exposure of the moist membrane to a UV-light source for 2 minutes. At this time, lanes containing the RNA ladders were cut from the rest of the membrane and stained with 0.02% methylene blue in 0.3 M Na(Ac) pH 5.5 according to Herrin and Schmidt, 1988. These lanes were later used to estimate the size of the detected bands.

Roche's hexanucelotide random primer kit was used to prepare ^{32}P-labeled probes from purified PCR products. DIG-labeling of probes was accomplished with PCR. These PCRs were performed as described above except the dNTP mixture was supplemented with dUTP-DIG (0.02 mM dUTP-DIG plus 0.18 mM dTTP). The muscle isoform specific probe was prepared by using the primer-pair ACE MCK 5U/ACE MCK 5L (Table 5). The mitochrondrial isoform specific probe was prepared by using the primer-pair 5′-d(CCG CCC GGG CAG GTG AAG C)-3′/5′-d(AGA GCC TTG GCC

ATG CAG TTG TTG TGT)-3′ (62° C annealing temperature). The brain isoform specific probe was prepared by using primer-pair GIB BCK 1U/GIB BCK 1L (see Table 7). Pre-hybridizations were for ≥ 1.0 hr. at 50° C while hybridizations were incubated overnight at 50-to-53° C. Both steps were in DIG Easy Hyb according to Roche's instructions. Membranes were then washed according to DIG Wash and Blocking buffer kit instructions (Roche). Final washes were done at 65-to-70° C. All steps were done in heat-sealed pouches. Colorimetric or chemiluminescent detection of DIG-labeled probes were developed according to Roche's instructions. In all cases, bands were visualized using Kodak's BIOMAX MR film.

Computer programs.

Oligonucleotide primers designed for PCR, preliminary multiple sequence alignments, preliminary similarity analyses, and contig construction were carried out with the programs supplied with the Dnastar package from Lasergene and NCBI's ClustalW (Thompson et al., 1994). Final multiple sequence alignments, similarity and identity analyses, and dendogram constructions were carried out using the program packages: Data Analysis in Molecular Biology and Evolution (DAMBE) (Xia and Xie, 2001), Phylip (Felsenstein, 1984), TreeView (Page, 1996), BioEdit (Hall T.A., 1999), and GeneDoc (Nicholas and Nicholas, 1997). Homologous sequence searches and BLAST searches were performed through the GenBank database. Figures depicting aligned sequences were prepared with the aid of BioEdit.

BIOGRAPHY OF THE AUTHOR

Paul T. Winnard Jr. was born in Pittsfield, Massachusetts on October 24, 1956. He was raised in Pittsfield, Massachusetts and graduated from Taconic High School in 1974. He attended Merrimack College and graduated in 1984 with a Bachelor of Science degree in Chemistry. He attended The University of New Hampshire and graduated in 1987 with a Master of Science degree in Biochemistry. He worked at Massachusetts General Hospital in the Department of Immunopathology until 1989. He worked at the Massachusetts Institute of Technology in the Department of Toxicology until 1991. He worked at The University of Massachusetts Medical Center in the Department of Radiology until 1995.

After receiving his degree, Paul will be joining The Department of Magnetic Resonance Imaging and Radiology at The Johns Hopkins School of Medicine as a post-doctorate fellow. Paul is a candidate for the Doctor of Philosophy degree in Biochemistry and Molecular Biology from The University of Maine in December, 2001.